

COM-08-023
Revision 0
September 1981
64.316.0042

DYNAMIC ANALYSIS OF
WETWELL-TO-DRYWELL
VACUUM BREAKERS
FOR
QUAD CITIES STATION
UNITS 1 & 2

Prepared for:
COMMONWEALTH EDISON COMPANY

Prepared by:
NUTECH
San Jose, California

Prepared by:

A. K. Moonka

A. K. Moonka
Specialist

Approved by:

G. P. Chew

G. P. Chew
Engineering Manager

Reviewed by:

V. N. Vagliente

Dr. V. N. Vagliente, P.E.
Project Engineer

Issued by:

H. W. Massie, Jr.

H. W. Massie, Jr.
Project Manager

Date:

9/29/81

8307190067 830712
PDR ADCK 05000237
P PDR

REGULATORY DOCKET FILE COPY

nutech
ENGINEERS

REVISION CONTROL SHEET

SUBJECT: Dynamic Analysis of Wetwell- to-Drywell Vacuum Breakers for Quad Cities Units 1&2
 REPORT NUMBER: COM-08-023
 Rev. 0

A.K. Moonka, Specialist
 NAME/TITLE

AKM
 INITIAL

V.N. Vagliente
 Principal Engineer
 NAME/TITLE

VNV
 INITIAL

P.C. Riccardella
 Engineering Director
 NAME/TITLE

[Signature]
 INITIAL

T.R. Mager
 Consultant I
 NAME/TITLE

TRM
 INITIAL

S.S. Tang
 Engineer
 NAME/TITLE

[Signature]
 INITIAL

T.S. Hsu
 Specialist
 NAME/TITLE

TSH
 INITIAL

EFFECTIVE PAGE(S)	REV	PRE- PARED	ACCURACY CHECK	CRITERIA CHECK	EFFECTIVE PAGE(S)	REV	PRE- PARED	ACCURACY CHECK	CRITERIA CHECK
1-1 thru 3-3	0	AKM	VNV	[Signature]	B-11 thru B-36	0	AKM	VNV	[Signature]
3-4 thru 3-11	0	AKM	SST	VNV					
3-12 thru 3-16	0	AKM	VNV	[Signature]					
4-1 thru 4-3	0	TRM	AKM	VNV					
5-1 thru 5-6	0	AKM	VNV	[Signature]					
5-7 thru 6-1	0	TRM AKM	AKM VNV	[Signature] [Signature]					
6-6 thru B-10	0	AKM	TSH	[Signature]					

QEP-001.1-00.

CERTIFICATION BY REGISTERED PROFESSIONAL ENGINEER

I hereby certify that this stress report has been reviewed by me and that I am a duly Registered Professional Engineer and that I am competent to review this document. I also certify that this stress report is correct and complete and satisfies the requirements of the ASME Boiler and Pressure Vessel Code, Section III, 1977 Edition including the Summer 1977 Addenda and is in compliance with the Design Specifications COM-08-022, Rev. 0 and COM-08-024, Rev. 0.

Certified by:

V. N. Vagliente
V. N. Vagliente

Civil Engineer

State of California

Registration No. C-28343

Date: Sept. 29, 1981

Certified by:

B. J. Whiteway
B. J. Whiteway

Professional Engineer

State of Illinois

Registration No. 62-39621

Date: SEPT. 29, 1981

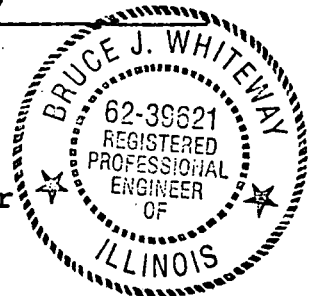


TABLE OF CONTENTS

	<u>Page</u>
LIST OF FIGURES	v
LIST OF TABLES	vi
ABSTRACT	vii
1.0 INTRODUCTION	1-1
1.1 Scope	1-1
1.2 Vacuum Breaker Function	1-2
1.3 Vacuum Breaker Design Load due to chugging	1-3
1.4 ASME Code Criteria	1-6
1.5 Atwood & Morrill Valve Details	1-10
1.6 Summary of Earlier Modifications	1-11
2.0 METHOD OF ANALYSIS	2-1
2.1 Analysis Summary	2-1
2.2 Discussion of Assumptions	2-2
2.3 Rigid Body Dynamics Model	2-4
2.4 Impact and Stress Models	2-9
2.5 Material Properties	2-11
2.6 Load Combination	2-13

TABLE OF CONTENTS (concluded)

	<u>Page</u>
3.0 RESULTS	3-1
3.1 Dynamic Analysis Results	3-1
3.2 Stress Analysis	3-4
3.2.1 Stresses in the Valve Components	3-4
3.2.2 Valve Attachment Point Stresses	3-12
3.2.3 Comparison of Calculated Stresses to Code Allowables	3-16
4.0 CONCLUSIONS	4-1
4.1 Identification of Overstressed Components	4-1
4.2 Material Replacement Recommendations	4-1
5.0 DESIGN OF BLIND FLANGES	5-1
6.0 REFERENCES	6-1
APPENDIX A - Description of Drywell to Wetwell Design Forcing Function	A-1
APPENDIX B - Valve Analysis Details	B-1

LIST OF FIGURES

<u>Figure</u>	<u>Title</u>	<u>Page</u>
1-1	Vacuum Breaker Location	1-12
1-2	Typical Drywell-to-Wetwell Vacuum Breaker Pressure Differential Due to LOCA	1-13
1-3	Vacuum Breaker Valve Geometry	1-14
1-4	Vacuum Breaker Valve Seat Details	1-15
1-5	Valve Shaft and Arm Details	1-16
2-1	Single Degree of Freedom Model	2-15
2-2	Pressure Loading Definition	2-16
2-3	Typical Valve Response	2-17
2-4	Linearity of Stress with Impact Velocity	2-18
2-5	Valve Closing Impact Model Results: Comparison of 100 in/sec and 200 in/sec Approach Velocities	2-19
2-6	Valve Closing Impact Model Results: Initial Velocity Linearity Check	2-20
2-7	Valve Disc Assembly and Force System	2-21
2-8	Valve Closing Impact Model	2-22

LIST OF TABLES

<u>Table</u>	<u>Title</u>	<u>Page</u>
1-1	Vacuum Breaker Type and Design Load	1-5
1-2	Summary of Stress Intensity Limits	1-9
1-3	Stress Intensity K-Factor for Design Service and Test Load Combinations	1-10
2-1	Rigid Body Model Properties	2-8
2-2	Atwood & Morrill Valve Material Properties Summary (Most Probable Values)	2-12
2-3	Load Combinations	2-13
2-4	Revised Load Combinations	2-14
3-1	Maximum Impact Velocities	3-3
3-2(a)	Stresses in the Vacuum Breaker Components for Closing Impact Velocity of 4.631 Radians/Second	3-6
3-2(b)	Stresses in the Bolts and Keys for Closing Impact of 4.631 Radians/Second	3-7
3-3(a)	Stresses in the Vacuum Breaker Components for Closing Impact Velocity of 4.831 Radians/Second	3-8
3-3(b)	Stresses in the Bolts and Keys for Closing Impact of 4.831 Radians/Second	3-9
3-4(a)	Stresses in the Vacuum Breaker Components for Closing Impact Velocity of 5.006 Radians/Second	3-10
3-4(b)	Stresses in Bolts and Keys for Closing Impact of 5.006 Radians/Second	3-11
3-5	Vacuum Breaker Mounting Bolt Stresses	3-16
4-1	Vacuum Breaker Material Replacement Recommendations	4-3
5-1	Blind Flange Material Requirements	5-7

ABSTRACT

This report presents the methodology and results of dynamic structural analyses performed for the internally mounted drywell-to-wetwell vacuum breakers for Quad Cities Units 1 and 2. The ability of the vacuum breakers to withstand the design loading due to chugging and load combinations as outlined in the Mark I Program Structural Acceptance Criteria (Reference 1) has been determined.

The vacuum breaker valves have been analyzed in accordance with ASME Boiler and Pressure Vessel Code, Section III, Subsection NC for Class 2 components, 1977 Edition including the Summer 1977 addenda. Results of the structural analyses indicate that the shaft and the weight lever are overstressed. Therefore, it is recommended that they be replaced with components made of stronger materials.

This report also includes a section describing the design of blind flanges to accommodate replacement of some of the vacuum breaker valves.

1.0 INTRODUCTION

1.1 Scope

The work described in this report includes the dynamic structural analyses performed to determine the ability of the vacuum breaker valves to withstand the design loading due to chugging, hydrodynamic and seismic loads as outlined in the Mark I Program Structural Acceptance Criteria (Reference 1). Quad Cities Station Units 1 and 2 have twelve drywell-to-wetwell vacuum breaker valves in the vent system. It is noted that the vacuum breakers are not a part of the overall Mark I modification program.

Material identification giving specific type and grade was not available for some of the existing vacuum breaker components. Therefore, metallurgical engineering judgement was used, where necessary, to identify typical material taking into consideration the valve component and the time of valve manufacture.

A sizing analysis performed by NUTECH for Quad Cities vacuum breakers showed that not all twelve vacuum breakers are needed for vacuum relief. Therefore, this report includes a section describing the design of blind flanges to accommodate replacement

of some of the vacuum breaker valves in the future by the Commonwealth Edison Company.

1.2 Vacuum Breaker Function

A vacuum breaker is a normally closed check valve installed between the wetwell air space and the drywell (Figure 1-1). Its function is to limit negative pressure on Mark I Containment drywell vessels. The vacuum breaker maintains a wetwell pressure less than or equal to the drywell pressure by permitting air flow from the wetwell to the drywell when the wetwell is pressurized and the drywell is depressurizing slowly.

During a typical Loss of Coolant Accident (LOCA) steam from a pipe break forces the drywell air into the wetwell through the vent system. When the Emergency Core Cooling System (ECCS) flow raises the water level in the reactor to the elevation of the break, water cascading out of the break condenses the steam and depressurize the drywell. The vacuum breaker then opens to equalize pressure between the wetwell and drywell. This prevents wetwell water from entering the vent system and also limits the negative pressure differential on the drywell and vent system. A typical drywell-to-wetwell vacuum breaker pressure differential due to LOCA is shown in Figure 1-2.

1.3 Vacuum Breaker Design Load Due to Chugging

Cyclic pressures and valve oscillations were found to occur during the chugging phase of the tests conducted in the Mark I Containment at the Full Scale Test Facility (FSTF). Based on FSTF data, a vacuum breaker load definition was developed to permit structural analyses of typical vacuum breakers. This load definition is the vent system (vacuum breaker outlet) pressure minus the pressure at downcomer exit and is referred to as the forcing function.

The design load forcing functions were developed by Continuum Dynamics, Inc. (CDI, Reference 2) under subcontract to General Electric Company. CDI used a dynamic model of a Mark I pressure suppression system, which was capable of predicting pressure transients at specified locations in the vent system. With this dynamic model and FSTF data, a load definition resulting in pressure differential (load) across the vacuum breaker disc was quantified as a function of time. In addition, since FSTF sizing is not directly applicable to an individual Mark I plant, CDI has developed a methodology which permits them to develop forcing functions for plant unique applications. The plants with internally mounted vacuum breakers were divided into three groups according to containment geometry characteristics and a design load was developed for each group. Table 1-1 lists the plants by

vacuum breaker type and design load. This table shows that the applicable design load for 18" Atwood & Morrill internally mounted vacuum breakers in Quad Cities Units 1 and 2, is the Group I forcing function.

Table 1-1

Vacuum Breaker Types and Design Loads

Plant	Design Load	Vacuum Breaker
Browns Ferry 1, 2, 3 Pilgrim	Group I	GPE 18" Internal
Brunswick 1, 2 Cooper Hatch 1,2 Peach Bottom 2, 3	Group II	
Duane Arnold Fermi 2	Group III	
Hope Creek	Group III	GPE 24" Internal
Monticello Quad Cities 1, 2	Group I	A&M 18" Internal
Dresden 2, 3 Millstone Oyster Creek Vermont Yankee	Plant Unique	A&M 18" External
FitzPatrick Nine Mile Point 1	Plant Unique	A&M 30" External

1.4 ASME Code Criteria

The Quad Cities vacuum breakers have been evaluated in accordance with the ASME Boiler and Pressure Vessel Code, Section III, Subsection NC for Class 2 Components 1977 Edition including the Summer 1977 Addenda based on the Mark I Program Structural Acceptance Criteria (Reference 1). The alternative design rules defined in Subarticle NC-3200 were used. Accordingly, the theory of failure used for combining stresses is that the maximum shear stress occurs at a point equal to one-half the difference between the algebraic largest and the smallest of the three principal stresses at the point.

Terms used in the evaluation relating to stress analysis are defined as follows:

- 1) Stress intensity is the absolute difference between the largest and smallest principal stresses at a given point.
- 2) Primary stress is any normal or shear stress developed by an imposed loading which is necessary to satisfy the laws of equilibrium of external and internal forces and moments. The basic characteristic of a primary stress is that it is not self-

limiting, i.e., it can result in gross failure or deformation.

- 3) Membrane stress is the component of normal stress which is uniformly distributed and equal to the average of stress across the thickness of the section.
- 4) General primary membrane stress (P_m) is the average primary stress across a given section excluding effects of discontinuities and concentrations.
- 5) Primary bending stress (P_b) is the component of primary stress that is proportional to distance from the centroid of the solid section. Excluded are effects of discontinuities and concentrations.
- 6) Local primary membrane stress (P_L) is produced by pressure or other mechanical loading associated with a primary or discontinuity effect producing excessive distortion in the transfer of load.
- 7) Design stress intensity (S_m) for various materials are obtained from the ASME Code, Section III,

Appendices, Table I-1.0 and from MIL Handbook 5A (Reference 10).

- 8) The only Secondary Stress (Q) is the thermal stress caused by the temperature differential between the wetwell airspace and the vent system. The governing factors in thermal stress calculation are the temperature differential, the coefficient of thermal expansion and the restraints on the system. With the exception of the disc, which is made of wrought aluminum and free to expand, all major components of the valve are made of steel and have the same coefficient of thermal expansion and are allowed to expand freely. Therefore the thermal stress due to the uniform temperature gradient is insignificant.
- 9) Fatigue evaluation in the vacuum breaker valve components is not required because the total number of pressure and metal temperature cycles are much lower than 1000, per the ASME Code, Section III, Subsection NC3219.2.

The requirement for acceptability of a design is that the calculated stress intensities shall not exceed specified allowable

limits. These limits differ depending on the stress category (primary, secondary, etc.) from which the stress intensity is derived and the Service Level. A summary of stress intensity limits as given in the ASME Code Section III, Subsection NC-3217, is presented below:

Table 1-2

Summary of Stress Intensity Limits

<u>Calculated</u> <u>Stress Intensity</u>	<u>Allowable</u> <u>Stress Intensity Limit</u>
P_m	$< KSm$
P_L	$< 1.5KSm$
$(P_m \text{ or } P_L) + P_b$	$< 1.5KSm$

K varies depending on Service Level. K values for various load combinations as given in the ASME Code, Table NC-3217-1, are presented in Table 1-3.

Table 1-3

Stress Intensity K Factors for Design Service
and Test Load Combinations

<u>Service Limits</u>		<u>K</u>
Design	(A)*	1.0
Normal	(A)	1.0
Upset	(B)	1.1
Emergency	(C)	1.2
Faulted	(D)	2.0
Test		1.25 for hydraulic
		1.15 for pneumatic

* () Indicates Service Level.

1.5 Atwood & Morrill Valve Details

The major parts of the Atwood & Morrill 18" Internal Vacuum Breaker Valve, as presently installed in the Quad Cities plants, are shown in Figures 1-3, 1-4, and 1-5. The overall geometry is illustrated in Figure 1-3. The valve body is made of cast steel about 7/8" thick. The disc is made of wrought aluminum about 1" thick, with a stainless steel post. The disc is bolted to a

stainless steel disc arm which in turn is keyed to the shaft. Note, from Figure 1-4, that the gasket (called disc seat by A&M) can be compressed about 50% before metal to metal contact occurs between the disc and body ring. The shaft penetrates the valve body and has counterweights attached to one end as shown in Figure 1-5. The disc can swing between seat contact (fully closed) and body contact (fully open). Gravity loads hold the valve in closed position.

1.6 Summary of Earlier Modifications

In 1974, CECO replaced the integral post with a threaded pin made of stainless steel. In 1979, the results of the Short Term program analysis (References 3 and 4) indicated that the cast aluminum discs were susceptible to failure in a brittle fracture mode. Therefore the cast aluminum discs were replaced by discs made of wrought aluminum. At this time, the drywell-to-wetwell vacuum breaker valves in Quad Cities Station Units 1 and 2 have wrought aluminum discs with stainless steel posts as shown in Figure 1-3.

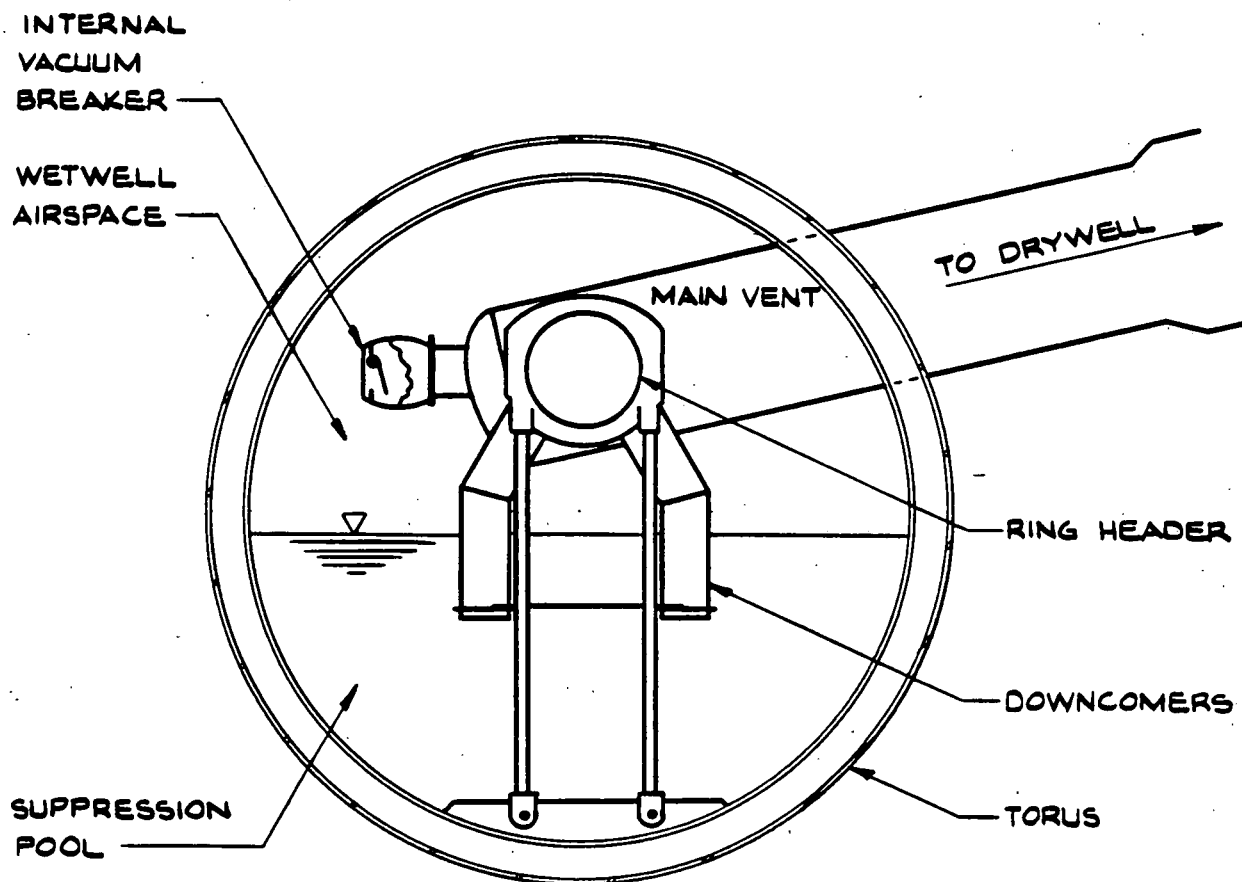


Figure 1-1. Vacuum Breaker Location

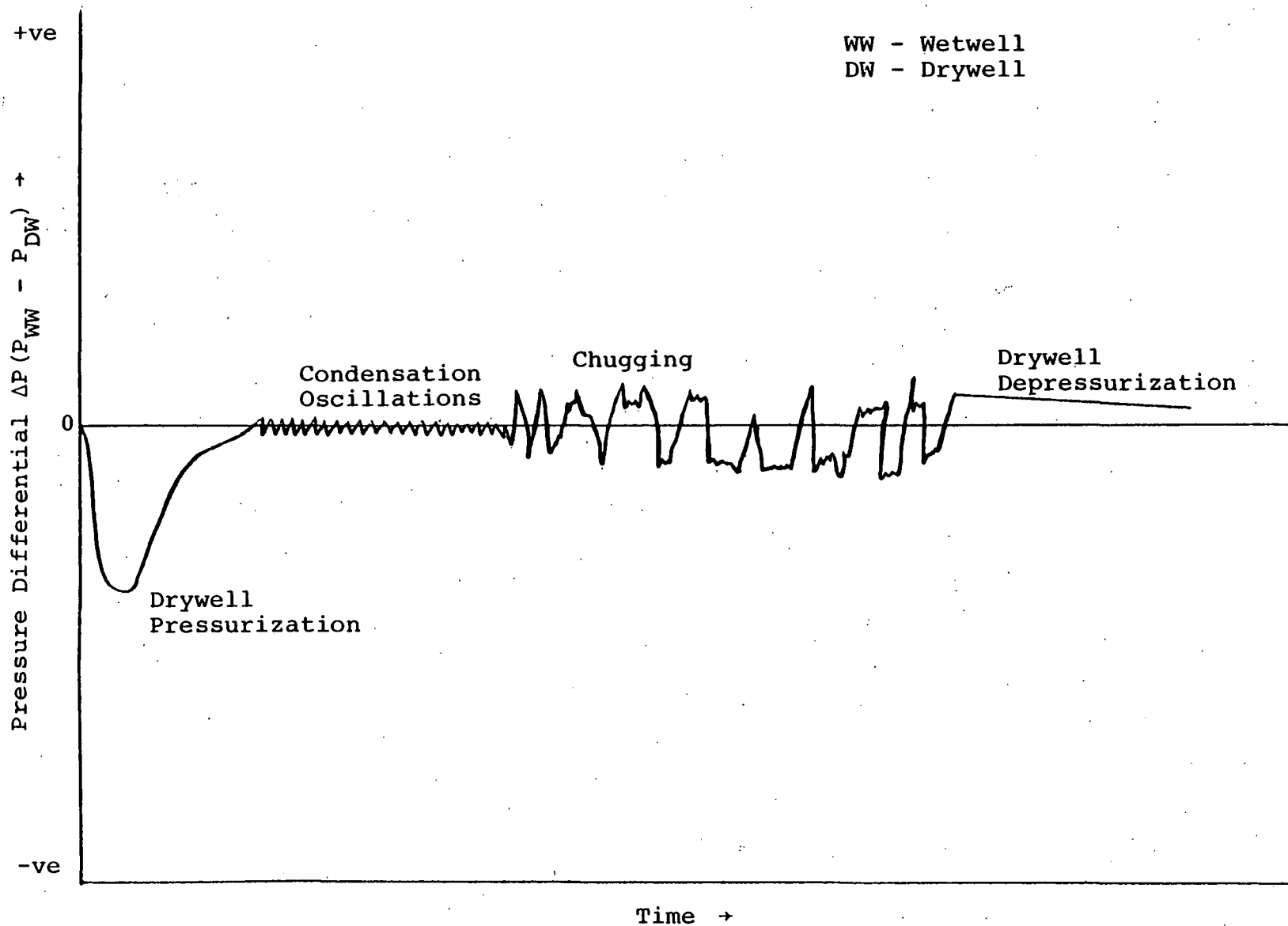


Figure 1-2. Typical DW/WW Vacuum Breaker Pressure Differential Due to LOCA

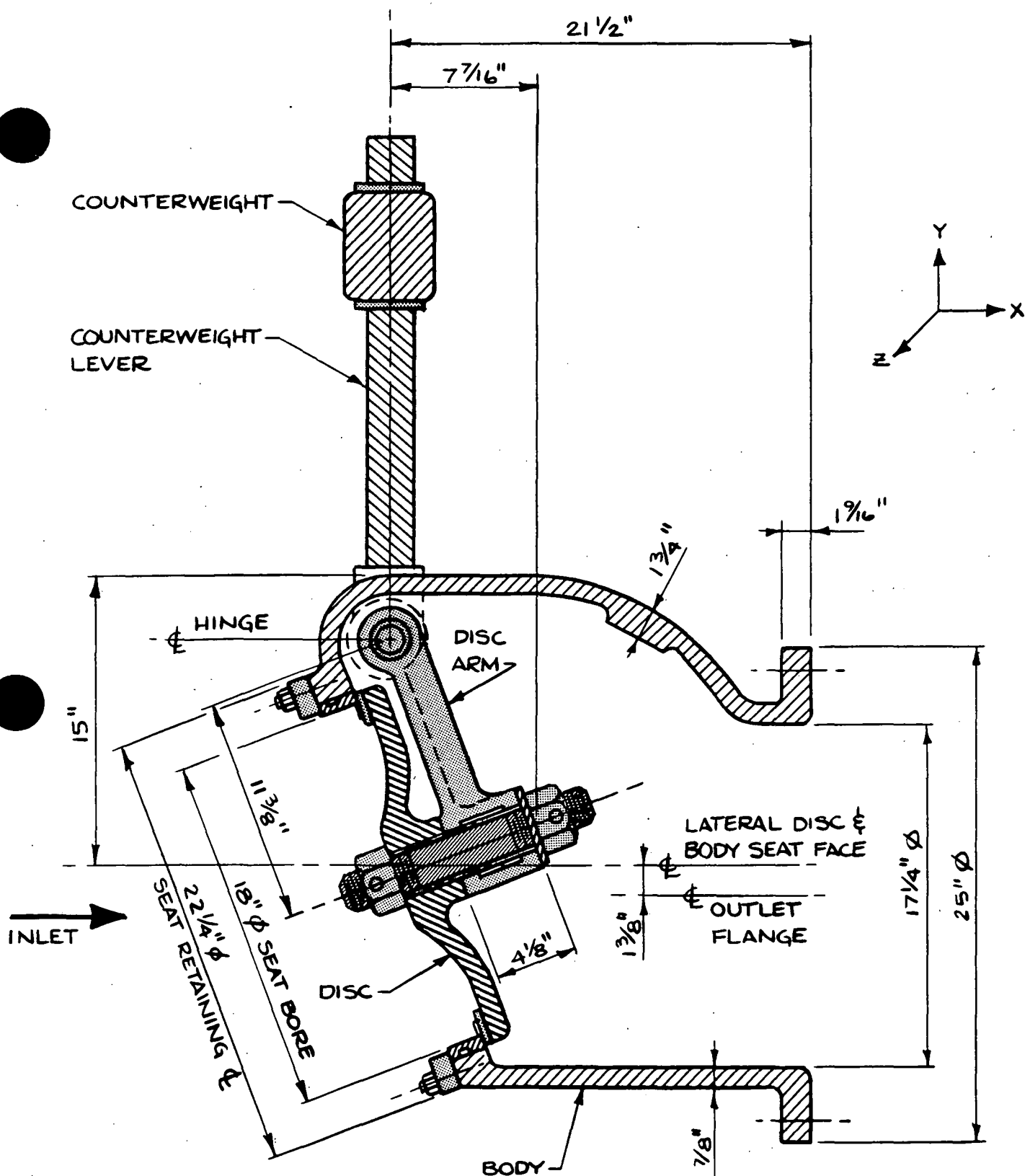


Figure 1-3. Vacuum Breaker Valve Geometry

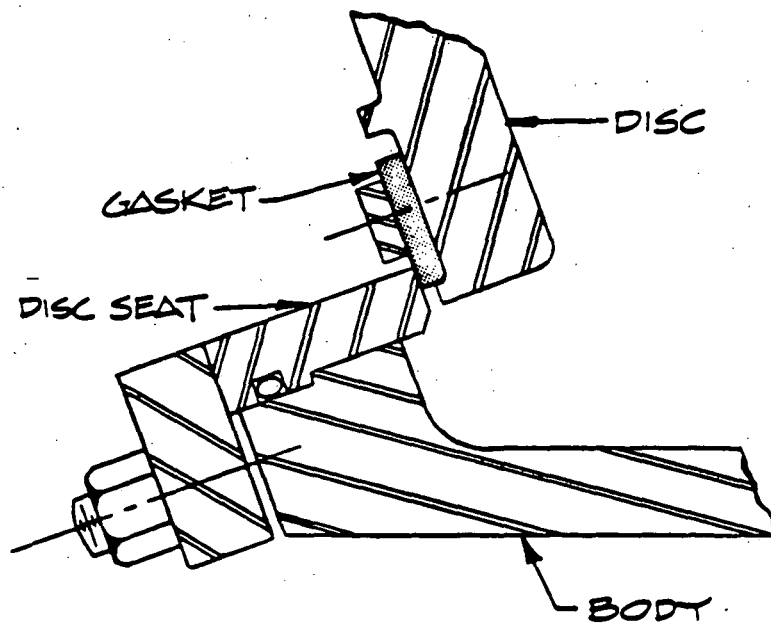


Figure 1-4. Vacuum Breaker Valve Seat Details

COM-08-023
Revision 0

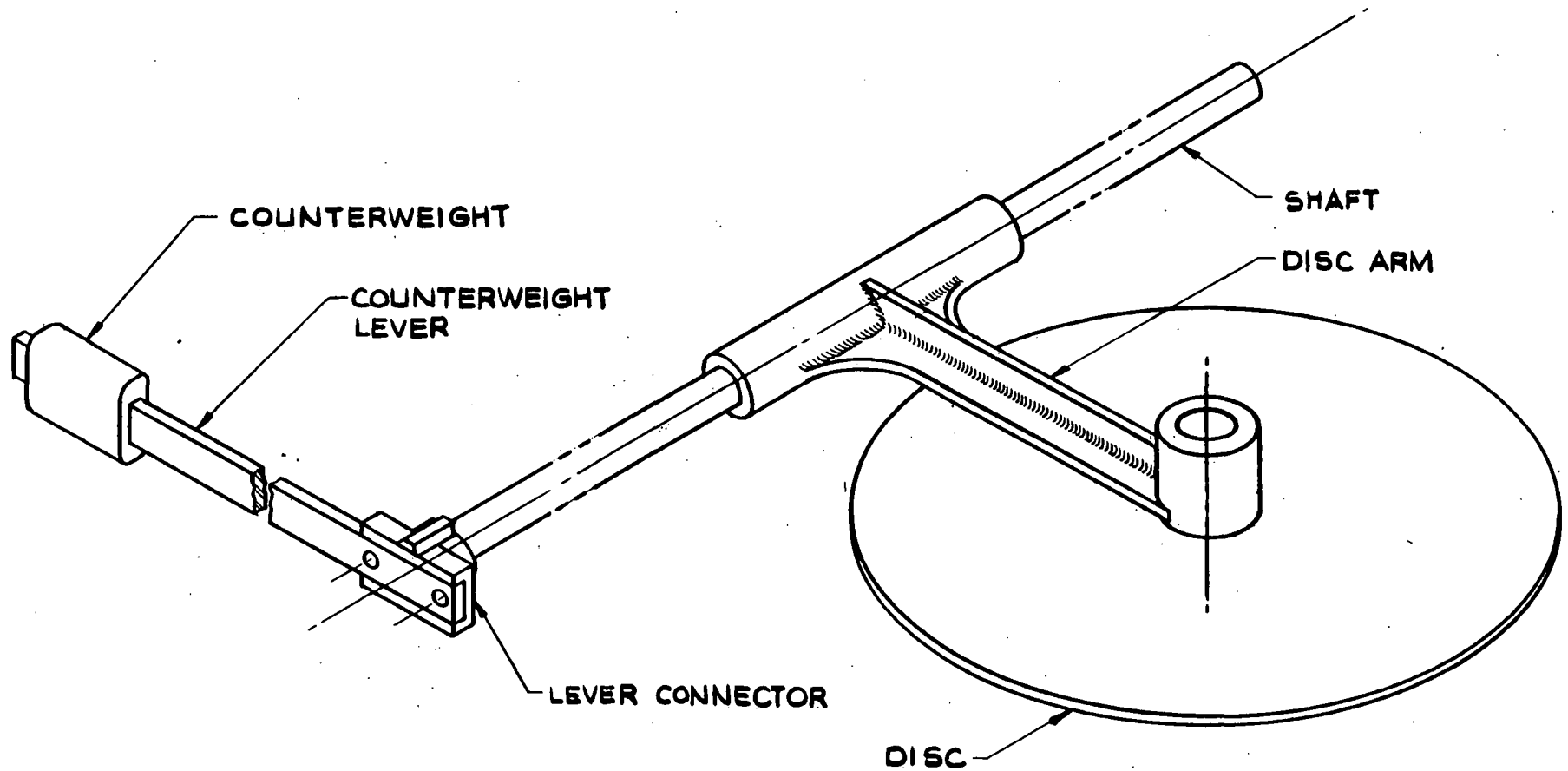


Figure 1-5. Valve Shaft and Arm Details

2.0 METHOD OF ANALYSIS

2.1 Analysis Summary

The A&M vacuum breaker valve is analyzed using the following procedure:

- a. First the moving parts of the valve are modeled as a rigid body for a single degree of freedom dynamic model (Figure 2-1). This model is used to determine the maximum impact velocities due to the design pressure loading (Figure 2-2).
- b. Second, finite element models of the disc, arms, shaft and counterweight were used to calculate the coefficients of restitution and stresses during impact. It was assumed in these models that the disc/counterweight assembly approached impact as a rigid body.
- c. Third, material properties were estimated and stress intensities were calculated scaling the stresses from the impact model corresponding to the angular velocity of impact predicted by the rigid body model.

The stress resultants from the detailed finite element models developed for the Short Term Program (References 3 and 4) are scaled to obtain the new stress resultants for the impact velocities due to the design load. Although the cast aluminum disc has been replaced by a wrought aluminum disc with a stainless steel post, the behavior of the disc during the impact is expected to vary only slightly so that the detailed finite element analysis results from the Short Term Program are still valid. This approach is considered effective.

The stress intensities are calculated from the stress resultants and compared to ASME Code allowables.

2.2 Discussion of Assumptions

It was assumed that the coefficient of restitution was independent of impact velocity. This is an exact relation of linear elastic systems, and is a valid assumption for systems, such as vacuum breakers, which represent only small departures from linearity.

It was also assumed that stress is a linear function of impact velocity. This assumption can be shown to be conservative by the following analysis of a single degree of freedom system.

Since the total energy remains constant, the kinetic energy just before impact is equal to the potential (strain) energy during impact when the velocity is zero:

$$KE = 1/2 MV^2 = PE = 1/2 K \cdot \delta^2$$

where: K = stiffness
 δ = displacement

Furthermore:

$$\text{load} = K \cdot \delta$$

$$\text{stress} = \sigma = \text{constant} \times \text{load} = C \cdot K \cdot \delta$$

Solving for displacement:

$$\delta = \frac{\sigma}{CK}$$

Substituting this displacement into the energy equations:

$$1/2 MV^2 = 1/2 K \frac{\sigma^2}{C^2 K^2}$$

Solving for stress yields:

$$\sigma = CV (KM)^{0.5}$$

Therefore, for a simple linear elastic system, the stress is linear with velocity. During impact, the vacuum breaker has an increasing stiffness as the disc first contacts the gasket and then the metal. The resulting stress versus velocity would be non-linear as shown in Figure 2-4. But, if a high impact velocity is used for the stress calculation, it is conservative to interpolate linearly back to zero.

The validity of this assumption was further checked by analyzing the impact of the valve at two impact velocities. The displacement results of these analyses are presented in Figures 2-5 and 2-6. It was found that there was a negligible departure from linearity.

2.3 Rigid Body Dynamics Model

The analytical model used for the rigid body dynamics analysis treats the moving parts of a valve as a single degree of freedom system rotating about a pivot point at the shaft location. The mass and mass moment of inertia about the centroid of each of the rotating components, (disc, arms, counterweights and shafts) were

lumped at the centroids which were connected to the shaft by rigid mass-less links. A computer program was set up to solve the equations of motion for the model oscillating between two specified stopping positions (the seat and the body impacts). A coefficient of restitution was imposed at each impact location. The load definitions were incorporated as digitized pressure loading tables. The program provided print and plot results of the rotational time history of the system, including angular rotation, angular velocity, angular acceleration, and pressure load on the disc.

The valve disc assembly and the force system acting on it are shown in Figure 2-7 for the valve. The motion of the disc assembly about the shaft axis is given by:

$$T = I \ddot{\alpha}$$

and

$$T = -W L_w \sin (\alpha_w + \alpha) + A_D L_D \Delta p \cos (\alpha) - K \alpha$$

combining yields:

$$-W L_w \sin (\alpha_w + \alpha) + A_D L_D \Delta p \cos (\alpha) - K \alpha = I \ddot{\alpha}$$

where

A_D	=	area of the disc
I	=	mass moment of inertia of the disc & counterweight assembly
L_D	=	moment arm from center of the disc pressure area to the pivot point
L_W	=	moment arm from center of gravity of the disc and counterweight assembly to the pivot point
T	=	total torque acting on the disc and counterweight assembly
W	=	total weight of the disc and counterweight assembly
α	=	angular displacement of the disc assembly
α_w	=	at rest (initial) angle of the center of gravity of the assembly from the vertical plane
$\ddot{\alpha}$	=	angular acceleration of the disc center of gravity
$\Delta p \cos(\alpha)$	=	net pressure differential between the outside and the inside of the vacuum breaker
K	=	a torsional spring to ground

The classical fourth order Runge-Kutta method was used to solve the equation of motion numerically for the imposed differential pressure loading function.

The forcing function obtained from CDI (Group I forcing function) is the vent system pressure minus the pressure at the bottom of the downcomer. This forcing function was converted to the vacuum breaker load across the disc (Δp) as follows:

Let

P_v = vent system pressure
 P_d = pressure at bottom of downcomer
 P_w = wetwell air space pressure
ff = Group I forcing function = $P_v - P_d$
sh = submergence head = $P_d - P_w = 1.59$ psi
corresponding to 3.67 ft. submergence head

Then,

Δp = vacuum breaker load across the disc
= $P_w - P_v$
= $-P_d + P_w - P_v + P_d$
= $-(P_d - P_w) - (P_v - P_d)$
= $-sh - ff$

The rigid body properties of the valve are presented in Table 2-1.

Table 2-1
Rigid Body Model Properties

Property (units)	A&M 18" Internal Valve
A_D (in^2)	283.53
L_D (in)	11.375
I ($\text{lb-sec}^2\text{-in}$)	55.65
W (lbs)*	108.54
α_{LB} (deg)**	20.0
α_{UB} (deg)**	65.0

NOTE:

* W is the total weight of the moving parts (disc assembly, counterweight arm and counterweight)

** α_{LB} and α_{UB} are the angular displacements of the disc assembly in the fully closed and fully open position (see Figure 2-7).

2.4 Impact and Stress Models

Finite element impact model of the entire valve was used to study the seat (valve fully closed) impact phenomena. This model is illustrated in Figure 2-8. The model was made up of axisymmetric, isoparametric finite elements; plate and shell elements; beam, mass and spring elements; and non-linear gap elements (which can support compressive loading but had no tensile capacity) to model the impact surfaces. This model was used to conduct non-linear, time-history analyses of the impact event using a general purpose finite element computer program (ANSYS). The general modeling philosophy was to use extremely fine detail in the vicinity of the impact point to accurately describe the local deformation of the impact surfaces.

Decreasing refinement was used with increasing distance from the impact point, as the objective in these regions was to obtain displacement time histories for input to more detailed stress models.

Detailed finite element stress models were used to calculate the stresses in the disc, shaft, counterweight and disc arm in the vacuum breaker valve.

Linear elastic material behavior was assumed for all elements except gap elements. Thus, with the exception of the gap

elements, the analyses were linear. Although some plasticity is expected in the immediate vicinity of impact, the material in these regions is expected to cyclically harden after the first few impacts such that linear behavior would occur thereafter.

Dynamic response from the impact and stress models were assumed to scale linearly with impact velocity as discussed previously.

The coefficient of restitution is the ratio of the velocity after impact to the velocity before impact. The angular velocity corresponding to the rigid body momentum of the assembly was used. The approach angular velocity was known since it was an input to the impact analysis. The angular velocity of the assembly after the impact was calculated from the principle of conservation of angular momentum as follows:

$$\overline{J\omega} = \sum_{i=1}^n J_i \omega_i$$

or

$$\omega = \frac{\sum J_i \omega_i}{\sum J_i} = \frac{\sum M_i r_i V_i}{\sum M_i r_i^2}$$

where

\overline{J} = total mass moment of inertia

$\bar{\omega}$ = average rigid body angular velocity
 M = mass
 r = radius from mass to axis of rotation
 V = linear velocity
 Σ = summation extends over all masses (i) in the disc counterweight assembly

More details of the impact and stress models and results are presented in Appendix B.

2.5 Material Properties

The vacuum breaker drawings received from Atwood & Morrill for some components did not contain sufficient material callouts to specifically identify the material type and grade used. In most cases, generic terms such as "steel" or "cast aluminum" were called out with no additional descriptive information. Therefore, it was necessary to apply metallurgical engineering judgement regarding typical valve component materials considering the time the vacuum breakers were manufactured.

The results of this effort are presented in Table 2-2. Standard material specifications for each component are listed in the second column of this table. Where the word "assume" does not appear in the table (such as for the shaft) then the material specification listed was actually indicated on the drawing.

Table 2-2

**Attwood & Morrill Valve Material Properties Summary
(Most Probable Values)**

Part Name	Material Specification	Yield Stress (ksi)	Ultimate Tensile Stress (ksi)
Weight Lever	Steel (<u>assume</u> AISI 1008 or AISI 1018)	24.0	45.0
Lever Connector	Cast Steel, ASTM A-216 Gr. WCB	36.0	70.0
Weight Lever Bolts	Steel (<u>assume</u> A-193, Gr. B7)	105.0	125.0
Keys (Shaft-Lever Connector, Disc Arm)	Steel AISI 1095	139.0	154.0
Shaft	Stainless Steel, Type 410	40.0	75.0
Disc Arm	Cast Steel A-352, Gr. LCB	35.0	65.0
Disc	Wrought Aluminum	40.0	45.0
Disc Seat	Ethylene Propylene (<u>assume</u> Parker E692-75)	---	1.23
Retaining Ring & Screws	Aluminum (<u>assume</u> annealed 1100 or cold worked 2024)	22.0	34.0
Body Ring	Stainless Steel Type 304	35.0	85.0
Seat Retaining Plate	Steel A-300, CL. 1	30.0	55.0
Seat Retaining Plate Bolts & Nuts	Steel A-193, Gr. B7	105.0	125.0
Body	Cast Steel A-352 <u>assume</u> Gr. LCB	35.0	65.0

2.6 Load Combination

The Design Specification (Reference 5) lists the design requirements for vacuum breaker replacement parts. The valve is analyzed for chugging, pool swell, seismic and SRV loads.

The eleven load combinations given in Table 5.2-1 (the design specification) when combined with Section 5.1.4 of the design specification (Reference 5) can be reduced to the eight load combinations described in Table 2-3 below. The safety relief valve discharge loads are negligible.

Table 2-3
Load Combinations

Service Level (ASME)		A			B			C	
Combination Number		1	2	3	4	5	6	7	8
Load		X	X	X	X	X	X	X	X
Pressure (psid)	Chugging 15 to 32								
Seismic	OBE SSE			X	X	X	X	X	X
Pool Swell			X			X			X

Also knowing that chugging causes the worst loads and stress on valve components and the seismic loads alone are insignificant (0.3g horizontal and 0.08g vertical, corresponding to SSE), the eight load combinations of Table 2-3 can be reduced to six load combinations described in Table 2-4, below.

Table 2-4
Revised Load Combinations

Service Level		A		B		C	
Combination Number		1	2	3	4	5	6
Load		X	X	X	X	X	X
Pressure (psid)	Chugging 15 to 32						
Seismic	OBE			X	X		
	SSE					X	X
Pool Swell			X		X		X

Stresses are calculated for each of these six load combinations and results are presented in Section 3.0.

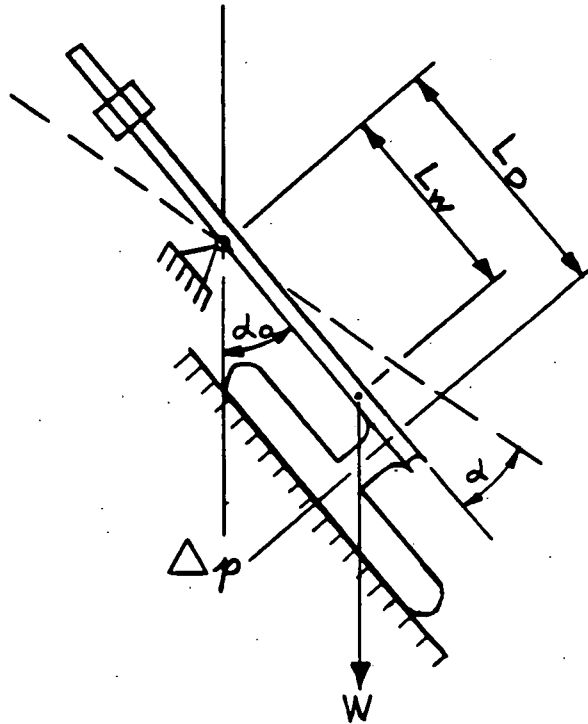


Figure 2-1. Single Degree of Freedom Model

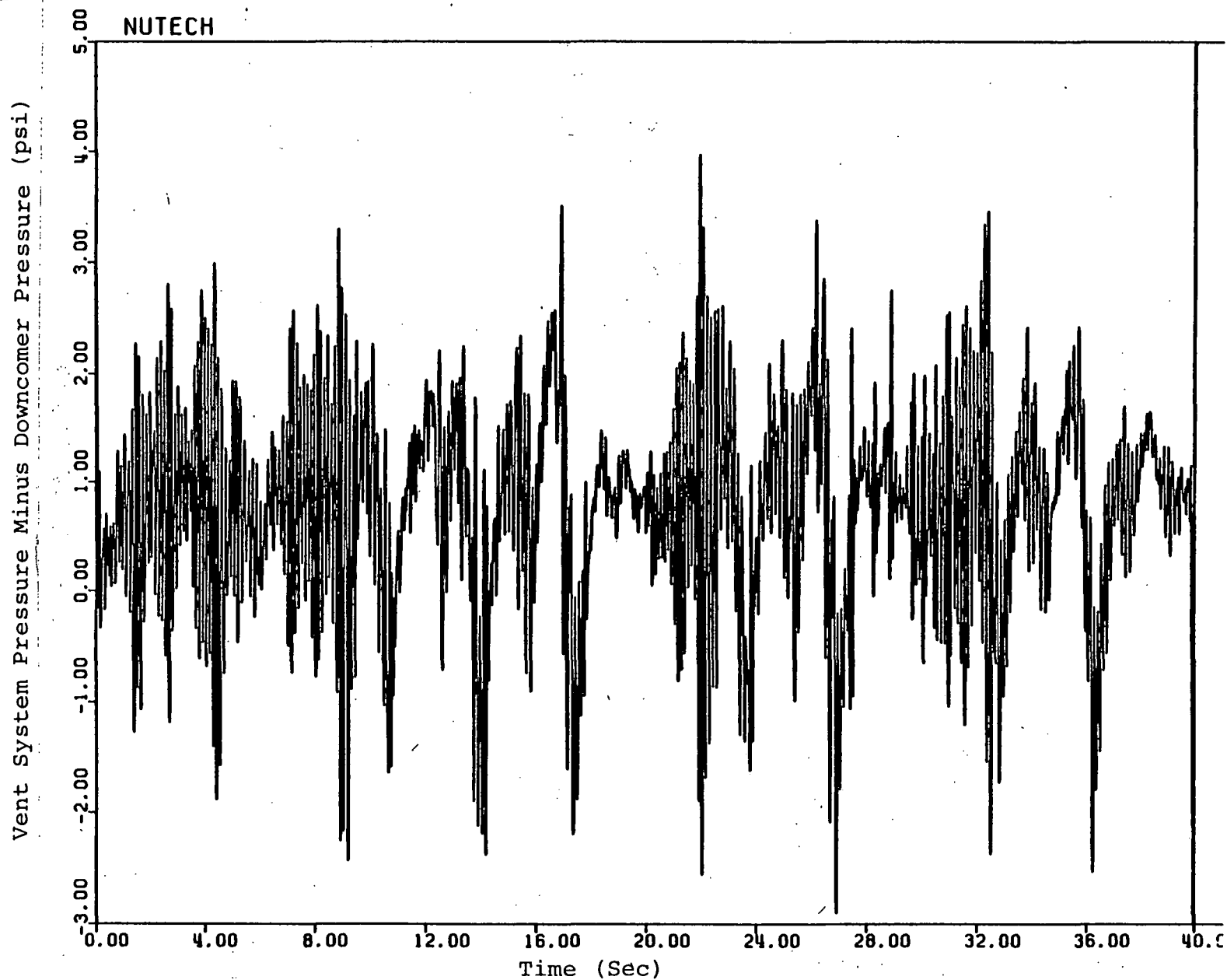


Figure 2-2. Group I Forcing Function (Pressure Loading Definition)

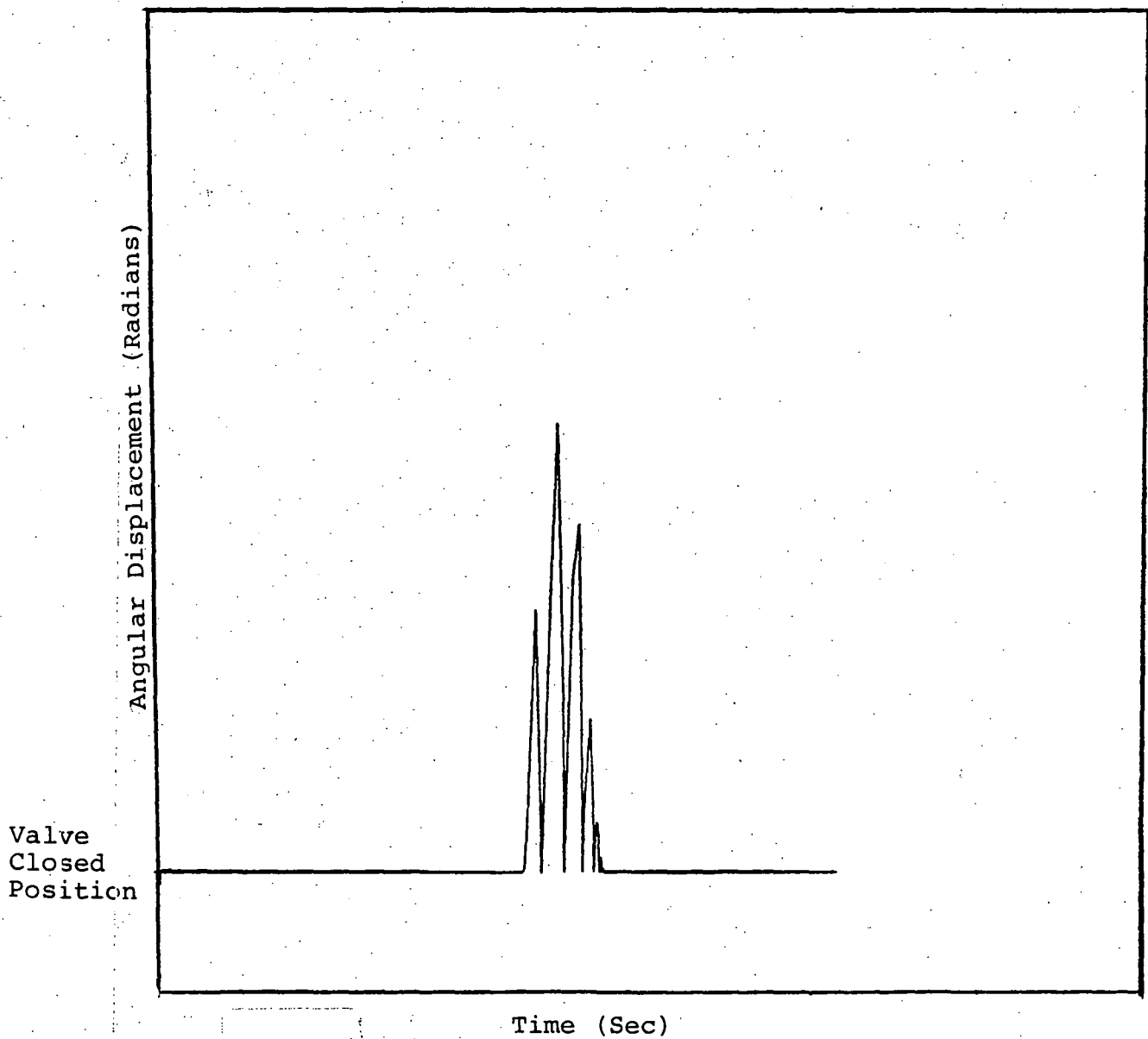


Figure 2-3. Typical Valve Response

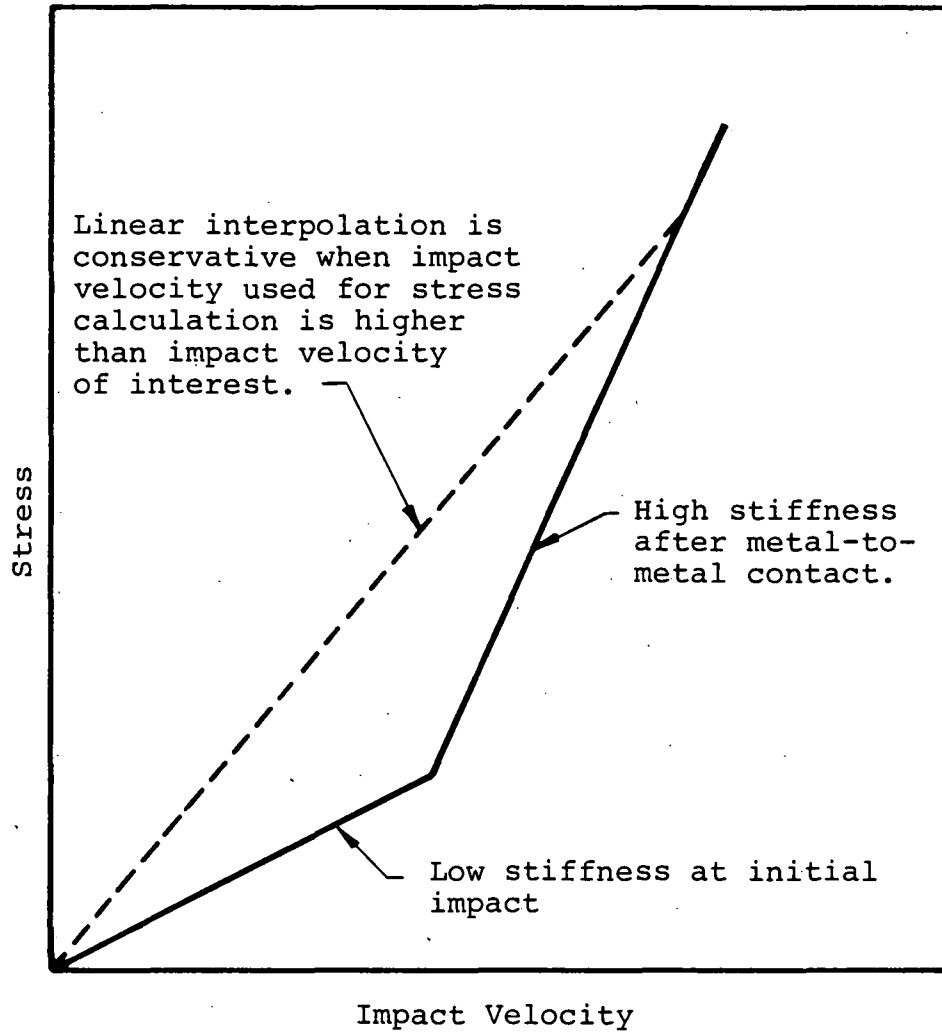


Figure 2-4. Linearity of Stress with Impact Velocity

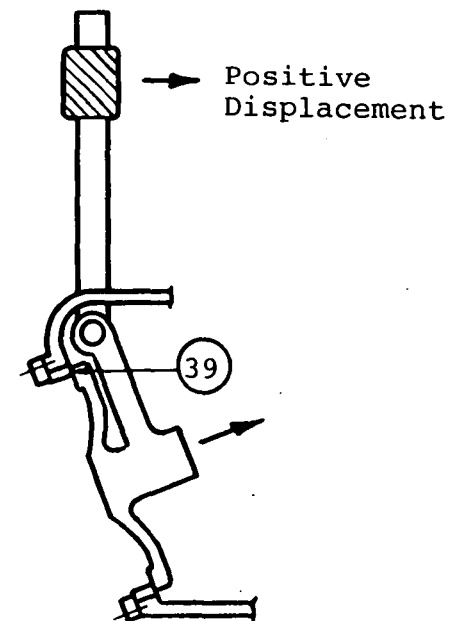
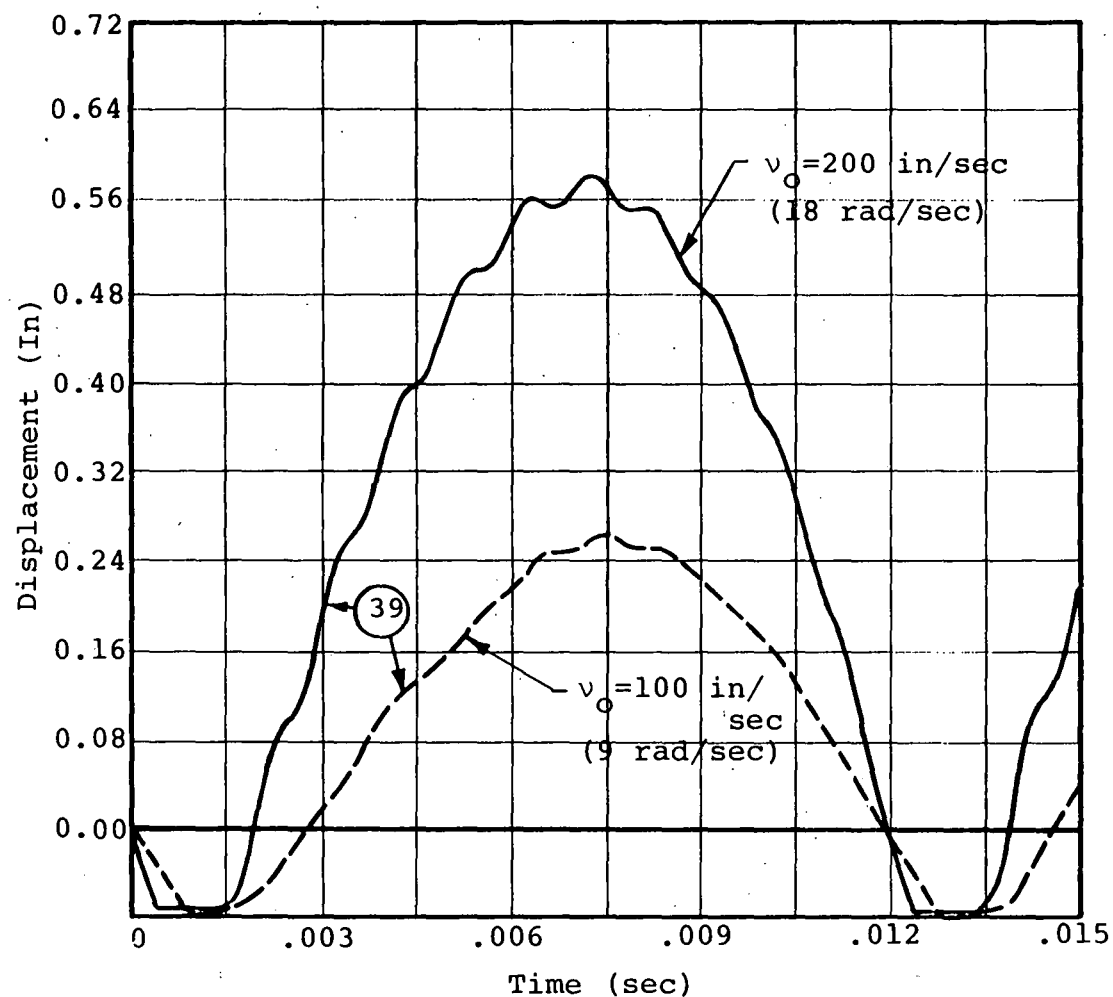


Figure 2-5. Valve Closing Impact Model Results: Comparison of 100 in/sec and 200 in/sec Initial Approach Velocity

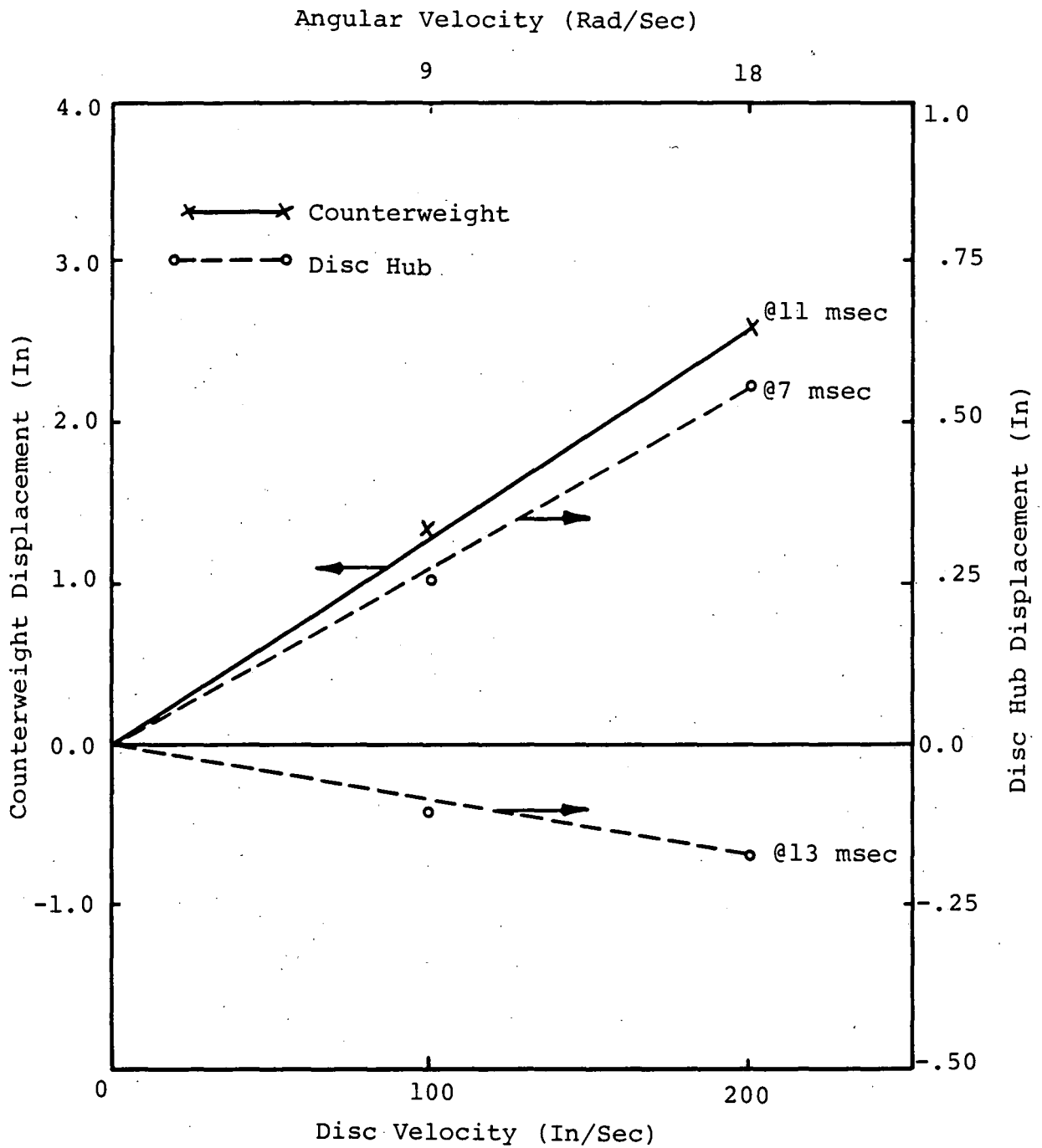


Figure 2-6. Valve Closing Impact Model Results: Initial Velocity Linearity Check

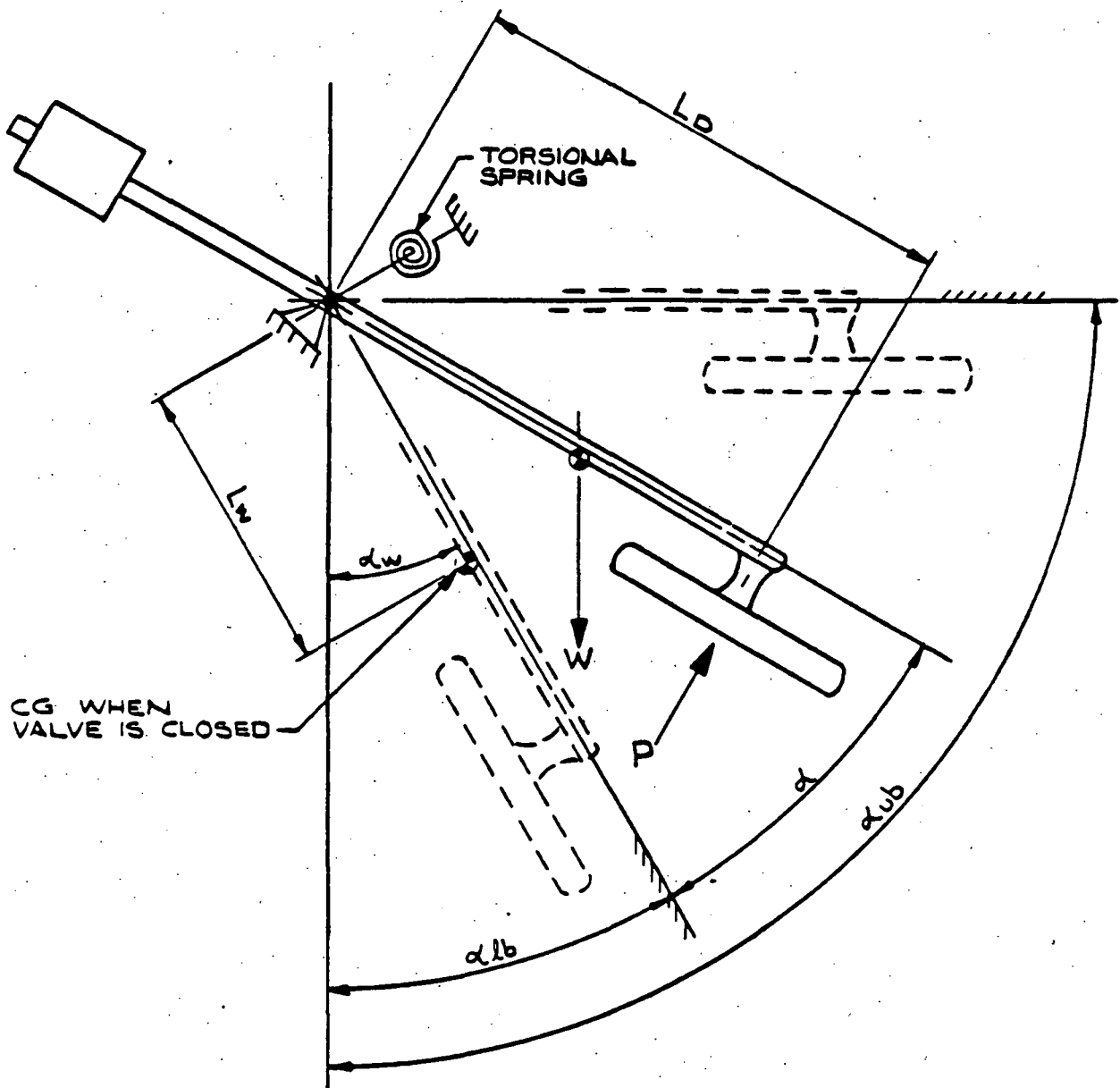


Figure 2-7. Valve Disc Assembly and Force System

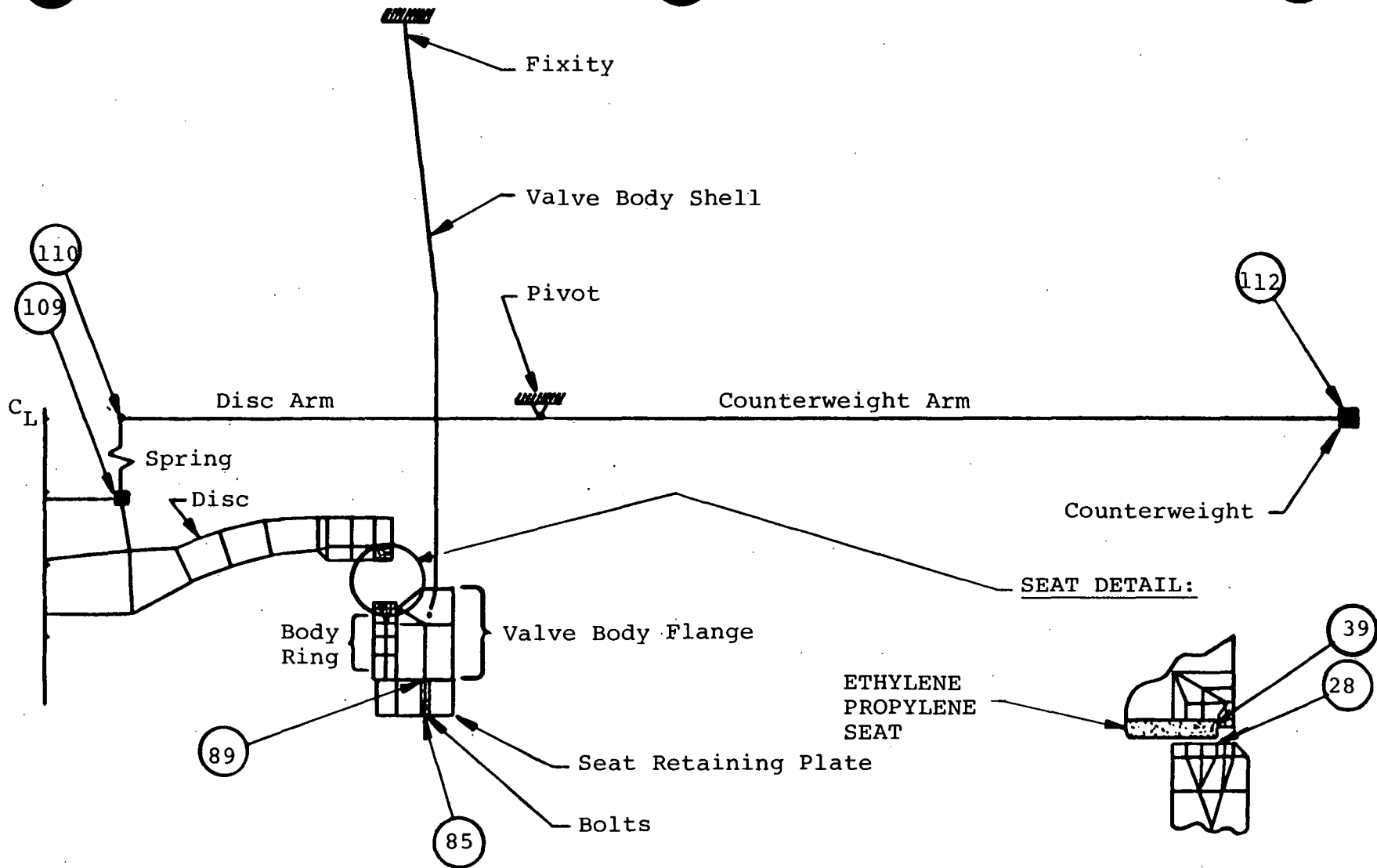


Figure 2-8. Valve Closing Impact Model

3.0 RESULTS

3.1 Dynamic Analysis Results

Dynamic analysis of the vacuum breaker was carried out using the method of analysis described in Section 2.3. A number of cases were run using NUTECH proprietary computer program DISCO for the chugging load and the loads associated with earthquakes.

Since the valve disc chatters during chugging, the maximum velocities for load combination cases 1, 3 and 5 (chugging, chugging plus OBE seismic and chugging plus SSE seismic), as given in Table 2-4, are obtained as follows.

The maximum valve opening due to the design chugging load is 7.18 degrees, which also coincides with the opening angle resulting in maximum seat impact velocity. There are no upper (body) impacts. The resultant seismic coefficient is assumed to act at the center of gravity (C.G.) of the moving components at the instant of time at which the valve is in the maximum opening position due to chugging. Since the DISCO computer program does not have the option of using seismic coefficients directly, the resulting torque at the shaft C.G. is converted into an equivalent pressure differential (Δp) at the disc. This Δp is

then used in DISCO in the closing direction with valve initial angle at 7.5 degrees open.

Also, since DISCO applies an additional load due to gravity (lg) with each applied load case, a third run is made applying only the gravity load (free fall) with valve initially at 7.5 degrees and resulting impact velocity is obtained.

From these results, the impact velocity due to combined (seismic plus chugging) loading is obtained in the following manner. It should be noted, it is also very unlikely that the two events would occur at the same time and at the worst possible time corresponding to the peak chugging (closing) load. Hence, this method is conservative.

$$\begin{aligned} \dot{\alpha}_{\max} \text{ (Due to chugging} &= \dot{\alpha}_{\max} \text{ (chugging)} \\ &+ \text{ seismic)} &+ \dot{\alpha}_{\max} \text{ (seismic)} \\ & &- \dot{\alpha}_{\max} \text{ (free fall)} \end{aligned}$$

where

$\dot{\alpha}$ is the impact velocity.

The details of the analysis are given in Appendix B (B.1).

The results of the various cases run are tabulated in Table 3-1.

Table 3-1
Maximum Impact Velocities

Maximum Impact Velocity	Chugging	Chugging + Seismic (OBE)	Chugging + Seismic (SSE)
$\dot{\alpha}_{\max}$ (seat) rad/sec	4.631	4.831	5.006
$\dot{\alpha}_{\max}$ (body) rad/sec	--	--	--

-- no upper (body) impact occurred.

3.2 Stress Analysis

The stresses were calculated for the six load combination cases as described in Table 2-4. Since load cases 1, 3 and 5 affect the moving parts of the valve, stresses for these load cases are calculated using computer program DISCO for dynamic analysis and ANSYS finite element program for stress analysis. The results of these analyses are presented in Section 3.2.1.

Load combination cases 2, 4 and 6 are treated as static loads and stresses are calculated at valve attachment points (vacuum breaker mounting bolts) as described in Section 3.2.2.

3.2.1 Stresses in the Valve Components

The new loads (bending moment, shear and torsion) on valve components for load combination cases 1, 3 and 5 (as given in Table 2-4) are obtained by scaling the results of a similar analysis performed for the Short Term Program (References 3 and 4). The method of analysis is described in Section 2.4 and the details of the analysis are described in Appendix B (B.2 and B.3). The stress intensities were calculated and compared with ASME Code allowables. Stress Intensity for each load case is compared with allowable stress intensity for the appropriate Service Level.

The results of this analysis are tabulated in Tables 3-2, 3-3 and 3-4.

Table 3-2 (a)

Stresses In The Vacuum Breaker Components For Closing Impact Velocity Of 4.631 Radians/Second
(Chugging Load) - Service Level A (K = 1.0)

PART NAME	MATERIAL SPECIFICATION			PRIMARY MEMBRANE STRESS INTENSITY* (KSI)			PRIMARY LOCAL STRESS INTENSITY* (KSI)			MEMBRANE + BENDING STRESS INTENSITY* (KSI)			REMARKS
	MATERIAL	σ_y (KSI)	σ_u (KSI)	CALCULATED P_M	ALLOWABLE = $K S_M$		CALCULATED P_L	ALLOWABLE=1.5K S_M		CALCULATED $(P_M \text{ or } P_L) + P_b$	ALLOWABLE=1.5K S_M		
					ROOM TEMP.	300°F		ROOM TEMP.	300°F		ROOM TEMP.	300°F	
Shaft	Stainless Steel, Type 410	40	75	0.00	25.0	21.7	0.00	37.5	32.5	49.24	37.5	32.5	Original Material (67)
	ASTM A-564, Gr. 630 age hardened at 1100°F	115	140	0.00	46.7	46.7	0.00	70.0	70.0	49.24	70.0	70.0	Recommended replacement in 1981
Weight Lever	Steel, Assume AISI 1008 or 1018	24	45	1.96	15.0	14.2	1.96	22.5	21.3	31.90	22.5	21.3	Original Material
	ASTM A-564, Gr. 630 age hardened at 1100°F	115	140	1.96	46.7	46.7	1.96	70.0	70.0	31.90	70.0	70.0	Recommended replacement in 1981
Lever Connector	Cast Steel ASTM A216, Gr. WCB	36	70	1.58	23.3	21.3	1.58	35.0	31.95	15.67	35.0	31.95	
Disc Arm	Cast Steel A-352, Gr. LCB	35	65	1.86	21.7	20.7	1.86	32.5	31.05	30.80	32.5	31.05	
Disc	Wrought Alum. 6061-T651	40	45	1.79	15.0	11.1	1.79	22.5	16.6	10.49	22.5	16.6	
Disc Seat	Ethylene Propylene Parker, E692-75	--	1.23	0.23	N/A	N/A	0.23	N/A	N/A	0.23	N/A	N/A	σ_c only
Disc Seat Retaining Ring	Aluminum Assume			0.00	11.3	9.4	0.00	17.0	14.1	2.82	17.0	14.1	σ_b only
Disc Seat Retaining Ring Screws	Annealed 1100 or Cold Worked 2024	22	34	3.04	11.3	9.4	3.04	17.0	14.1	3.04	17.0	14.4	σ_t only
Body Ring	Stainless Steel, TP 304	30	75	1.71	23.3	22	1.71	35.0	33.0	1.71	35.0	33.0	σ_M only
Seat Retaining Plate	Steel A-300, CLI	30	55	0.00	18.3	17.7	0.00	27.4	26.6	1.67	27.4	26.6	σ_b only
Body	Cast Steel A-352 Assume Gr. LCB	35	65	0.93	21.7	20.7	0.93	32.5	31.05	0.93	32.5	31.05	σ_M only

S_M - Design Stress Intensity, N/A - not applicable

*Per ASME B&PV Code, Sec. III, Subsection NC for Class 2 Components, 1977 Ed. through Summer 1977 Addenda

Table 3-2 (b)

Stresses In The Bolts And Keys For Closing Impact Of 4.631 Radians/Second

PART NAME	MATERIAL SPECIFICATION			CALCULATED STRESS (KSI)	ALLOWABLE STRESS (KSI) FOR BOLTS, ALLOWABLE = $2S_M$ FOR KEYS, ALLOWABLE = S_y	REMARKS
	MATERIAL	σ_y (KSI)	σ_u (KSI)			
Weight Levers Bolts	Assume A-193, Gr. B7	105	125	30.10	70.0	Recommend Replacement
Keys (Shaft - Disc Arm, Lever Connector)	AISI 1095	139	154	59.18	139.0	
Seat Retaining Plate Nuts & Bolts	A-193, Gr. B7	105	125	7.36	70.0	

Table 3-3 (a)

Stresses In The Vacuum Breaker Components For Closing Impact Velocity Of 4.831 Radians/Second
(Chugging + OBE) - Service Level B (K = 1.1)

PART NAME	MATERIAL SPECIFICATION			PRIMARY MEMBRANE STRESS INTENSITY* (KSI)			PRIMARY LOCAL STRESS INTENSITY* (KSI)			MEMBRANE + BENDING STRESS INTENSITY* (KSI)			REMARKS
	MATERIAL	σ_y	σ_u	CALCULATED P_M	ALLOWABLE = $K S_M$		CALCULATED P_L	ALLOWABLE=1.5 $K S_M$		CALCULATED $(P_M \text{ or } P_L) + P_b$	ALLOWABLE=1.5 $K S_M$		
		(KSI)	(KSI)		ROOM TEMP.	300°F		ROOM TEMP.	300°F		ROOM TEMP.	300°F	
Shaft	Stainless Steel, Type 410	40	75	0.00	27.5	23.9	0.00	41.3	35.8	51.37	41.3	35.8	Original Material (67)
	ASTM A-564, Gr. 630 age hardened at 1100°F	115	140	0.00	51.4	51.4	0.00	77.0	77.0	51.37	77.0	77.0	Recommended Replacement in 1981
Weight Lever	Steel, Assume AISI 1008 or 1018	24	45	2.04	16.5	15.6	2.04	24.5	23.4	33.28	24.5	23.4	Original Material
	ASTM A-564, Gr. 630 age hardened at 1100°F	115	140	2.04	51.4	51.4	2.04	77.0	77.0	33.28	77.0	77.0	Recommended replacement in 1981
Lever Connector	Cast Steel ASTM A-216, Gr. WCB	36	70	1.65	25.6	23.4	1.65	38.5	35.2	16.35	38.5	35.2	
Disc Arm	Cast Steel A-352, Gr. LCB	35	65	1.94	23.9	22.8	1.94	35.8	34.2	32.13	35.8	34.2	
Disc	Wrought Alum. 6061-T651	40	45	1.87	16.5	12.2	1.87	24.8	18.3	10.94	24.8	18.3	
Disc Seat	Ethylene Propylene Parker, E692-75	--	1.23	0.24	N/A	N/A	0.24	N/A	N/A	0.24	N/A	N/A	σ_c only
Disc Seat Retaining Ring	Aluminum Assume Annealed	22	34	0.00	12.4	10.3	0.00	18.7	15.5	2.94	18.7	15.5	σ_b only
Disc Seat Retaining Ring Screws	Annealed 1100 or Cold Worked 2024			3.17	12.4	10.3	3.17	18.7	15.5	3.17	18.7	15.5	σ_t only
Body Ring	Stainless Steel, TP 304	30	75	1.78	25.6	24.2	1.78	38.5	36.3	1.78	38.5	33.0	σ_M only
Seat Retaining Plate	Steel A-300, CLI	30	55	0.00	20.1	19.5	0.00	30.1	29.2	1.74	30.1	29.2	σ_b only
Body	Cast Steel A-352 Assume Gr. LCB	35	65	0.97	23.9	22.8	0.97	35.8	34.2	0.97	35.8	34.2	σ_M only

S_M - Design Stress Intensity, N/A - not applicable

*Per ASME B&PV Code, Sec. III, Subsection NC for Class 2 Components, 1977 Ed. through Summer 1977 Addenda

COM-08-023
Revision 0

3-8

Table 3-3 (b)

Stresses In The Bolts And Keys For Closing Impact Of 4.831 Radians/Second

PART NAME	MATERIAL SPECIFICATION			CALCULATED STRESS (KSI)	ALLOWABLE STRESS (KSI) FOR BOLTS, ALLOWABLE = $2S_H$ FOR KEYS, ALLOWABLE = S_y	REMARKS
	MATERIAL	σ_y (KSI)	σ_u (KSI)			
Weight Lever Bolts	<u>Assume</u> A-193, Gr. B7	105	125	31.40	70.0	Recommend Replacement
Keys (Shaft - Disc Arm, Lever Connector)	AISI 1095	139	154	56.52	139.0	
Seat Retaining Plate Nuts & Bolts	A-193, Gr. B7	105	125	7.68	70.0	

Table 3-4 (a)

Stresses In The Vacuum Breaker Components For Closing Impact Velocity Of 5.006 Radians/Second
(Chugging + SSE) - Service Level C (K = 1.2)

PART NAME	MATERIAL SPECIFICATION			PRIMARY MEMBRANE STRESS INTENSITY* (KSI)			PRIMARY LOCAL STRESS INTENSITY* (KSI)			MEMBRANE + BENDING STRESS INTENSITY* (KSI)			REMARKS
	MATERIAL	σ_y (KSI)	σ_u (KSI)	CALCULATED P_M	ALLOWABLE = $K S_M$		CALCULATED P_L	ALLOWABLE=1.5 $K S_M$		CALCULATED $(P_M \text{ or } P_L) + P_b$	ALLOWABLE=1.5 $K S_M$		
					ROOM TEMP.	300°F		ROOM TEMP.	300°F		ROOM TEMP.	300°F	
Shaft	Stainless Steel, Type 410	40	75	0.00	30.0	26.0	0.00	45.0	39.0	53.23	45.0	39.0	Original Material (67)
	ASTM A-564, Gr. 630 age hardened at 1100°F	115	140	0.00	56.0	56.0	0.00	84.0	84.0	53.23	84.0	84.0	Recommended replacement in 1981
Weight Lever	Steel, Assume AISI 1008 or 1018	24	45	2.12	18.0	17.0	2.12	27.0	25.5	34.48	27.0	25.5	Original Material
	ASTM A-564, Gr. 630 age hardened at 1100°F	115	140	2.12	56.0	56.0	2.12	84.0	84.0	34.48	84.0	84.0	Recommended replacement in 1981
Lever Connector	Cast Steel ASTM A-216, Gr. WCB	36	70	1.71	28.0	25.6	1.71	42.0	38.3	16.94	42.0	38.3	
Disc Arm	Cast Steel A-352, Gr. LCB	35	65	2.01	26.0	24.8	2.01	39.0	37.26	33.29	39.0	37.3	
Disc	Wrought Alum. 6061-T651	40	45	1.93	18.0	15.8	1.93	27.0	23.7	11.34	27.0	23.7	
Disc Seat	Ethylene Propylene Parker E692-75	--	1.23	0.25	N/A	N/A	0.25	N/A	N/A	0.25	N/A	N/A	σ_c only
Disc Seat Retaining Ring	Aluminum Assume Annealed 1100			0.00	13.6	11.3	0.00	20.4	16.9	3.05	20.4	16.9	σ_b only
Disc Seat Retaining Ring Screws	or Cold Worked 2024	22	34	3.29	13.6	11.3	3.29	20.4	16.9	3.29	20.4	16.9	σ_t only
Body Ring	Stainless Steel, TP 304	30	75	1.85	28.0	26.4	1.85	42.0	39.6	1.85	42.0	39.6	σ_M only
Seat Retaining Plate	Steel A-300, CL1	30	55	0.00	22.0	21.2	0.00	32.9	31.9	1.81	32.9	31.9	σ_b only
Body	Cast Steel A-352 Assume Gr. LCB	35	65	1.01	26.0	24.8	1.01	39.0	37.3	1.01	39.0	37.3	σ_M only

S_M - Design Stress Intensity, N/A - not applicable

*Per ASME B&PV Code, Sec. III, Subsection NC for Class 2 Components, 1977 Ed. through Summer 1977 Addenda

Table 3-4 (b)

Stresses In The Bolts And Keys For Closing Impact Of 5.006 Radians/Second

PART NAME	MATERIAL SPECIFICATION			CALCULATED STRESS (KSI)	ALLOWABLE STRESS (KSI) FOR BOLTS, ALLOWABLE = $2S_M$ FOR KEYS, ALLOWABLE = S_y	REMARKS
	MATERIAL	σ_y (KSI)	σ_u (KSI)			
Weight Lever Bolts	Assume A-193, Gr. B7	105	125	32.54	70.0	Recommend Replacement
Keys (Shaft - Disc Arm, Lever Connector)	AISI 1095	239	154	58.57	139.0	
Seat Retaining Plate Nuts & Bolts	A-193, Gr. B7	105	125	7.96	70.0	

COM-08-023
Revision 0

3-11

3.2.2 Valve Attachment Point Stresses

Loads on the vacuum breaker mounting bolts due to pool swell impact and drag on the vent header, vent deflector, downcomer miter and vent system thrust are given in the Design Specification (Reference 5) in the form of response spectra for an assumed vacuum breaker weight of 1000 lbs and c.g. location at 15" from vacuum breaker nozzle. The peak spectral acceleration and the loads acting on the valve attachment point are proportional to its mass. Being unable to get an accurate weight of the vacuum breaker from the manufacturer (Atwood & Morrill), an approximate weight was calculated to be 725 lbs. Therefore, conservatively, a vacuum breaker weight of 1000 lbs was used in the load calculation.

The forces acting on the vacuum breaker at its center of gravity are obtained by multiplying the mass of the vacuum breakers by peak spectral accelerations in the applicable direction.

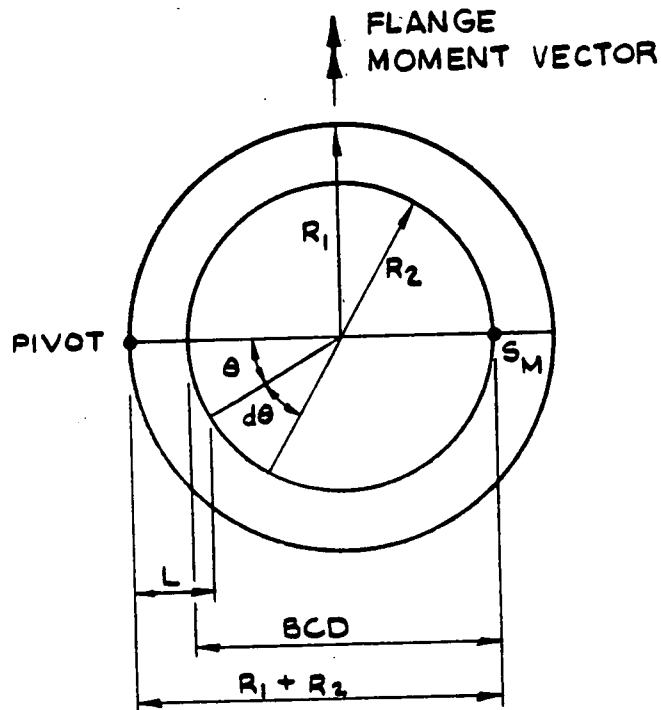
A maximum pressure differential of 32 psid (Reference 5) is multiplied by the surface area of the vacuum breaker mounting flange to obtain the axial forces on the bolts. Static seismic coefficients specified in Reference 5 are applied to vacuum breaker center of gravity to obtain forces and moments at the bolts.

The loads acting on the vacuum breaker mounting bolts are obtained by converting the moments into axial forces as described below:

CONVERSION OF FLANGE MOMENTS TO BOLT AXIAL FORCES

The following assumptions are made in order to convert flange moments to bolt axial forces:

1. Concentrated moment is at the pivot
2. Axial force in the bolts varies linearly along the diameter from the pivot point and is maximum at the diametrically opposite end



where:

R_1 = outer radius of the flange
 R_2 = bolt circle radius
 θ = angle measured from diameter through pivot
 L = distance from pivot
BCD = bolt circle diameter

Let S = axial force in lb/circumferential inch
 S_m = maximum force in lb/cir-in at diametrically
opposite location from pivot
 N = number of bolts

and S is proportional to location

$$S = S_m \frac{L}{R_1 + R_2} = S_m \frac{(R_1 - R_2 \cos \theta)}{(R_1 + R_2)} \quad (1)$$

$$dM = S \cdot R_2 d\theta \cdot L \quad (2)$$

$$dM = \frac{S_m L^2 R_2 d\theta}{R_1 + R_2}$$

Total Moment M at the Flange

$$M = \int_0^{2\pi} dM = \frac{S_m R_2}{R_1 + R_2} \int_0^{2\pi} L^2 d\theta$$

$$M = \frac{S_m R_2}{R_1 + R_2} \int_0^{2\pi} (R_1^2 + R_2^2 \cos^2 \theta - 2R_1 R_2 \cos \theta) d\theta$$

$$M = \frac{S_m R_2}{R_1 + R_2} \left[R_1^2 \theta + \frac{R_2^2 \theta}{2} - 2R_1 R_2 \sin \theta + R_2^2 \sin \theta \cos \theta \right]_0^{2\pi}$$

$$M = \frac{\pi S_m \cdot R_2 (2R_1^2 + R_2^2)}{(R_1 + R_2)} \quad (3)$$

Maximum force in any bolt

$$F_{\max} = \frac{2\pi R_2 S_m}{N} \quad \text{or} \quad S_m = \frac{F_{\max} \cdot N}{2\pi R_2} \quad (4)$$

From (3) and (4)

$$M = \frac{F_{\max} (2R_1^2 + R_2^2) N}{2(R_1 + R_2)}$$

$$F_{\max} = \frac{2M (R_1 + R_2)}{N(2R_1^2 + R_2^2)} \quad (5)$$

Using equation 5 given above, the moments are converted to bolt axial forces and added to the initial axial force to get the total maximum axial force due to each loading case in any given bolt. The stresses are obtained by dividing these forces by the

bolt cross sectional area. Detail calculations are given in Appendix B and the results are presented in Table 3-5.

Table 3-5
Vacuum Breaker Mounting Bolt Stresses

Load Combination Number	Description	Bolt Tensile Stress (ksi)	Remarks
2	32 psid + pool swell	3.44	Bolt Stresses are insignificant
4	32 psid + OBE + pool swell	3.46	
6	32 psid + SSE + pool swell	3.48	

3.2.3 Comparison of Calculated Stresses to Code Allowables

The calculated stresses were compared with the allowable limits as per ASME, B & PV Code, Sec III, Subsection NC for class 2 components, 1977 Edition through Summer 1977 addenda as given in Table 3-2 through 3-4. It is observed that the existing shaft and weight lever are overstressed and hence they should be replaced with those made of stronger materials, as recommended.

4.0 CONCLUSIONS

4.1 Identification of Overstressed Components

Based on the results presented in Section 3.0 of this report it is concluded that the shaft and the weight lever are overstressed. It is, however, noted that since the material for existing weight lever is not known, the term overstressed applies to the best-estimate material assumed using metallurgical engineering judgment.

It is recommended that these valve components be replaced by components made of stronger materials (described in Section 4.2).

4.2 Material Replacement Recommendations

To assure the valves proper re-assembly and functionality with the new parts, some of the mating parts should also be replaced. These include inner and outer shaft bushings made of bushing material compatible with the new shaft material, and O-rings. Since the weight lever is to be replaced, the weight lever bolts and lever connector should be replaced as well. The disc arm keys, have a high load applied to them and due to uncertainties concerning the existing material should be replaced. Table 4-1 contains a list of the vacuum breaker parts

to be replaced and the recommended material for replacements.

Also contained in Table 4-1 is the rationale for the selection of the replacement materials.

Table 4-1

Vacuum Breaker Material Replacement Recommendations

Part Name	Existing Material			Recommended Replacement Material			Rationale for Selection of Replacement Material
	Spec. No.	Min. Yield Strength (KSI)	Min. Tensile Strength (KSI)	Spec. No.	Min. Yield Strength (KSI)	Min. Tensile Strength (KSI)	
Shaft	Steel Type 410	40	75	ASTM A564 Type 630	115	140	High Strength, Corrosion Resistance, Availability
Weight Lever	Assume AISI 1008 or 1018	35	60	ASTM A564 Type 630	115	140	High Strength, Corrosion Resistance, Availability
Weight Lever Bolts	Assume ASTM A193, Grade B7	105	125	ASTM A193, Grade B7	105	125	High Strength, Corrosion Resistance, Availability
Weight Lever Nuts	Assume ASTM A194, Grade 2H	Proof Load, 59,650 lbf	N/A	ASTM A194 Grade 2H	Proof Load, 59650 lbf	N/A	Standard nut material used with bolt replacement material
Weight Lever Washers	AISI 1020	N/A	N/A	AISI 1020	N/A	N/A	Already available at Part Fabricators' shop
Shaft Keys	AISI 1095	139	154	AISI 1095	139	154	High Strength, Already Available at part Fabricators' Shop, Used in the past in similar environment with no problems.
Shaft Bushings	Steel	N/A	N/A	ASTM A582 Type 416	N/A	N/A	Compatible with Replacement Shaft Material, Available at part Fabricators' shop
Shaft O-rings	Ethylene-Propylene	N/A	N/A	Ethylene-Propylene	N/A	N/A	Standard O-ring material, available at part fabricators' shop
Lever Connector	Cast Steel ASTM A216, Grade WCB	36	70	Cast Steel ASTM A216, Grade WCB	36	70	Adequate strength, casting already available

COM-08-023
Revision 0

4-3

5.0 DESIGN OF BLIND FLANGES

Based on a sizing analysis performed by NUTECH for Quad Cities vacuum breakers, which indicate that not all twelve vacuum breakers are needed for vacuum relief, Commonwealth Edison Company may at some point of time remove a number of vacuum breakers from the vent system. The opening between the drywell and wetwell at the vacuum breaker mounting location must be sealed off with blind flanges.

This section describes the design calculations performed for these blind flanges. Appendix XI of the ASME Boiler and Pressure Vessel Code specifically covers design of certain types of flanges. Blind flanges are not included in Appendix XI. Therefore, analysis is performed to conform to stress allowables of the ASME Code Section III, Subsection NC. The following assumptions apply for this design:

1. Since the blind flange will be bolted circumferentially at sixteen locations to the vacuum breaker mounting flange, the blind flange has been assumed to be clamped along its bolt circle.
2. The applicable loads are as given in the design specification (Reference 7).

3. Based on the dimensions of the mounting flange and the expected loading, the thickness of the blind flange is assumed to be $1\frac{1}{2}$ ". Analysis is used to verify this assumption, as described below:

From Reference 8, the vacuum breaker mounting flange dimensions are:

Outer Diameter, O.D.	= 25"
Inner Diameter, I.D.	= $19\frac{1}{8}$ "
Bolt Circle Diameter, BCD	= $22\frac{3}{4}$ "
Number of Bolts	= 16
Bolt Diameter, d	= $1\frac{1}{8}$ "
Finished Thickness, t	= $1\frac{5}{16}$ "
Bolting Material	= A-307

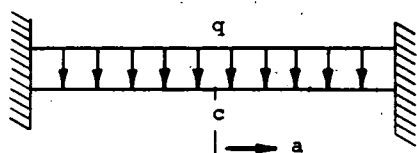
The following details are specified for the blind flanges:

Material = ASME SA516, Gr. 70
Outer Diameter, O.D. = 25"
Thickness = $1\frac{1}{2}$ "
Bolt Hole Diameter = $1\frac{1}{4}$ "
Bolt Circle Diameter = $22\frac{3}{4}$ "

The stresses due to temperature and pressure loading are calculated and combined as follows:

- a) From Reference 9, Table 24, Case 10, for uniformly distributed pressure loading on a clamped circular plate:

$$M_{ra} = \frac{-qa^2}{8} \quad (5.1)$$



where

M_{ra} = radial moment

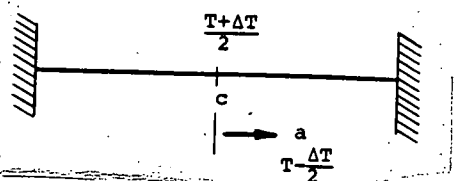
q = ΔP

a = radial distance

r = radius

$$\sigma_b = \frac{6M}{t^2} \quad (5.2)$$

- (b) From Reference 9, Table 24, Case 15, for a temperature differential ΔT :



$$M_{ra} = \frac{-\gamma D (1-\nu^2) \Delta T}{t} \quad (5.3)$$

where

y = coefficient of
thermal expansion

$$D = \frac{Et^3}{12(1-\nu)}$$

From (5.1), (5.2) and (5.3) maximum bending stress in the blind flange can be calculated as follows:

$$\sigma_b = \frac{6M}{t^2} = - \left[\frac{3}{4} \frac{\Delta P \cdot r^2}{t^2} + \frac{y E(1+\nu)}{2} \Delta T \right] \quad (5.4)$$

The most severe load combination applicable to the blind flange is Case 6 of the load combinations shown in Table 2-4. In addition, a temperature differential of 110°F is applied per Section 5.1.2 of the design specification (Reference 7). The seismic coefficients are converted into an equivalent Δp on the blind flange as described below and used in the design. From Reference 7, SRSS value of seismic coefficient corresponding to Safe Shutdown Earthquake (SSE) is

$$a_{SRSS} = \sqrt{0.3^2 + 0.3^2 + 0.08^2} = 0.432g$$

The weight of the blind flange = density of steel x volume of
blind flange

$$W_{\text{Blind Flange}} = 0.290 \times \frac{\pi}{4} (25)^2 \times 1.5$$

$$W_{\text{Blind flange}} = 213.53 \text{ lbs}$$

Total force acting on the blind flange due to Safe Shutdown
Earthquake is:

$$F_{\text{SSE}} = 213.53 \times .43 = 92.25 \text{ lbs}$$

The equivalent pressure differential is:

$$\Delta p = \frac{92.25}{\frac{\pi}{4} (25)^2} = 0.19 \text{ psi (assume 1 psi)}$$

Therefore, conservatively the following values are used to obtain
the maximum stress in the blind flange.

$$q = \Delta P = 33 \text{ psi}$$

$$r = \text{bolt circle radius} = 11.375''$$

$$t = \text{thickness of the plate} = 1.5''$$

$$y = \text{coefficient of thermal expansion} = 9.9 \times 10^{-6} \text{ in/in}^\circ \text{ F}$$

$$\nu = \text{Poisson's ratio} = 0.3$$

E = Young's modulus = 30×10^6 psi

$\Delta T = 110^\circ\text{F}$

Substituting these values in Equation (5.4)

$$\sigma_b = - \left[\frac{3}{4} \frac{(33)(11.375)^2}{(1.5)^2} + \frac{(9.9 \times 10^{-6})(30 \times 10^6)(1+.3)}{2} \right] \times 110$$

$$\sigma_b = - [1.42 + 21.24]$$

$$\sigma_b = -22.62 \text{ ksi} \ll 3.0 S_M = 67.5 \text{ ksi}$$

Table 5-1 contains a list of components required for the blind flange installation. Also provided is the rationale for the selection of the materials.

Table 5-1

Blind Flange Material Requirements

Part Name	Spec. No.	Material Min. Yield Strength (ksi)	Min. Tensile Strength (ksi)	Rationale For Selection of Materials
Blind Flange	ASME SA 516 Grade 70	38	70	ASME Section III Code material recommended for pressure vessel plates for moderate and low temperature service
Gasket	Silicone Compound or Equivalent (40 Durometer)	N/A	N/A	Gasket material used in similar applications at Quad Cities
Flange Bolts (16 required per flange)	ASME A193 Grade B7	105	125	ASME Section III Code bolting material, high strength, corrosion resistance, availability
Flange Nuts (16 required per flange)	ASME A194 Grade 2H	Proof Load 59,650 lbf	N/A	Standard nut material used with ASME A193 bolts
Flange Washers (16 required per flange)	AISI 1020	N/A	N/A	Availability

COM-08-023
Revision 0

5-7

REFERENCES

1. Mark I Containment Program, Structural Acceptance Criteria, Plant Unique Analysis Application Guide, GE document NEDO-24583-1, October 1979.
2. Mark I Containment Program, Mark I Wetwell-to-Drywell Vacuum Breaker Functional Requirements, GE Document NEDE-24802, April 1980.
3. NUTECH Letter Report from P.C. Riccardella to R.H. Kohrs (GE) No. GEN-62-001, September 7, 1979, covering NUTECH Analysis of A&M Internal Vacuum Breakers for Short Term Program.
4. NUTECH Report No. GEN-67-015, "Dynamic Analysis of Wetwell-to-Drywell Vacuum Breakers for Mark I Program Short Term Loads", May 21, 1980 (File 31.317.0048).
5. NUTECH Report No. COM-08-022, "Design Specification for Replacement of Vacuum Breaker Valve Shaft and Weight Lever Assemblies, Quad Cities Station Units 1 & 2", Rev. 0, September 1981 (File 64.316.0054).
6. NUTECH Internal Memo from S. Hong to T.J. Victorine dated June 29, 1981 (File 64.316.0005), "Quad Cities Vacuum Breaker Acceleration".
7. NUTECH Report No. COM-08-024, "Design Specification for Blind Flanges to Accommodate Replacement of Drywell-to-Wetwell Vacuum Breaker Valves, Quad Cities Station Units 1 & 2", Rev. 0, September, 1981 (File 64.316.0055).
8. Chicago Bridge & Iron Co. Drawings No. 206, Rev. 2 and 213, Rev. 3 (Contract No. 9-6735).
9. Roark, R.J. and Young, W.C., "Formulas for Stress and Strain", McGraw-Hill, 5th Edition.
10. MIL Handbook 5A, published by Research & Technology Division, Wright-Patterson AFB, Ohio 45433.

APPENDIX A

DESCRIPTION OF DRYWELL-TO-WETWELL
DESIGN FORCING FUNCTION

COM-08-023
Revision 0

A-1.

The drywell-to-wetwell vacuum breaker design forcing function used in the structural analyses is shown in Figure A-1 as a time history of the differential pressures across the valve disc. The technical basis for the computer model used to generate the forcing function is described in GE document NEDE-24802 (Reference A-1).

The applicable design loading for Quad Cities vacuum breakers is Group I forcing function (Reference A-2). Appropriate submergence head was added to the forcing function supplied by GE to obtain the pressure differential across the disc.

NUTECH

Wetwell Pressure Minus Vent System Pressure (psi)

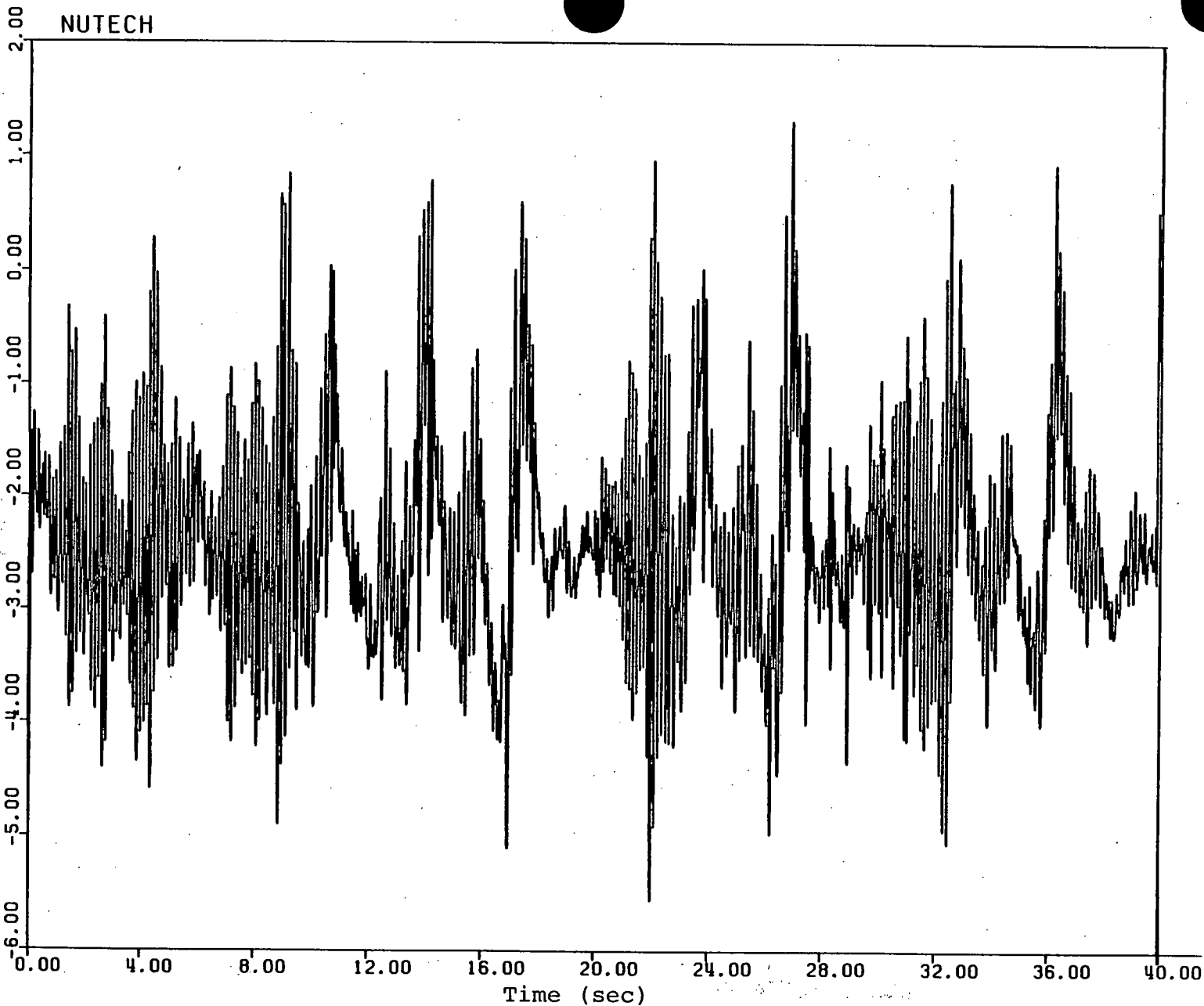


Figure A-1. Gr. I.F.F. + 1.59 psi Submergence Head
Pressure Time History

COM-08-023
Revision 0

A-3

nutech
ENGINEERS

REFERENCES FOR APPENDIX A

- A-1 G.E. document NEDE-24802 "Mark I Containment Program: Mark I Wetwell-to-Drywell Vacuum Breaker Functional Requirements", April 1980.
- A-2 G.E. Letter No. MI-G-64 of May 15, 1980 from D.L. Butcher to K.B. Ramsden of the Commonwealth Edison Company.

APPENDIX B

VALVE ANALYSIS DETAILS

COM-08-023
Revision 0

B-1

APPENDIX B

TABLE OF CONTENTS

<u>Section</u>	<u>Title</u>	<u>Page</u>
B.1	Single Degree of Freedom Model	B-5
B.2	Impact Model	B-11
B.3	Detailed Stress Models	B-16
B.3.1	Detailed Disc Model	B-16
B.3.2	Detailed Valve Internals Model	B-17
B.3.3	Stress Summary	B-18
B.4	Valve Attachment Point Stresses	B-28
B.5	References	B-36

APPENDIX B

LIST OF TABLES

<u>Table</u>	<u>Title</u>	<u>Page</u>
B.1-1	Dynamic Properties of A&M 18" Internal Valve	B-7
B.1-2	Single Degree of Freedom Model Results for A&M 18" Internal Valve	B-8
B.4-1	Valve Attachment Point Stresses.	B-35

APPENDIX B

LIST OF FIGURES

<u>Figure</u>	<u>Title</u>	<u>Page</u>
B.1-1	Single Degree of Freedom Model	B-9
B.1-2	Valve Response Due to Chugging Load	B-10
B.2-1	Valve Closing Impact Model	B-14
B.2-2	Valve Closing Impact Model Results. Impact Surface, Disc and Counterweight Displacement vs. Time, 200 In/Sec Approach Velocity	B-15
B.3-1	Valve Detailed Disc Model Geometry	B-19
B.3-2	Stress Contour Plot of Von Mises Equivalent Stress at Time of Maximum Stress	B-20
B.3-3	Parallel Surface Stress Distribution in Detailed Disc Model	B-21
B.3-4	Detailed Valve Internals Model	B-22
B.3-5	Finite Element Model of Valve Internals	B-23
B.3-6	Stopping Function - Deceleration Motion at Disc (Down-Impact) Velocity = 9 Rad/Sec	B-24
B.3-7	Valve Internal Assembly Counterweight Arm Moment	B-25
B.3-8	Valve Internal Assembly Shaft Torque	B-26
B.3-9	Valve Internal Assembly Disc Arm Moment	B-27

B.1 SINGLE DEGREE OF FREEDOM MODEL

A single degree of freedom model was used to analyze the rigid body rotation of the disc about its pivot point. The design load definition from Appendix A was used as pressure versus time loads on the disc surface. Gravity loads were considered. Friction and damping were neglected. Coefficients of restitution obtained from the impact analysis were used where impacts occurred.

The model is shown in Figure B.1-1 and the properties are tabulated in Table B.1-1. The dimensions for the valve were obtained from Reference B-1. The equivalent loading (Δp) across the disc due to seismic loading is obtained as follows.

From reference B-2, seismic coefficients (SRSS value) corresponding to safe shutdown earthquake (SSE) and operational basis earthquake (OBE) are .432 g's and .216 g's respectively. Also, total mass of disc, disc arm and weight assembly is 108.54 lbs and c.g. is located at a distance of 3.48" from shaft c.g.

This torque is converted into an equivalent Δp that would produce the same torque at the shaft C.G. when applied to the disc for input into DISCO.

Let G = seismic coefficient
 \bar{L} = C.G. location of the disc, disc arm and weight assembly, measured from shaft C.G.
 \bar{L} = 3.48"
 \bar{M} = weight of disc, disc arm and weight assembly
 A_D = Area of the disc
 Δp = Pressure differential across disc
 L_{DP} = distance of disc center of pressure from shaft C.G. location

Therefore, torque at shaft = $G \times \bar{L} \times \frac{\bar{M}}{g} = A_D \times \Delta p \times L_{DP}$

$$\text{or } \Delta p = \left(\frac{\bar{M}\bar{L}}{g} \right) \left(\frac{1}{A_D \times L_{DP}} \right) \times G$$

Substituting the values

$$(\Delta p)_{SSE} = \left(\frac{108.54 \times 3.48}{g} \right) \left(\frac{1}{283.53 \times 11.375} \right) \times .432g$$

$$(\Delta p)_{SSE} = 0.0505 \text{ PSI}$$

$$(\Delta p)_{OBE} = 1/2 (\Delta p)_{SSE} = 0.02527 \text{ PSI}$$

The results of the rigid body analysis are presented in Table B.1-2. The response of the valve to the chugging load is shown in Figure B.1-2.

Table B.1-1

Dynamic Properties for A&M 18" Internal Valve

Item	Units	Rigid Body Model
Mass of Disc	lb sec ² /in	0.1613
Mass of Weight	lb sec ² /in	0.0543
Mass of Disc Arm	lb sec ² /in	0.0269
Mass of Weight Arm	lb sec ² /in	0.0384
Radius to Disc	inch	11.395
Radius to Weight	inch	21.233
Radius to Disc Arm	inch	5.333
Radius to Weight Arm	inch	10.064
Angle to Disc	radians	0.0597
Angle to Weight	radians	2.7925
Angle to Disc Arm	radians	0.0404
Angle to Weight Arm	radians	2.7925
Angle to Lower Bound	radians	0.3491
Angle to Upper Bound	radians	1.1345
Angle to Spring*	radians	0.0
Spring Stiffness	in-lb/rad	0.0
Coef. of Res., Lower	---	0.6
Coef. of Rest., Upper	---	0.7
Sum of Mass Moment of Inertia**	lb-sec ² -in	5.5655

* Angle is to zero load position

** Inertia about component CG's.

Table B.1-2
Single Degree of Freedom Model Results

Item	Units	Chugging Load	Seismic Load		Free Fall	$\dot{\Delta\alpha}$
			OBE	SSE		
Maximum Closing Impact Velocity $\dot{\alpha}_{\max}(\text{seat})$	Rad/sec	4.631	1.497	1.672	1.297	N/A
Maximum Valve Opening	Degrees	7.18	7.5	7.5	7.5	N/A
$\dot{\Delta\alpha}(\text{OBE})$ - free fall	Rad/sec	N/A	N/A	N/A	N/A	0.20
$\dot{\Delta\alpha}(\text{SSE})$ - free fall	Rad/sec	N/A	N/A	N/A	N/A	0.375

NOTE: There were no upper (body) impacts.

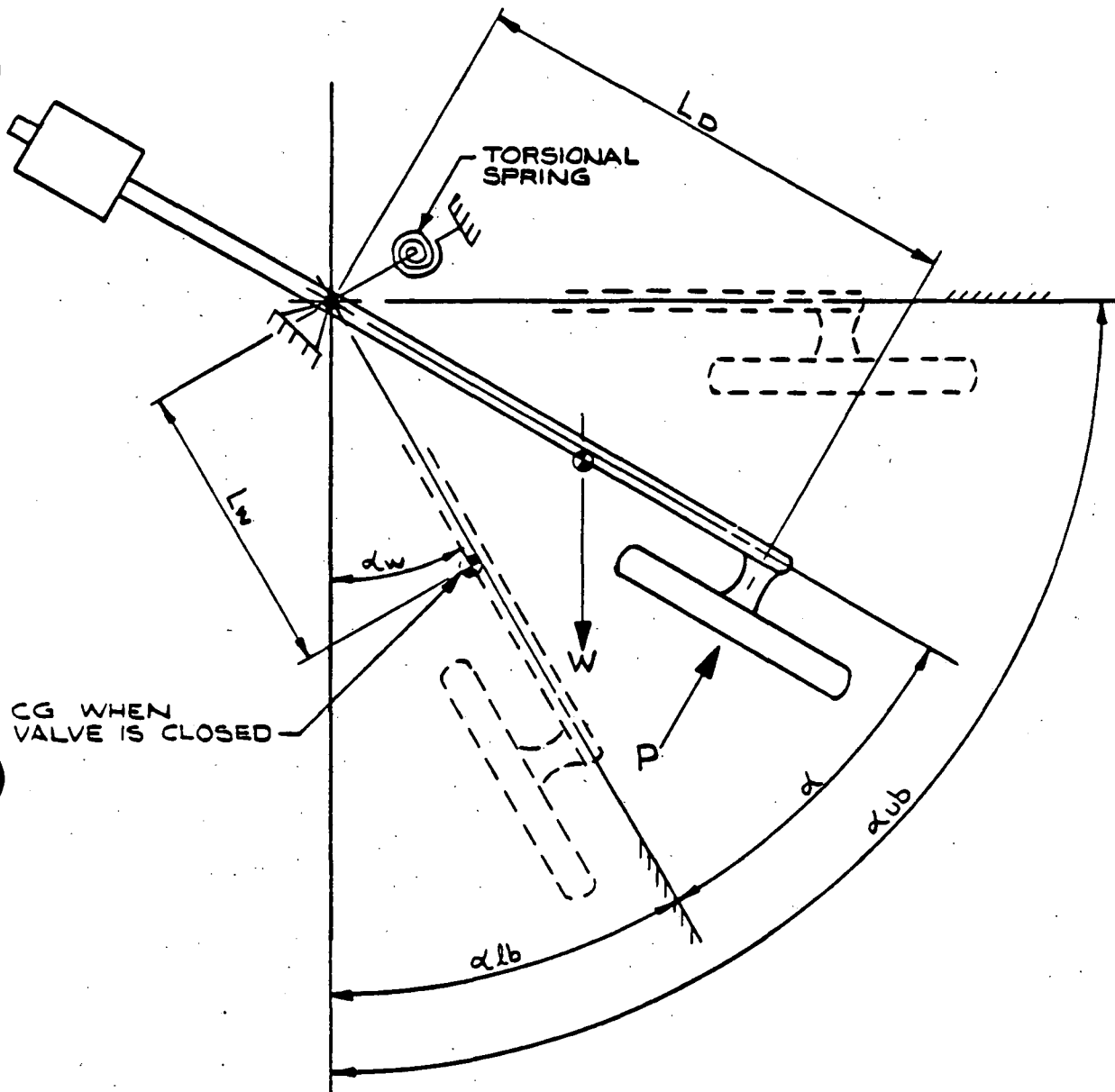


Figure B.1-1. Single Degree of Freedom Model

A finite element impact model of the entire valve was used to study the seat (valve fully closed) impact phenomenon. This model is illustrated in Figure B.2-1. The model is made up of axisymmetric, isoparametric solid elements; axisymmetric shell elements; beam, mass and spring elements; and non-linear gap elements (which can support compressive loading but have no tensile capacity) to model the impact surfaces. This model was used to conduct non-linear, time-history analyses of the impact events using the ANSYS (Reference B-3) general purpose finite element computer program. The general modeling philosophy was to use extremely fine detail in the vicinity of the impact point to accurately describe the local deformation of the impact surfaces. Decreasing refinement was used with increasing distance from the impact point. The objective of this analysis was to obtain displacement time-histories for input to more detailed stress models.

Significant assumptions in the analysis are as follows:

1. The geometry was approximated as axisymmetric. This involved approximating the actual three dimensional valve body shell by a cylinder of

average stiffness, and using a uniform average impact velocity for the entire disc seat.

2. Linear elastic material behavior was assumed for all elements. Thus, with the exception of the gap elements, the analysis was linear. Although some plasticity is expected in the immediate vicinity of impact, the material in these regions is expected to cyclically harden after the first few impacts such that linear behavior would occur thereafter. The elastic modulus of the non-linear gasket material was chosen to correspond to that at 50% deformation, since the metal tip on the disc impact surface restricts gasket deformation to approximately this value.
3. Dynamic response and stresses from the impact model were assumed to scale linearly with impact velocity. The validity of this assumption was confirmed through check runs at two different velocities.

The results of the closing impact analysis are presented in Figure B.2-2 in terms of displacement of various critical nodes in the model versus time. The analysis proceeds by imposing an

initial angular velocity to the disc/counterweight elements, and stepping through the impact event using extremely fine time steps (0.02 msec). The impact event is best described in terms of the node 39 displacement trace in Figure B.2-2. This node represents the metal impact surface on the rim of the disc. The displacement of this node proceeds at essentially the initial velocity for the first 0.5 msec, during which time the gasket material is being compressed. At this point, node 39 is stopped suddenly by the metal-to-metal impact for approximately 1 msec, and then rebounds in the opposite direction. At approximately the midpoint of this initial impact, a maximum relative deflection condition is observed between the disc rim (node 39) and the disc hub (node 109). During this entire impact, however, the counterweight (node 112) continues to move in the valve closing direction (because of the relatively soft connection between it and the disc), and does not reverse direction until approximately 11 msec. The inertia of this counterweight assembly is sufficient to completely reverse the disc, and send it back for a second, more severe impact at 12 msec. Finally, after this second impact, both the disc and counterweight are reversed and moving in the valve opening direction and the impact event is over. Note, however, that there is oscillation between the disc and counterweight.

B-14

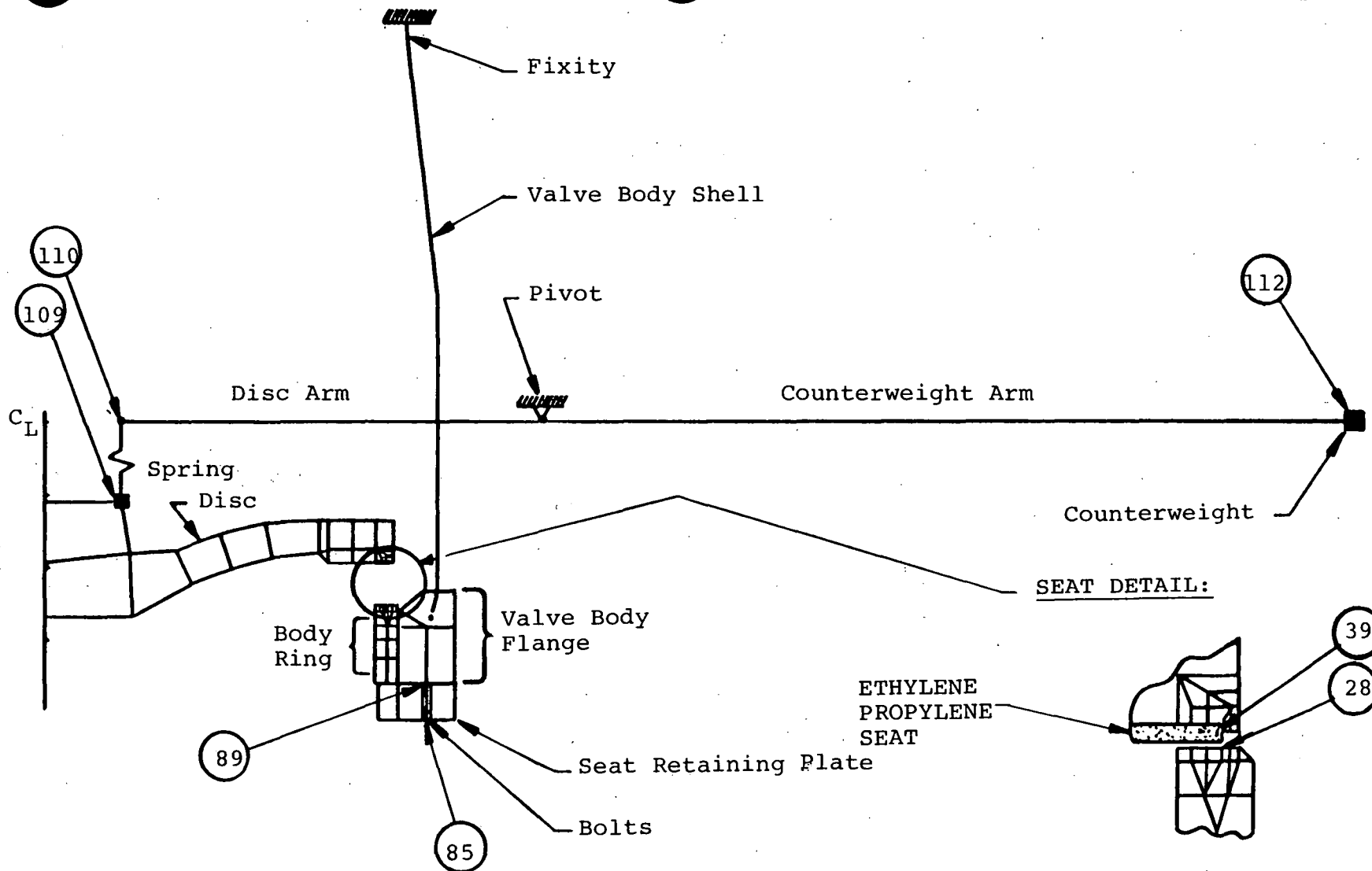
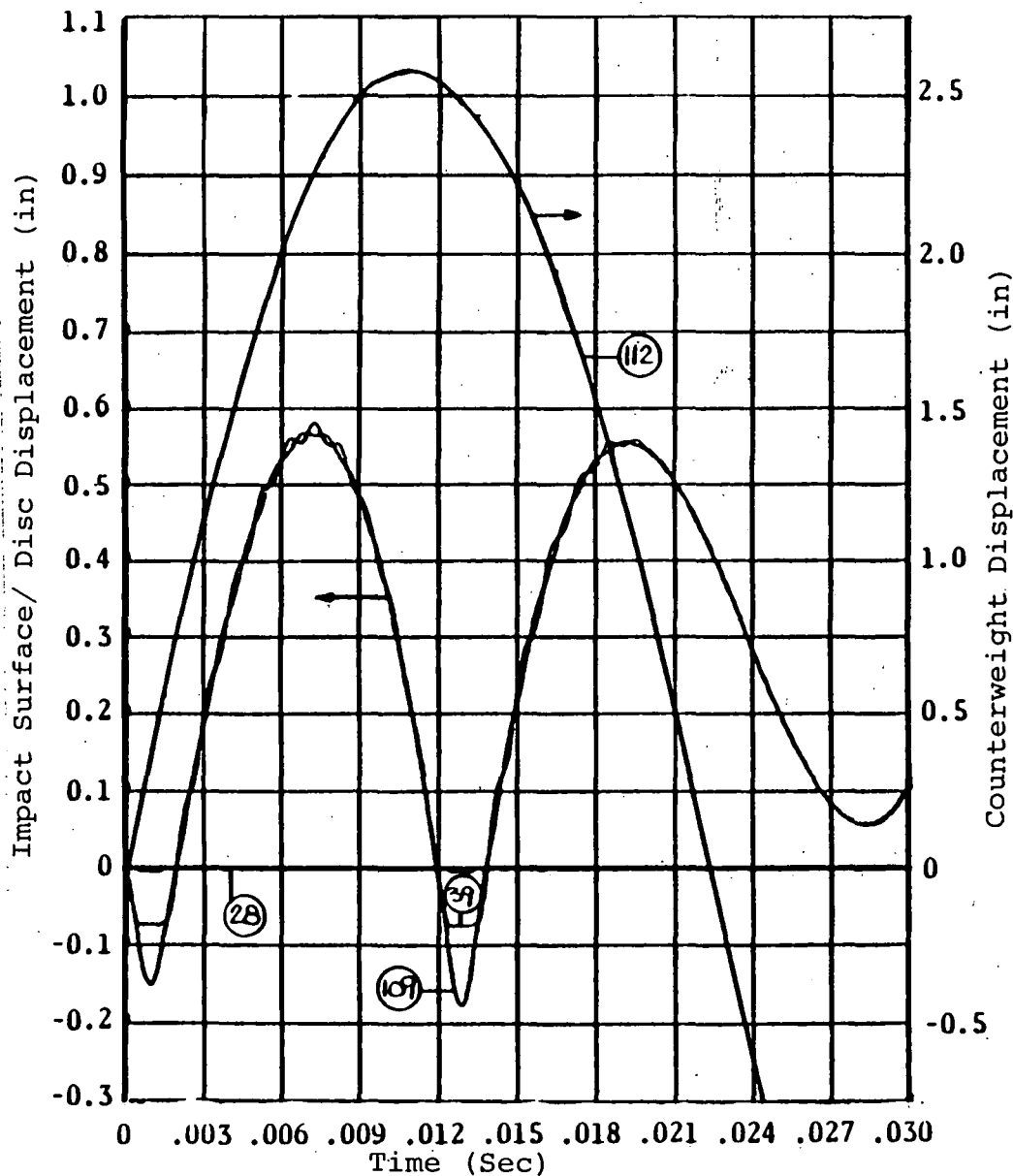


Figure B.2-1. Valve Closing Impact Model



POSITIVE DISPLACEMENT

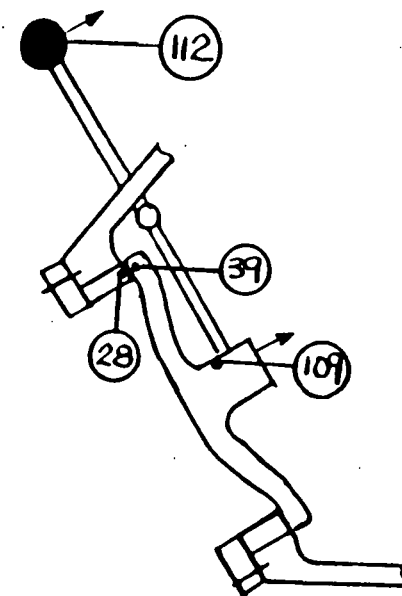


Figure B.2-2. Valve Closing Impact Model Results: Impact Surface, Disc and Counterweight Displacement vs. Time (200 in/sec Approach Velocity)

B.3 DETAILED STRESS MODELS

B.3.1 Detailed Disc Model

The detailed analysis of the stresses in the vacuum breaker disc was performed using the axisymmetric model illustrated in Figure B.3-1. Loading input to the model consisted of imposing, to selected nodes, displacement time-histories which were obtained from the results of the impact model analysis. In addition, an initial velocity (corresponding to a rotational velocity of 9 radians/sec of the moving valve components) was applied to the model prior to impact. The inertia effects of the moving disc were, therefore, introduced in the analysis. The displacements of a hub node and rim node, shown in Figure B.3-1 were controlled throughout the analysis following impact based on the impact model results for these nodes presented in Figure B.2-2. The 9 radians/sec velocity bounds the maximum input velocities found in the single degree of freedom analysis.

Results of the analysis are shown in Figures B.3-2 and B.3-3. Figure B.3-2 is a stress contour plot of Von-Mises equivalent stress at the time the maximum stress occurred in the disc. As the figure shows, the highest stress is located on the bottom (or outside) surface in the dished portion of the disc. Figure B.3-3 better illustrates the stress condition of the disc at the most

critical time during impact. At impact, the disc hub continues to move in the closing direction relative to the rim. The outside and inside disc surfaces, in the thinner dished area, experience tension and compression stresses, respectively, as shown in Figure B.3-3. The stress plots from this figure were used to determine bending and membrane stresses. These stresses were then used to calculate the stress intensity in the disc.

B.3.2 Detailed Valve Internals Model

A model of the moving parts of all components other than the actual disc of the Atwood & Morrill valve was made to investigate their dynamic response following impact. A schematic drawing of the model is shown in Figure B.3-4 and NASTRAN Finite element model is shown in Figure B.3-5. The initial rotational velocity of 9 radians/sec was input to the model to include the rotational inertia of the components as part of the input loading. Also, from the results of the impact model analysis, a displacement time-history, Figure B.3-6, was applied to the disc arm (at the disc centerline) after impact. The displacement specification at the disc end of the arm was, therefore, a stopping function being applied to the rotational inertia of the valve internal components. The model was analyzed using the computer program MSC/NASTRAN (Reference B-4).

Results of the analysis are presented in Figures B.3-7 through B.3-9. The plots show the resultant forces and moments versus time for the various components. The maximum values from these and similar plots for other components were used to determine the stresses and to compute the stress intensities.

B.3.3 Stress Summary

The stresses in the vacuum breaker valve components along with applicable allowable stress intensity limits for the various load combinations are given in Tables 3-2, 3-3 and 3-4 in the main text.

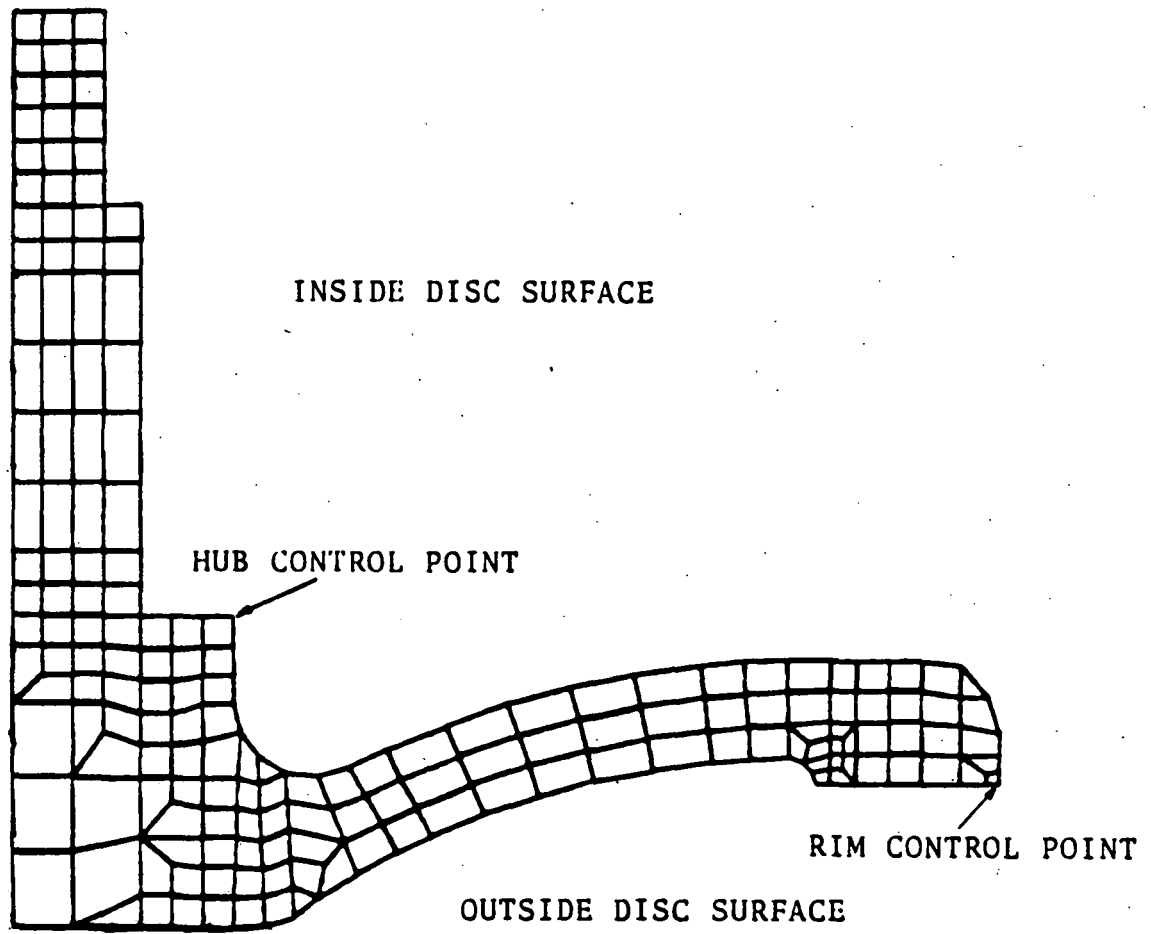


Figure B.3-1. Valve Detailed Disc Model Geometry

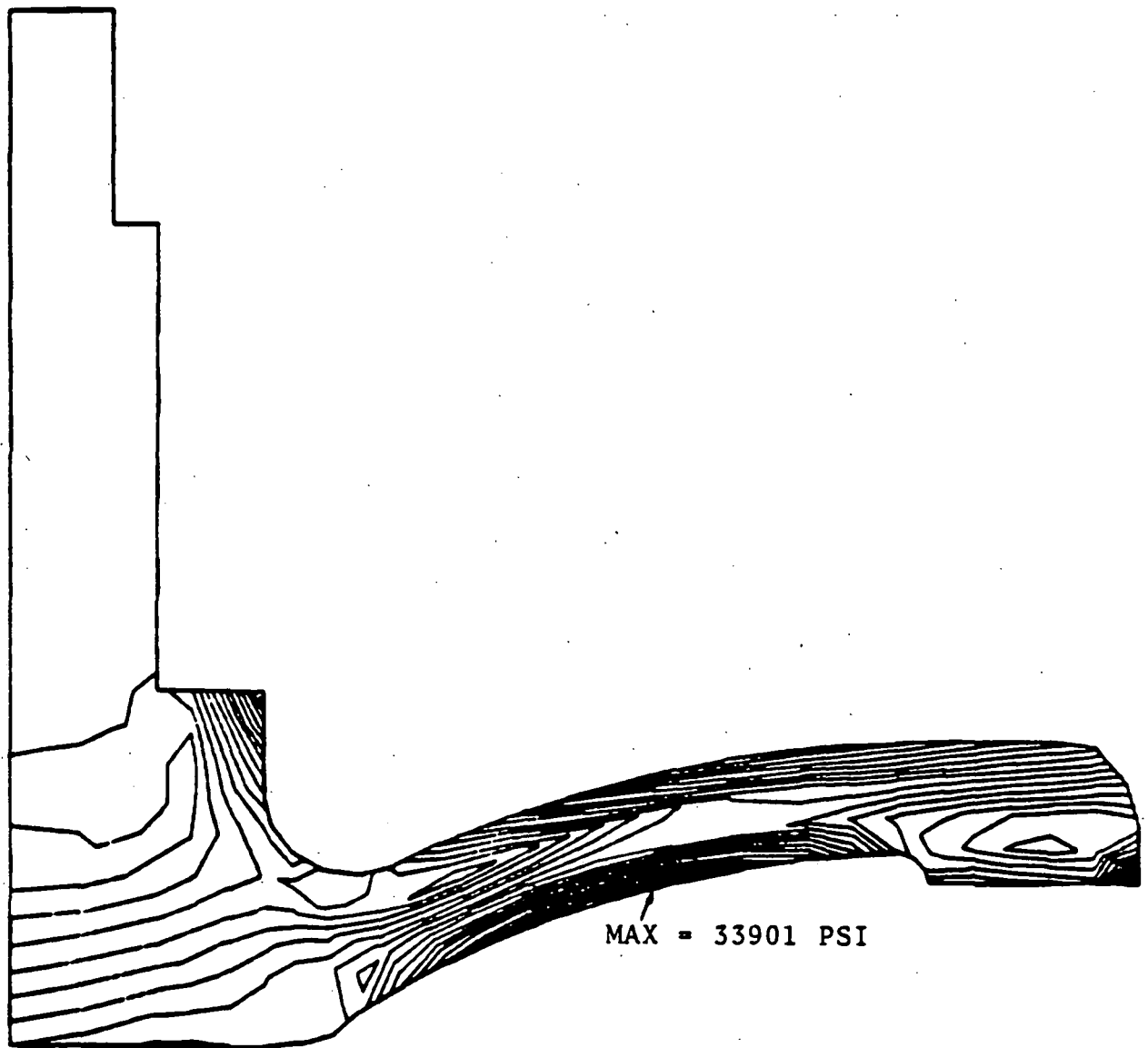


Figure B.3-2. Stress Contour Plot of Von Mises Equivalent Stress at Time of Maximum Stress

COM-08-023
Revision 0

B-20

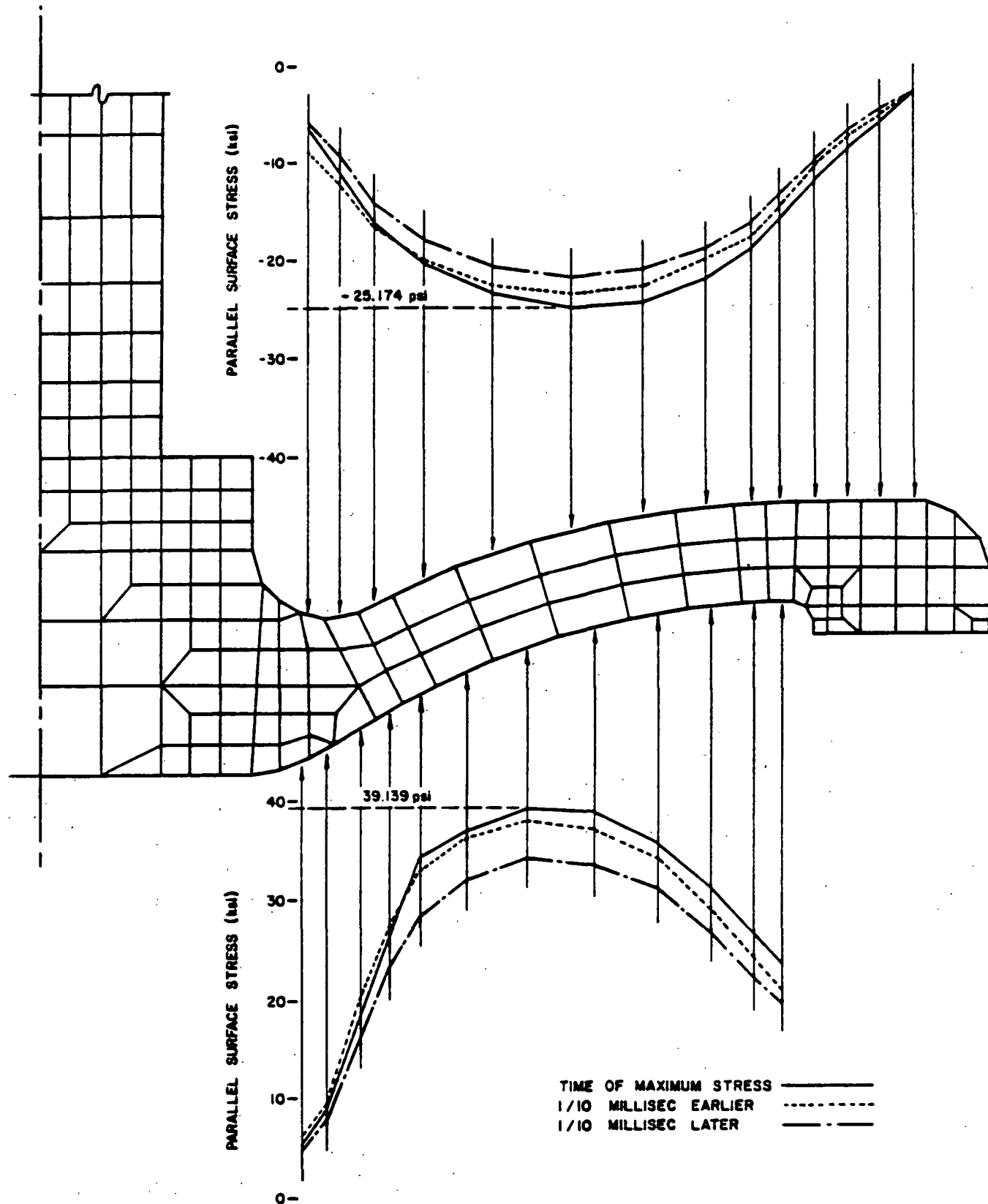


Figure B.3-3. Parallel Surface Stress Distribution in Detailed Disc Model

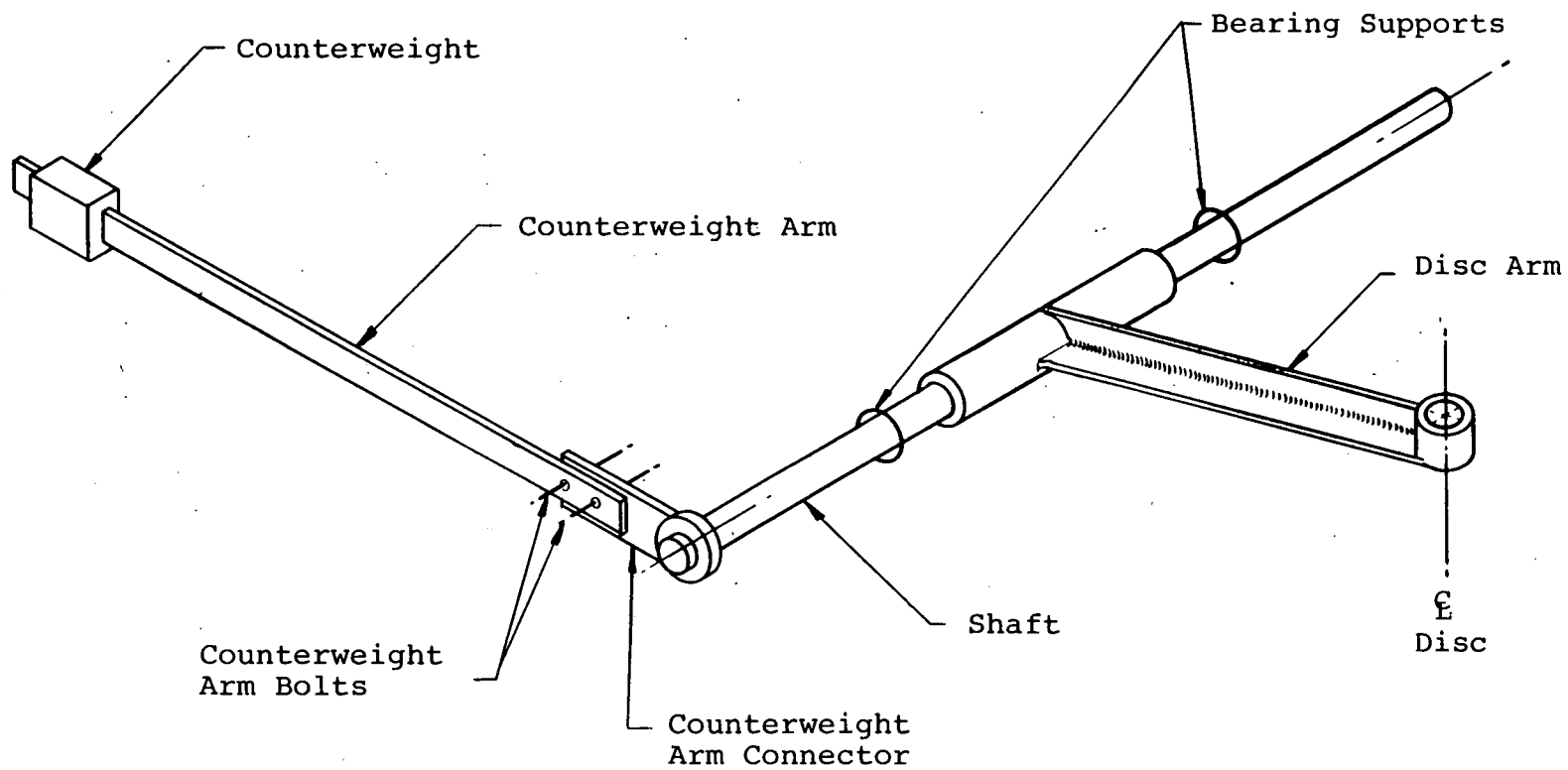


Figure B.3-4. Detailed Valve Internal Model

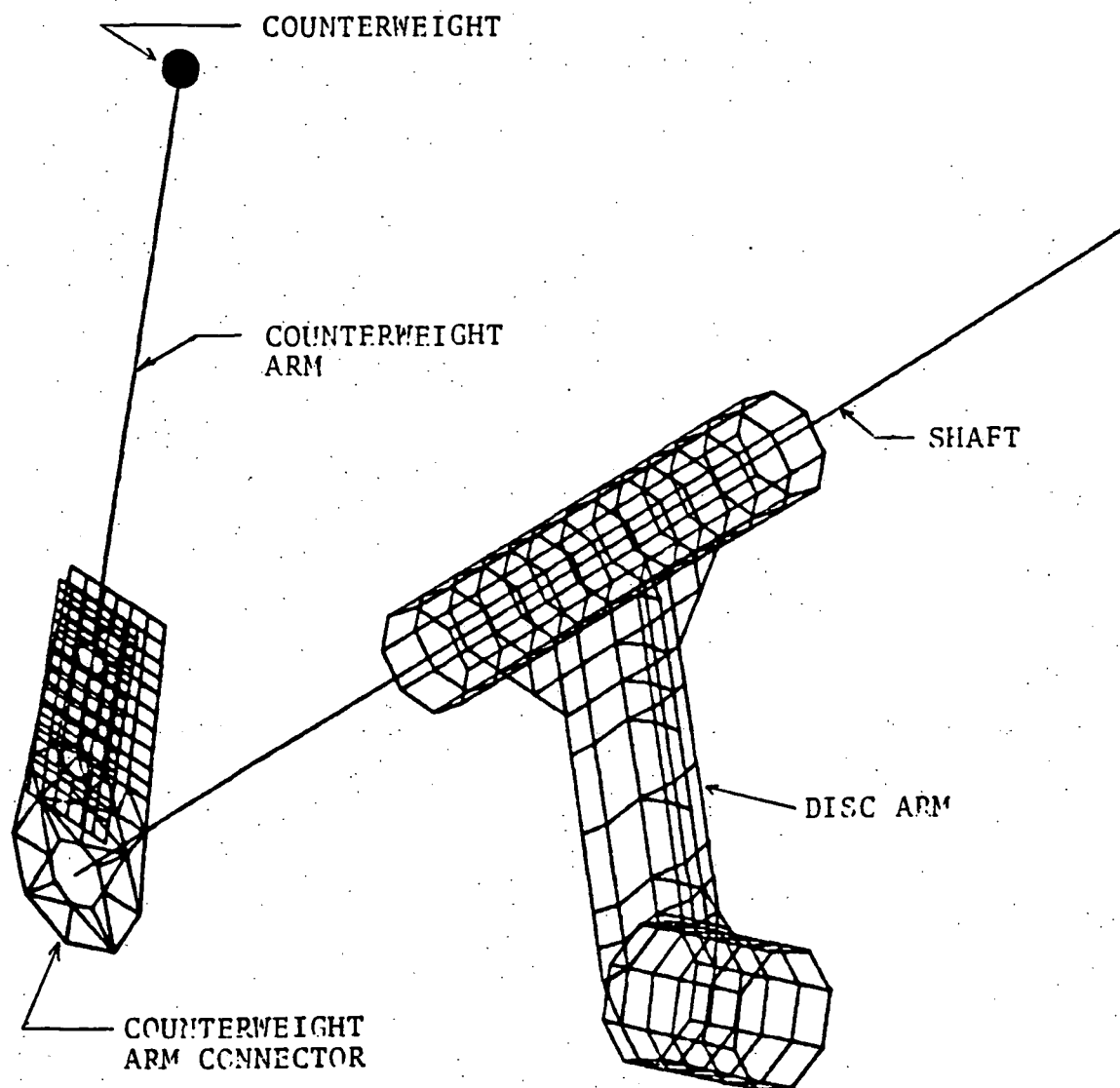


Figure B.3-5. Finite Element Model of Valve Internals
(NASTRAN-1)

COM-08-023
Revision 0

B-23

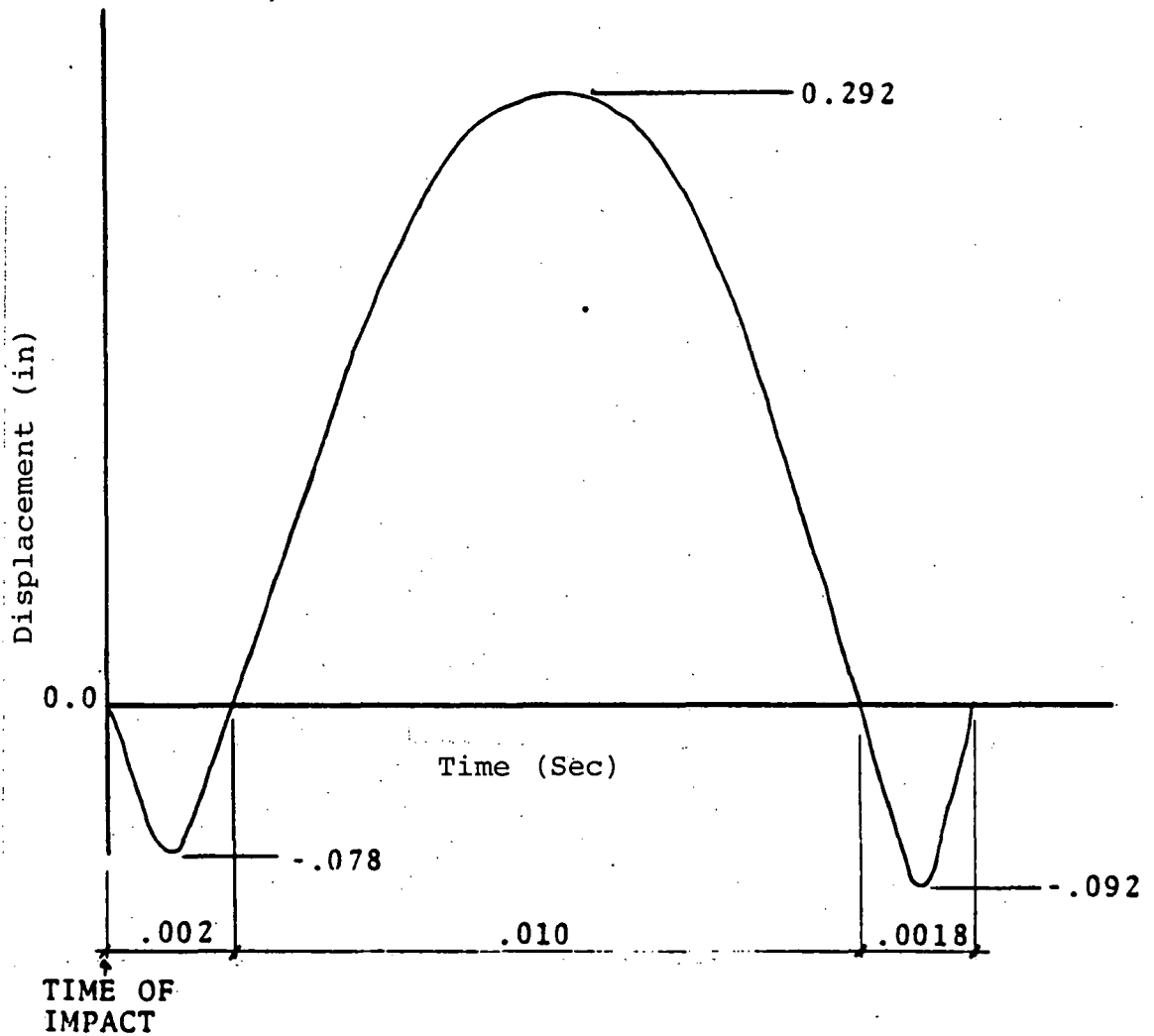


Figure B.3-6. Stopping Function - Deceleration Motion at Disc Hub (Down - Impact) Velocity = 9 Rad/sec

COM-08-023
Revision 0

B-24

COM-08-023
Revision 0

B-25

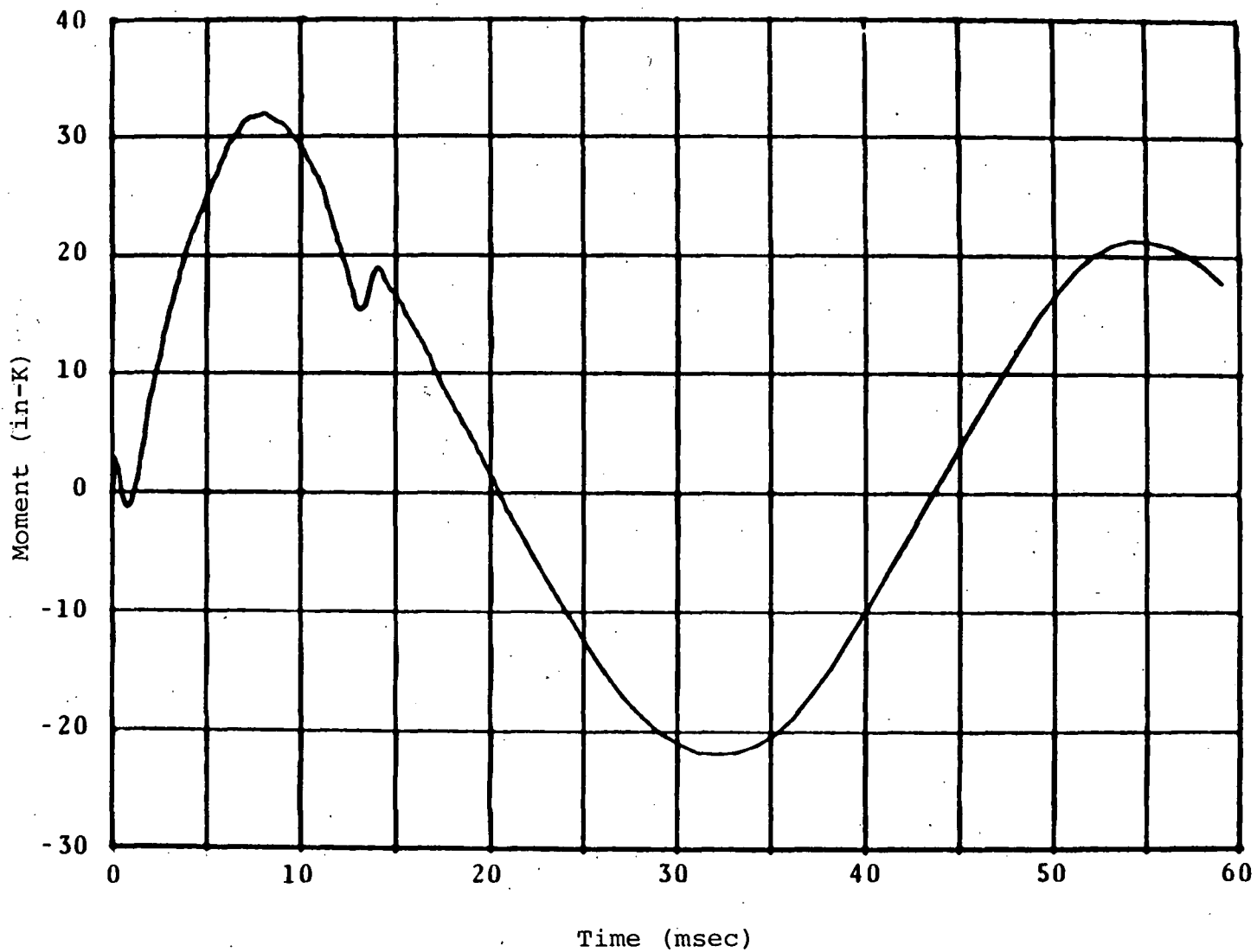


Figure B.3-7. Valve Internal Assembly, Counterweight Arm Moment

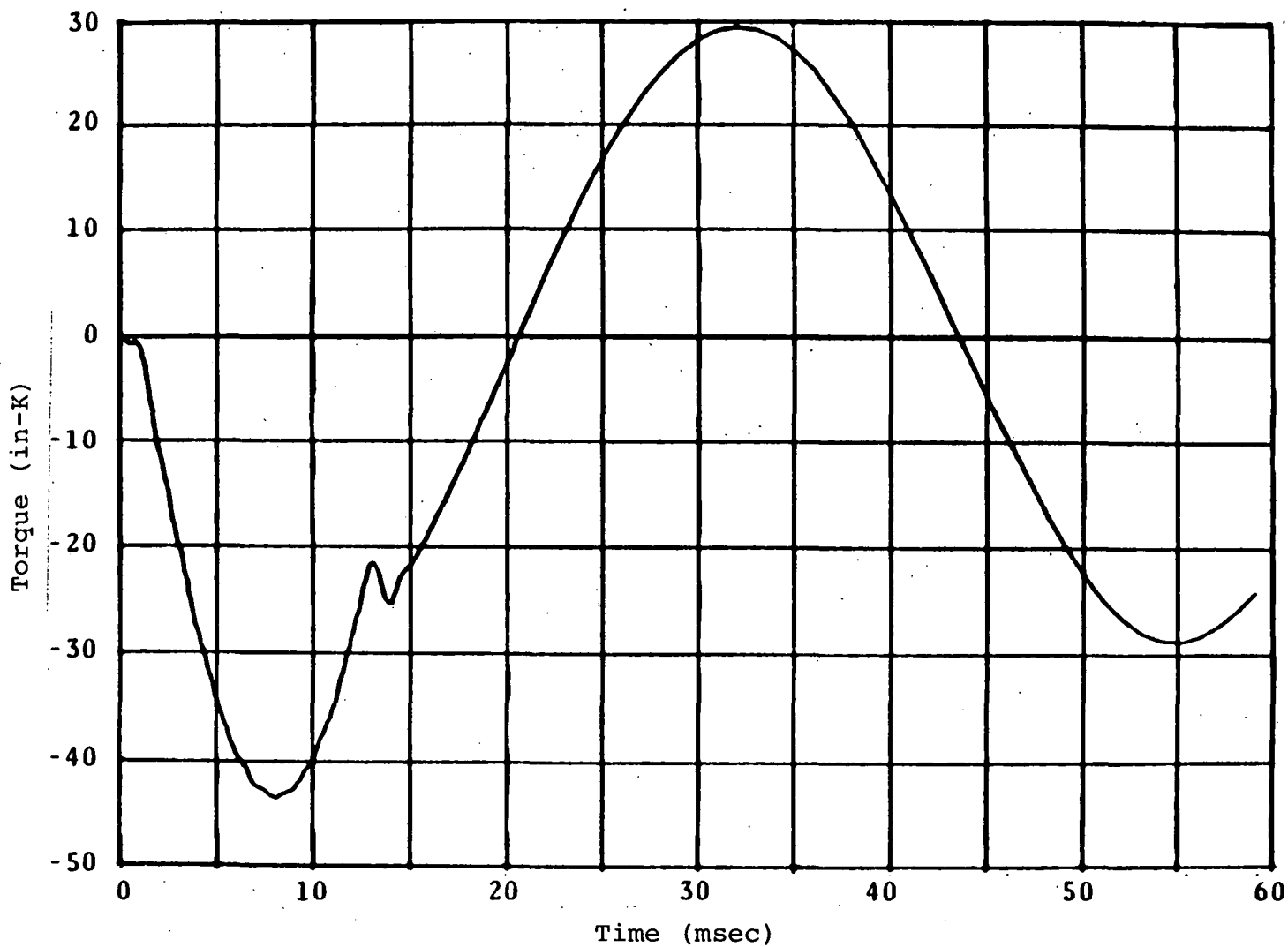


Figure B.3-8. Valve Internal Assembly, Shaft Torque

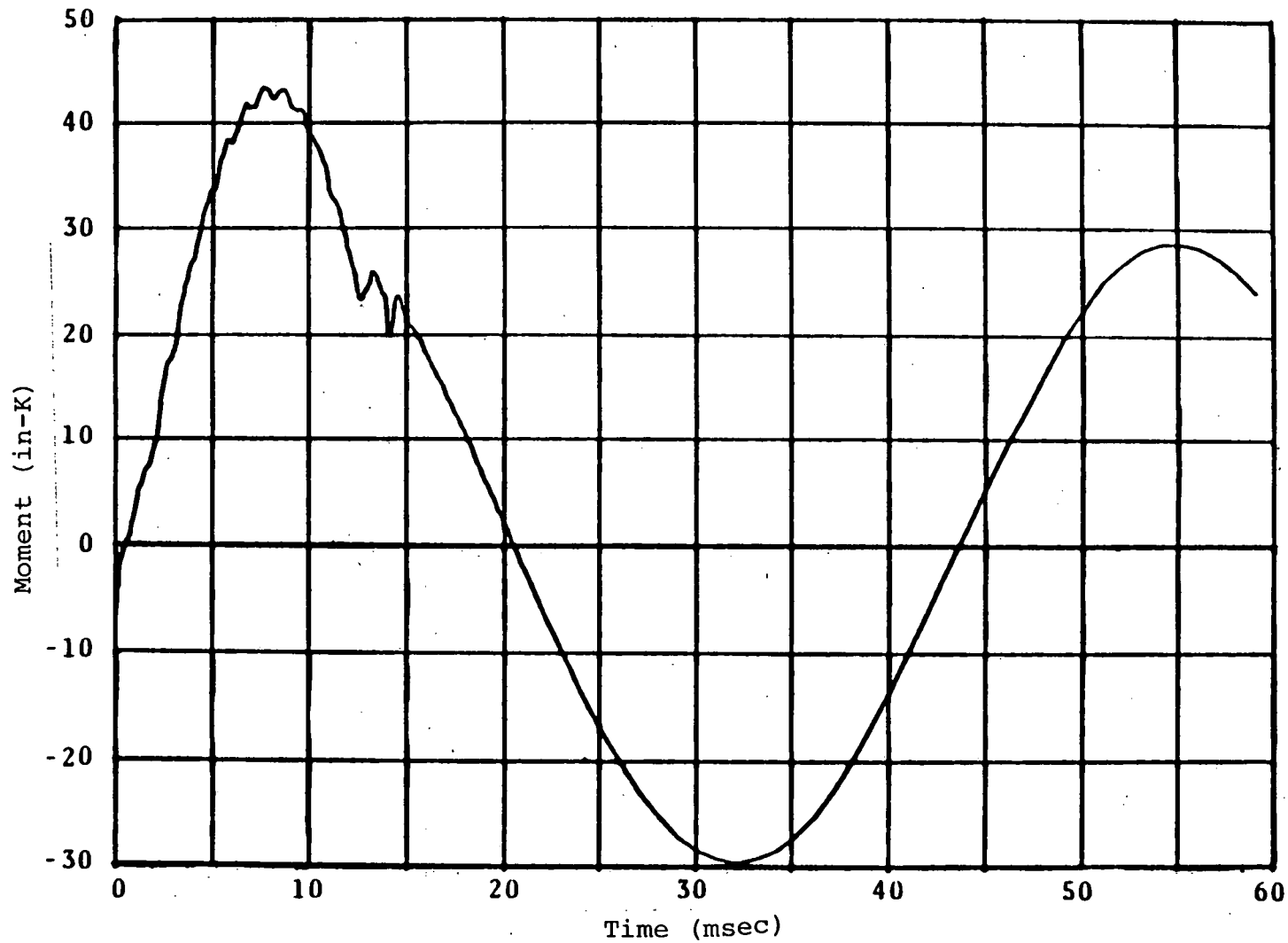


Figure B.3-9. Valve Internal Assembly, Disc Arm Moment

B.4

VALVE ATTACHMENT POINT STRESSES

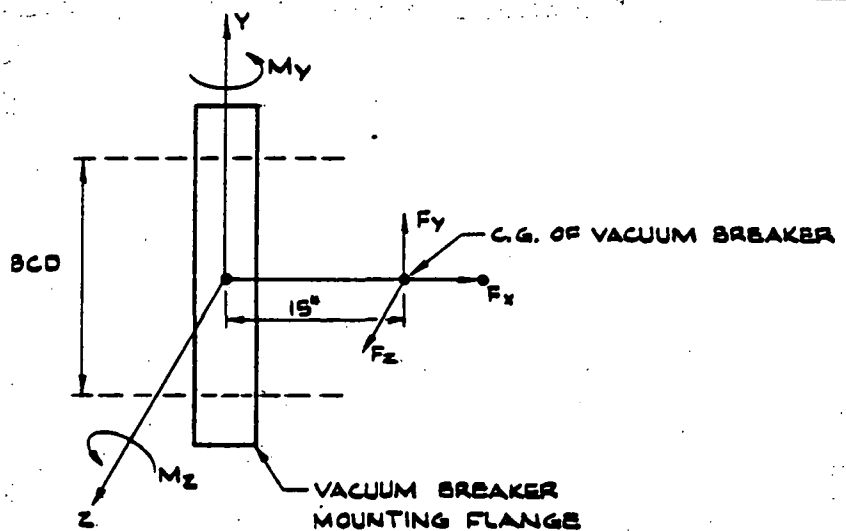
The valve attachment point stresses are calculated for the load combinations 2, 4 and 6 as given in Table 2-4 of the main text, as follows:

From Reference 6, the peak acceleration due to pool swell loads are:

$$\ddot{x} = 7.45g$$

$$\ddot{y} = 18.0g$$

$$\ddot{z} = 4.3g$$



Assuming a vacuum breaker weight of 1000 lbs, loads are calculated as follows:

Pool Swell loads

$$F_x = M_x = 1000 \times 7.45 = 7450 \text{ lbs.}$$

$$F_y = M_y = 1000 \times 18.0 = 18000 \text{ lbs.}$$

$$F_z = M_z = 1000 \times 4.3 = 4300 \text{ lbs.}$$

Gravity Load (weight of the valve)

$$F_y = 1000 \text{ lbs.}$$

Loads due to pressure differential (Δp) across the valve

$$F_y = \Delta p \times \text{Mounting flange area}$$

$$F_y = 32 \times \frac{\pi}{4} (25)^2$$

$$F_y = 15708 \text{ lbs.}$$

Seismic Loads

Loads corresponding to earthquakes are obtained by multiplying the seismic coefficients by the valve mass.

SSE Loads are obtained as follows

$$F_x = 0.3 \times 1000 = 300 \text{ lbs.}$$

$$F_y = 0.08 \times 1000 = 80 \text{ lbs}$$

$$F_z = 0.3 \times 1000 = 300 \text{ lbs.}$$

OBE loads are one-half of the SSE loads

$$F_x = 0.15 \times 1000 = 150 \text{ lbs}$$

$$F_y = 0.04 \times 1000 = 40 \text{ lbs}$$

$$F_z = 0.15 \times 1000 = 150 \text{ lbs.}$$

These values of loads are used to obtain the resultant loading on the valve mounting bolts for the various load combinations as follows.

Load Combination 2

Loading for this load combination consists of 32 psid pressure differential, pool swell and gravity loads.

Therefore

$$\begin{aligned} F_x &= 15708 \times 7450.0 + 0.0 = 23158 \text{ lbs.} \\ F_y &= 0.0 + 18000.0 \times 1000.0 = 19000 \text{ lbs.} \\ F_z &= 0.0 + 4300.0 + 0.0 = 4300 \text{ lbs.} \end{aligned}$$

$$M_y = F_z \times 15 = 4300 \times 15 = 64,500 \text{ in-lbs.}$$

$$M_z = F_y \times 15 = 19000 \times 15 = 285,000 \text{ in-lbs.}$$

Resultant Moment

$$M_R = \sqrt{M_y^2 + M_z^2} = \sqrt{(64500)^2 + (285000)^2}$$

$$M_R = 292207.55 \text{ in-lbs.}$$

Using Equation (5) (Section 3.2.2 of main text) the moment is converted into an equivalent axial force as seen by the bolt as follows:

$$F_{\max} = \frac{2M(R_1 + R_2)}{N(2R_1^2 + R_2^2)} \quad (B4.1)$$

where R_1 = outer radius of the flange

R_2 = bolt circle radius

N = number of bolts

M = moment

F_{\max} = maximum axial force on any single bolt due to M

Also R_1 = 12.5"

R_2 = 11.375"

N = 16

Substituting these values in Equation (B4.1)

$$\begin{aligned} (F_{\max}) \text{ due to } M_R &= \frac{2 \times 292207.55 (11.375 + 12.5)}{16 [2(12 \times 5)^2 + (11 \times 3.75)^2]} \\ &= 292207.55 \times .00675366 \text{ lbs.} \\ &= 1973.47 \text{ lbs} \end{aligned}$$

$$(F_a)_{\text{bolt}} \text{ due to } F_x = \frac{23158}{16} = 1447.38 \text{ lbs}$$

Total axial force for load combination Case 2 on any single bolt
= 1973.47 + 1447.38 = 3420.85 lbs.

Bolt Cross Section

$$A = \frac{\pi}{4} \left(1\frac{1}{8}\right)^2 = 0.994 \text{ sq. in.}$$

$$\sigma_{\text{bolt}} = \frac{3420.85}{.994} = 3.44 \text{ ksi}$$

$$(\sigma_{\text{bolt}})_{\text{case 2}} = 3.44 \text{ ksi}$$

Load Combination 4

Loading for this load combination consists of 32 psid pressure differential seismic (OBE) load and pool swell loads.

Therefore

$$F_x = 15708 + 150 + 7450 = 23308 \text{ lbs.}$$

$$F_y = 0.0 + 40 + 1000 + 18000 = 19040 \text{ lbs.}$$

$$F_z = 0.0 + 150 + 4300 = 4450 \text{ lbs.}$$

$$M_y = F_z \times 15 = 4450 \times 15 = 66750 \text{ in-lbs.}$$

$$M_z = F_y \times 15 = 19040 \times 15 = 285600 \text{ in-lbs}$$

Resultant Moment

$$M_R = \sqrt{(66750)^2 + (285600)^2} = 293296.6 \text{ in-lbs.}$$

$$(F_{\max})_{\text{due to } M_R} = .00675366 \times M_R$$

$$(F_{\max})_{M_R} = 1980.83 \text{ lbs.}$$

$$(F_a)_{\text{bolt due to } F_X} = \frac{23308}{16} = 1456.75 \text{ lbs}$$

$$(F_a)_{\text{Total}} = 3437.6 \text{ lbs.}$$

$$(\sigma_{\text{bolt}})_{\text{case 4}} = \frac{3437.6}{.994} = 3.46 \text{ ksi}$$

$$(\sigma_{\text{bolt}})_{\text{case 4}} = 3.46 \text{ ksi}$$

Load Combination 6

Loading for this load combination consists of 32 psid pressure differential, seismic (SSE) and pool swell loads.

$$F_X = 15708 + 300 + 7450 + 0 = 23458 \text{ lbs.}$$

$$F_Y = 0.0 + 80 + 18000 + 1000 = 19080 \text{ lbs.}$$

$$F_Z = 0.0 + 300 + 4300 + 0 = 4600 \text{ lbs}$$

$$M_Y = F_Z \times 15 = 4600 \times 15 = 69000 \text{ in-lbs.}$$

$$M_Z = F_Y \times 15 = 19080 \times 15 = 286200 \text{ in-lbs.}$$

Resultant Moment

$$M_R = \sqrt{(69000)^2 + (286200)^2} = 294,400 \text{ in-lbs.}$$

$$(F_{\max})_{\text{due to } M_R} = .00675366 \times 294,400$$

$$(F_{\max})_{M_R} = 1988.3 \text{ lbs}$$

$$(F_a)_{\text{bolt due to } F_x} = \frac{23458}{16} = 1466.13 \text{ lbs.}$$

$$(F_a)_{\text{total}} = 3454.43 \text{ lbs.}$$

$$(\sigma_{\text{bolt}})_{\text{case 6}} = \frac{3454.43}{.994}$$

$$(\sigma_{\text{bolt}})_{\text{case 6}} = 3.475 \text{ ksi}$$

The results are summarized in Table B.4-1.

Table B.4-1

Valve Attachment Point Stresses

LOAD COMBINATION NUMBER	DESCRIPTION	CALCULATED BOLT TENSILE STRESS (KSI)	REMARKS
2	32 psid + pool swell	3.44	Bolt stresses are insignificant
4	32 psid + OBE + pool swell	3.46	
6	32 psid + SSE + pool swell	3.48	

REFERENCES

- B-1 Drawing, Atwood & Morrill Co., Inc., Salem, Massachusetts:
- 20802-F Full Bore Vacuum Breaker Valves with Side Air Cylinder and Double Wgts and Levers
 - 20750-H 18 in. - 150 No. Std. Flg. Vacuum breaker Valve Body
 - 21811-C Disc 18 in. Vacuum Breaker Valve
 - 21816-C Disc Arm 18 in. Vacuum Breaker Valve
 - 22523-B Retaining Ring 18 in. Vacuum Breaker Valve
 - 22524-B Disc Seat 18 in. Vacuum Breaker Valve
 - 22529-B Seat Retaining Plate 18 in. Vacuum Breaker Valve
 - 22817-B Shaft 18 in. Vacuum Breaker Valve
 - 22922-B Lever Connection 14 in. 30 in. Diameter RCV's
 - 2398-C Standard List of Slide Weights with Interchangeable Ends.
- B-2 Rigid body dynamic analysis results, NUTECH File 64.316.0035, August 1981.
- B-3 G.J. DeSalvo and J.A. Swanson, ANSYS Engineering Analysis System, August 1, 1978.
- B-4 C.W. McCormick, ed., MSC/NASTRAN USER's MANUAL, MacNeal Schwendler Corp., 1976.
- B-5 DISCO USER MANUAL, NUTECH File 08.078.0100, April 1981.



C.D.I. TECH NOTE NO. 82-7

IMPROVED DYNAMIC VACUUM BREAKER

VALVE RESPONSE

FOR QUAD CITIES 1 & 2

Revision 1

Prepared by

CONTINUUM DYNAMICS, INC.

for

GENERAL ELECTRIC COMPANY

September 1982

8307190074 830712
PDR ADDCK 05000237
P PDR

IMPROVED DYNAMIC VACUUM BREAKER

VALVE RESPONSE

FOR QUAD CITIES 1 & 2

REVISION 1

PREPARED FOR

GENERAL ELECTRIC COMPANY

175 CURTNER AVENUE

SAN JOSE, CALIFORNIA 95125

UNDER PURCHASE ORDER NO. 205-XJ102

BY

CONTINUUM DYNAMICS, INC.

P.O. BOX 3073

PRINCETON, NEW JERSEY 08540

APPROVED BY

A handwritten signature in cursive script, reading "Alan Bilanin", is written over a horizontal line.

ALAN J. BILANIN
PRINCIPAL INVESTIGATOR

SEPTEMBER, 1982

DISCLAIMER OF RESPONSIBILITY

Neither the General Electric Company nor any of the contributors to this document makes any warranty or representation (express or implied) with respect to the accuracy, completeness, or usefulness of the information contained in this document or that the use of such information may not infringe privately owned rights; nor do they assume any responsibility for liability or damage of any kind which may result from the use of any of the information contained in this document.

SUMMARY

Improved plant-unique expected and design vacuum breaker impact velocities have been calculated for the Quad Cities 1 and 2 plants.

The valve displacement time history was predicted using a valve dynamic model which takes credit for the reduction of hydrodynamic torque across the vacuum breaker as a consequence of valve actuation. Expected vacuum breaker actuation velocities are reduced by 21% over a prediction which does not take credit for hydrodynamic torque reduction.

SUMMARY OF THE METHODOLOGY USED TO DEFINE PLANT-UNIQUE
WETWELL TO DRYWELL MARK I VACUUM BREAKER FORCING FUNCTIONS
FROM FSTF DATA

During the Mark I FSTF test series, wetwell to drywell vacuum breaker actuation was observed during the chugging phase of steam blowdowns. As a result of this observation, a methodology was developed which can be used to define the loading function acting on a vacuum breaker during chugging (Ref. 1). The methodology developed uses FSTF pressure time history data and adjusts the vent system and wetwell pressures to account for plant-unique geometry. For plants with internal vacuum breakers, the most critical parameter controlling the magnitude of the vacuum breaker forcing function is the drywell volume per vent area. Vacuum breaker forcing functions are specified as a time history of the differential pressure across the valve disc.

The steps taken in the development of the plant-unique forcing function model are shown in Figure 1. Step 1 involves the development of analytic dynamic models for the unsteady motion in the steam vent system (see Figure 2), at the steam water interface (see Figure 3) and in the suppression pool (see Figure 4) assuming that the condensation rate at the steam water interface is known. The dynamics in the vent system are assumed to be governed by one-dimensional acoustic theory and jump conditions across the steam water interface are the Rankine-Hugoniot relations. A one-dimensional model of the suppression pool was developed which accounts for compression of the wetwell airspace

STEP

1

Develop a dynamic model of the vent system, steam water interface and pool slosh with the condensation rate at the interface unknown.

2

Use measured drywell pressure to determine the condensation rate.

3

With the condensation rate determined, predict unsteady pressures at other vent locations to validate the model.

4

Use the condensation source at the vent exit to drive dynamic models of Mark I plants to determine unique vacuum breaker forcing functions.

Figure 1. Steps in determining plant unique vacuum breaker forcing functions.

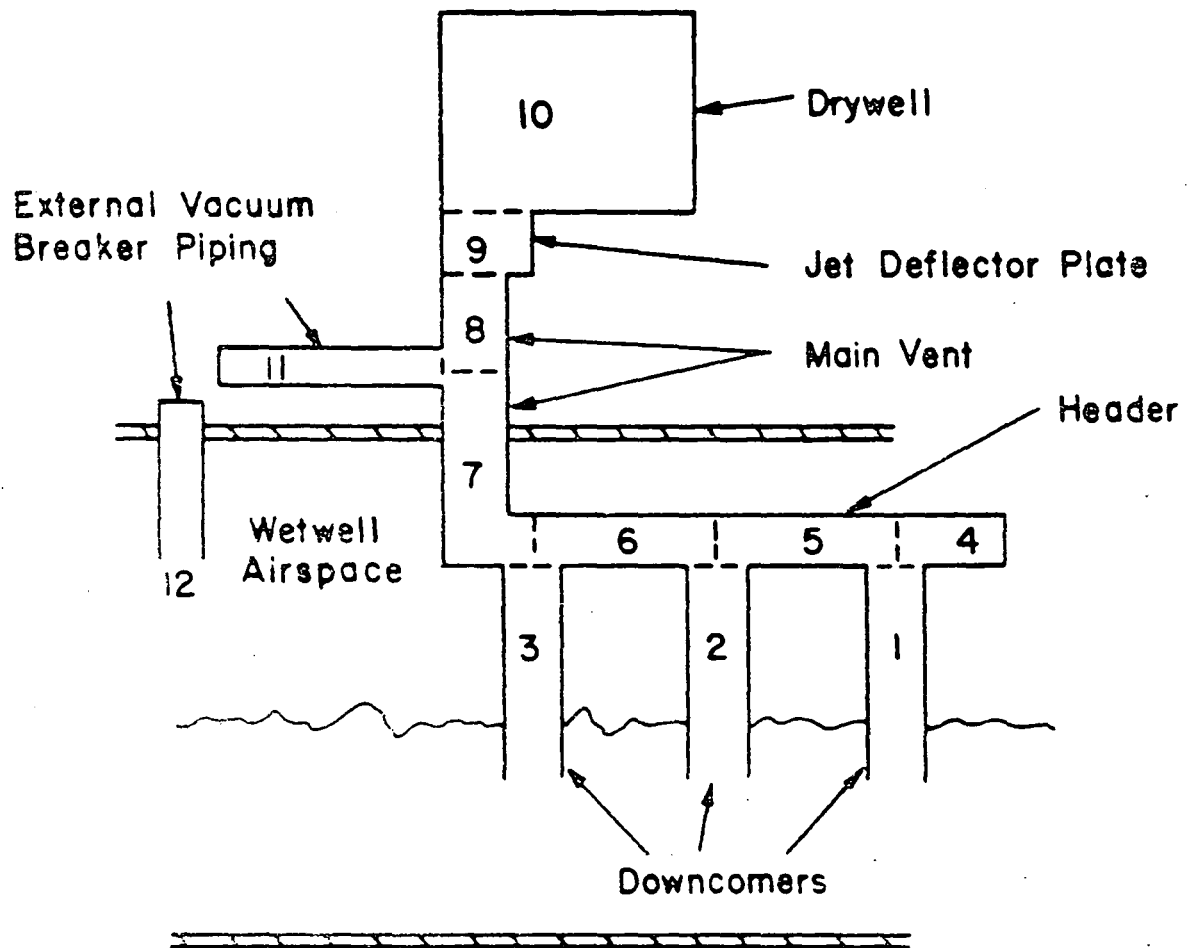


Figure 2. Schematic model of the vent system depicted by 12 dynamic components.

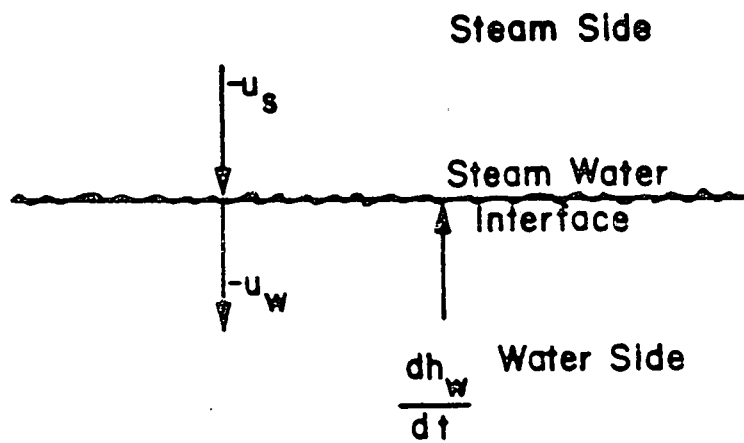


Figure 3. Details of the steam water interface.

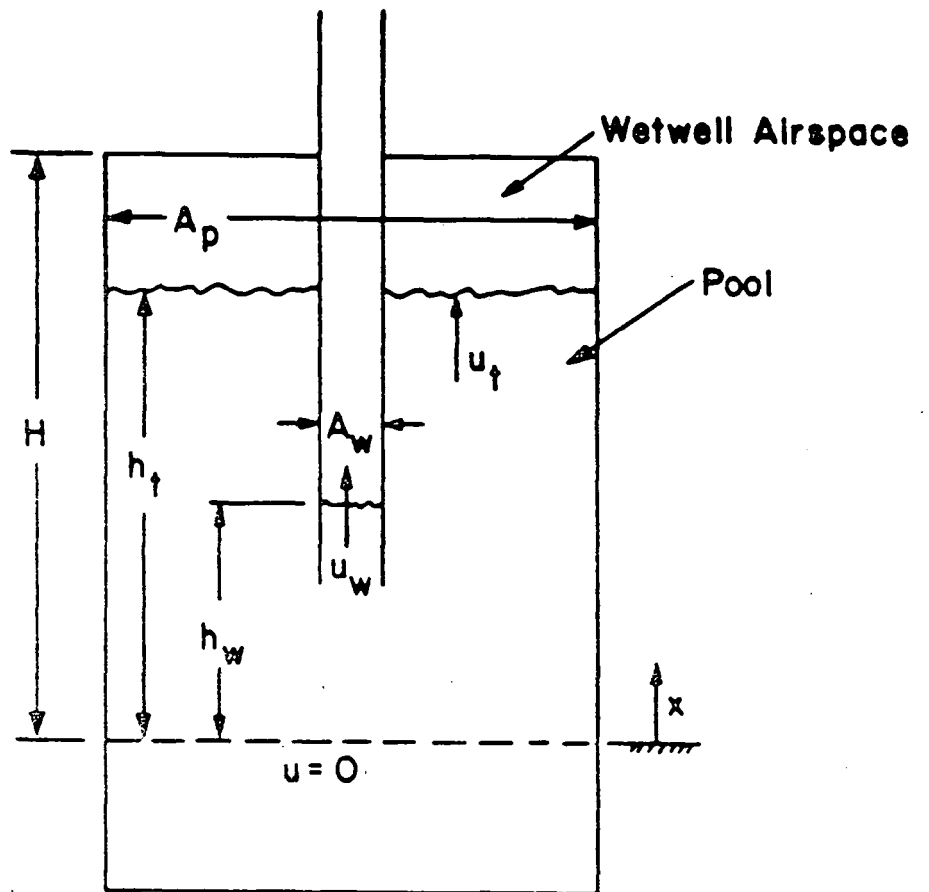


Figure 4. Details of the pool dynamic model around each downcomer.

with the lowering of the steam water interface in the downcomer. Assuming a unit condensation source in frequency space, a transfer function is then developed between the condensation source and the pressure in the drywell. Once this transfer function has been established, the condensation time history at the steam water interface can be extracted from a measured drywell pressure time history which is step 2 in Figure 1.

The model developed permits validation (step 3 in Figure 1) provided that an additional pressure time history, at another location in the suppression system, is available. With the condensation rate determined at the vent exit using a pressure time history from the drywell, the pressure history in the ring header was predicted and compared against measured data. The comparison was very favorable (Ref. 1).

In order to predict plant-unique vacuum breaker forcing functions, the key assumption is made that the condensation rate is a facility independent quantity. This assumption is supported by the observation that the condensation rate is fixed by local conditions at the vent exit; i.e., steam mass flow rate, non-condensibles and thermodynamic conditions, and that these local conditions vary slightly between plants. Using this condensation rate, the forcing function parameters given in Table 1 were used to compute expected and design loads across the Quad Cities 1 & 2 vacuum breakers (Ref. 1).

TABLE 1

Forcing Function Parameters
for Quad Cities 1 & 2

Parameter	Value Used In Computation*
Vent/pool area ratio	0.045
Drywell volume/main vent area ratio	413.62 ft**
Main vent area/downcomer area	0.99
Main vent length	37.32 ft
Header area/downcomer area	1.47
Header length	15.0 ft
Downcomer area	3.01 ft ²
Downcomer length	10.8 ft
Submergence head	3.67 ft water

* The modeled plant is FSTF

** Group 1 value used even though Quad Cities 1 & 2
are 491.40 ft.

SUMMARY OF THE METHODOLOGY OF THE MARK I/MARK II VACUUM
BREAKER VALVE MODEL (INCLUDING HYDRODYNAMIC EFFECTS)

During the Mark I shakedown tests, the vacuum breaker displacement time history was recorded. Use of a simple single-degree-of-freedom valve model resulted in large overly conservative predictions of the resulting valve dynamics. In an effort to reduce the conservatism in this test series, and additionally to relax the prediction of valve impact velocities in expected Mark II downcomer-mounted applications during chugging, a methodology was developed which uses the differential forcing function across the vacuum breaker (computed by the vent dynamic model) but includes the effect of torque alleviation as a consequence of valve flow (Ref. 2). With the valve in an open position, the pressure difference across the valve is not the pressure difference felt by the valve disc, because of flow effects across the open valve disc. This reduction in hydrodynamic torque is estimated by the following:

1. A linear analysis of the pressure field on either side of the closed valve permits the solution for pressure and velocity in the vicinity of the valve disc without flow.
2. The flow effect is modeled as a mathematical source/sink around the circumference of the open valve.
3. The local pressure and velocity fields permit evaluation of the strength of the flow source/sink.

4. The response of the valve to both flow and up and downstream pressure transients is computed as a superposition of these influences. In all cases flow tends to reduce the pressure load felt by the disc.

The 18" A&M valve characteristics for Quad Cities 1 & 2 are shown in Table 2.

TABLE 2

Vacuum Breaker Characteristics
for Quad Cities 1 & 2

Vacuum breaker type	18" A&M internal
System moment of inertia (lb-in-s ²)	55.645
System moment arm (in)	2.418
Disc moment arm (in)	11.375
System weight (lb)	108.54
Disc area (in ²)	283.53
System rest angle (rad)	1.021
Seat angle (rad)	0.3491
Body angle (rad)	1.1345
Seat coefficient restitution	0.6
Body coefficient restitution	0.7

RESULTS

The pressure time history shown in Figure 5 was used to drive a valve dynamic model with/without flow for the A&M valve with characteristics given in Table 2. The response of the valve for displacement and angular velocity are given in Figures 6 and 7. All results shown are for the expected pressure loading function with flow. Table 3 summarizes the valve impact data for both expected and design loading response.

.PRESSURE (PSI)

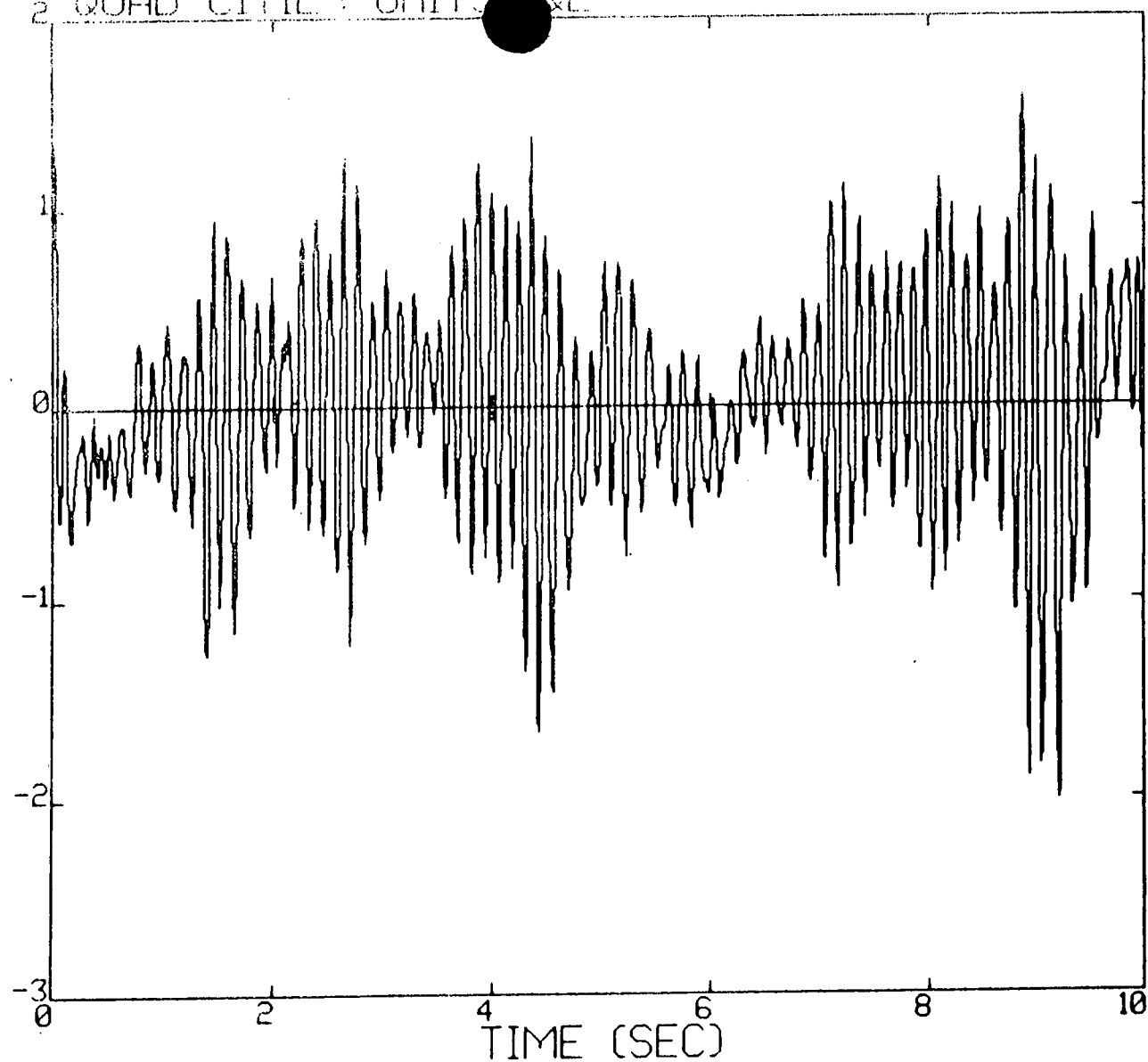


Figure 5a. Pressure time history predicted across a vacuum breaker located at the main vent-header junction in a Group 1 Mark I plant. Submergence head has not been added. 0 - 10 seconds.

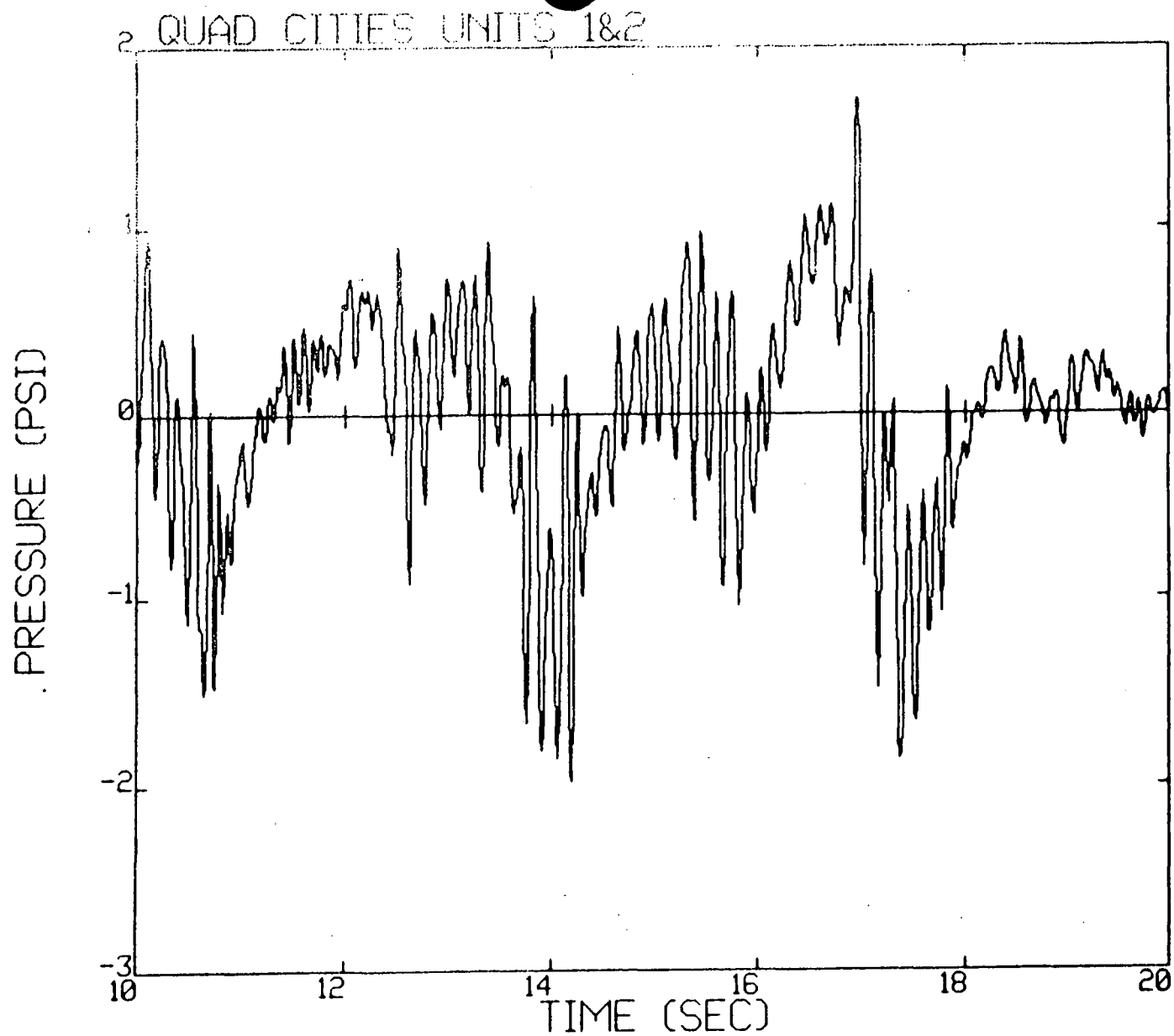


Figure 5b. 10 - 20 seconds.

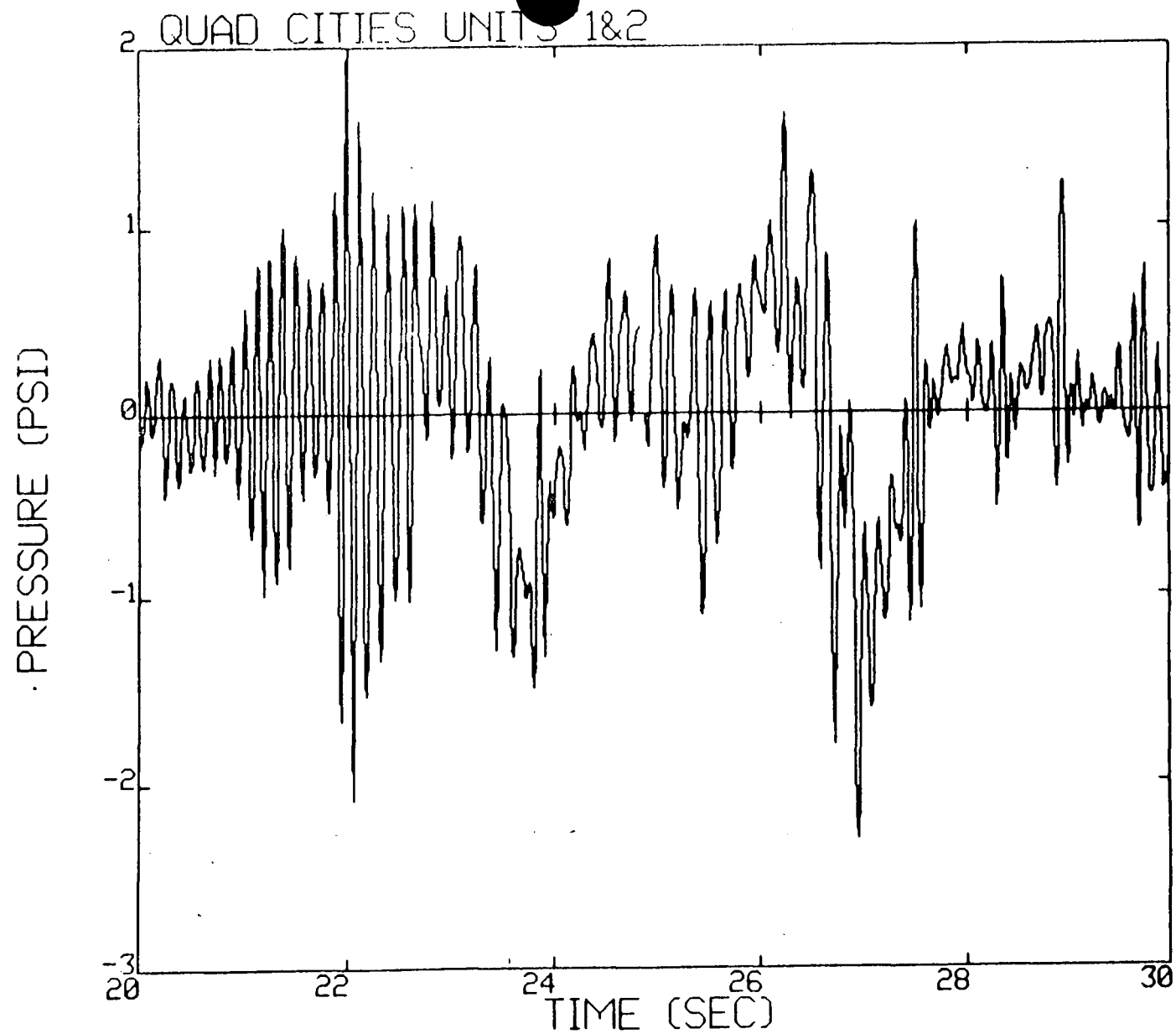


Figure 5c. 20 - 30 seconds.

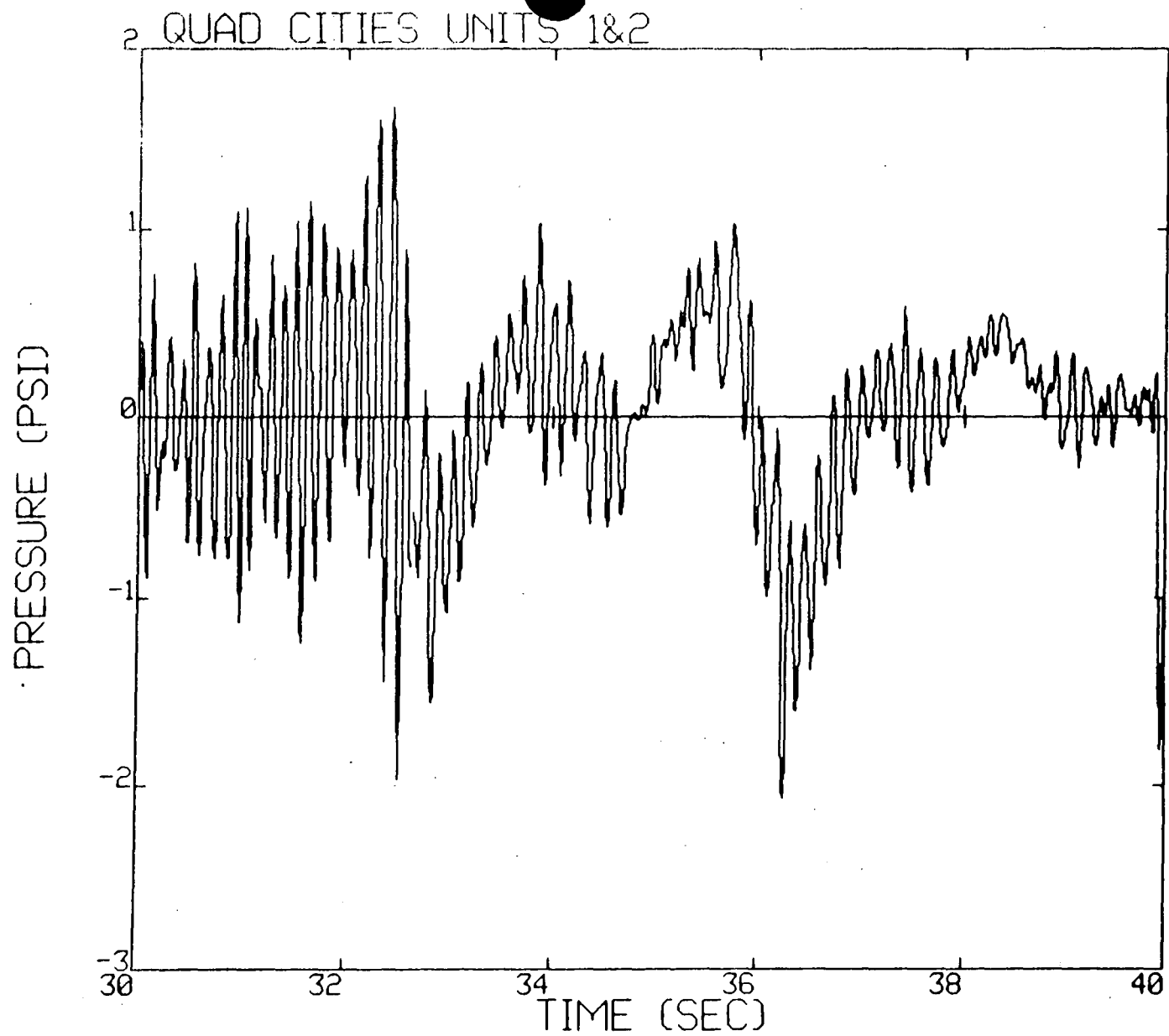


Figure 5d. 30 - 40 seconds.

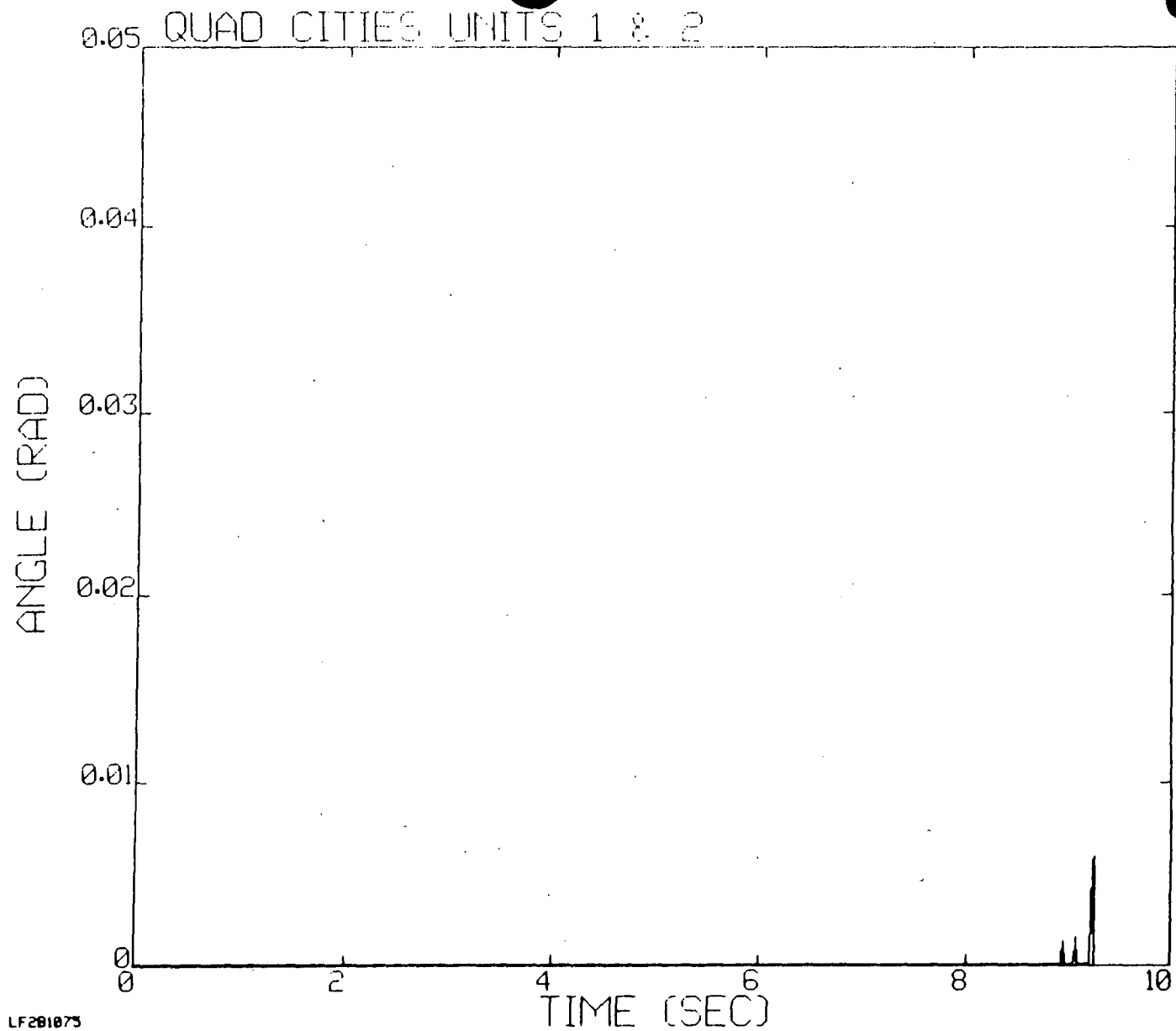


Figure 6a. Displacement time history of the 18" A&M internal valve in Quad Cities 1 & 2. 0 - 10 seconds.

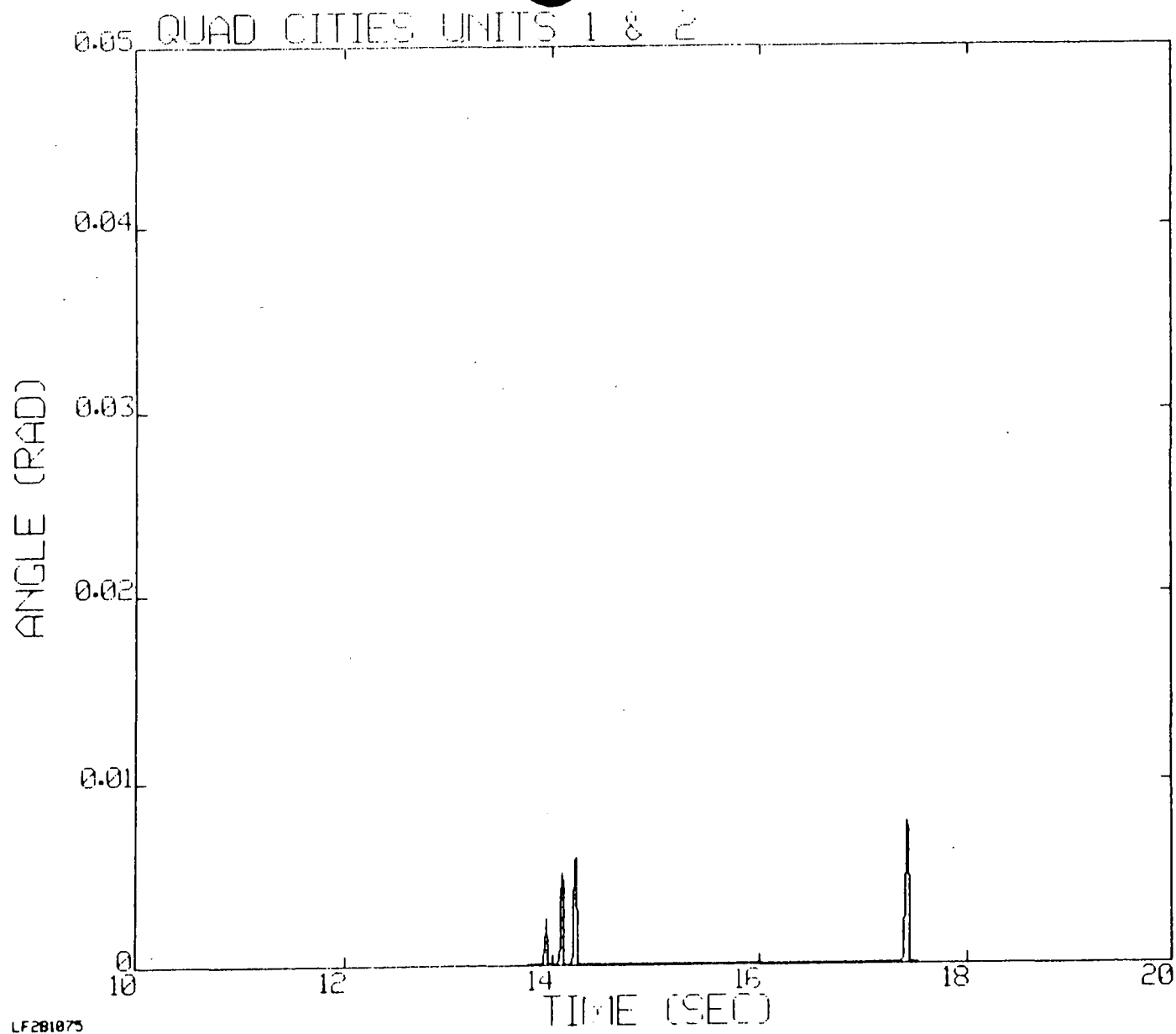


Figure 6b. 10 - 20 seconds.

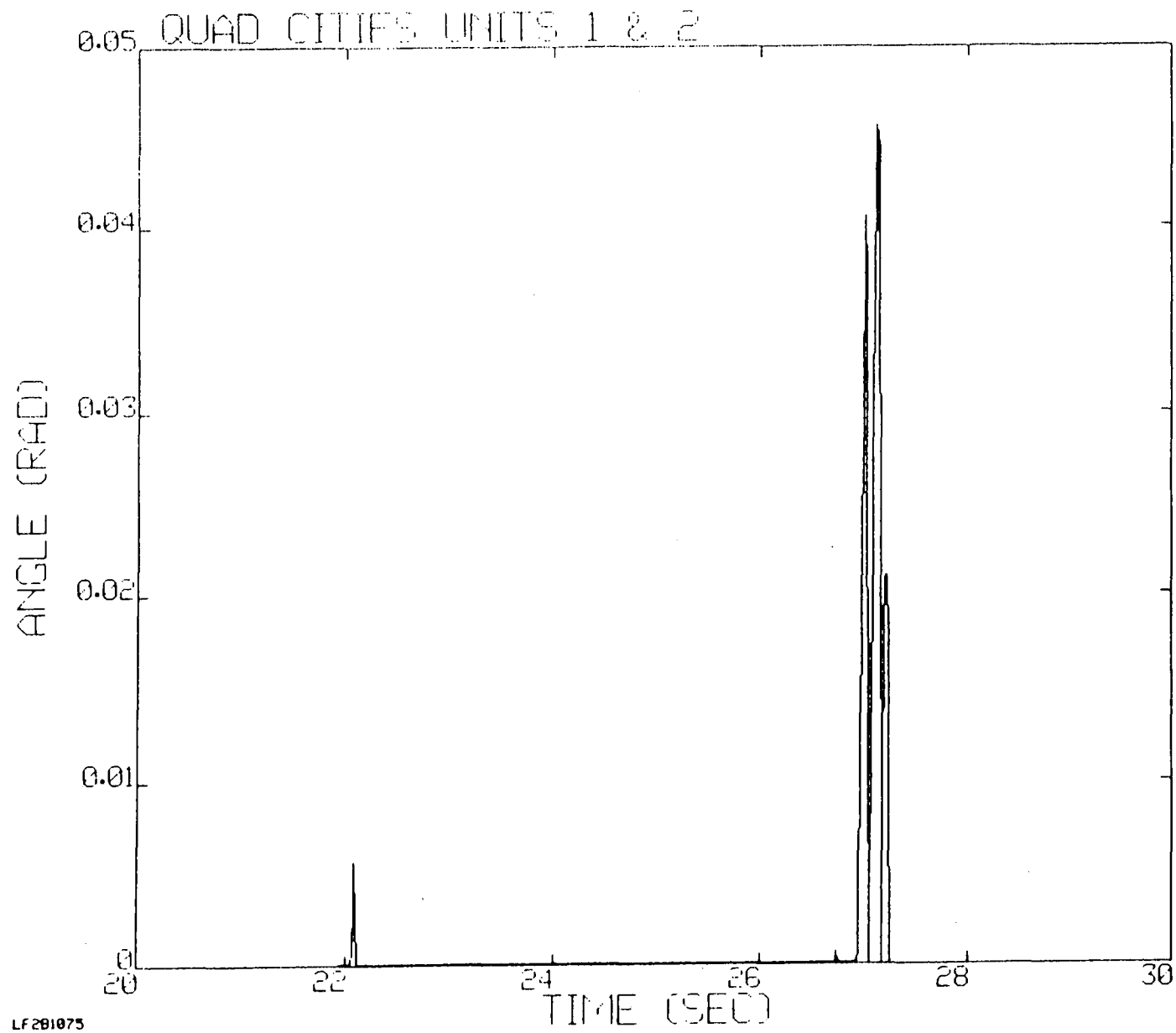


Figure 6c. 20 - 30 seconds.

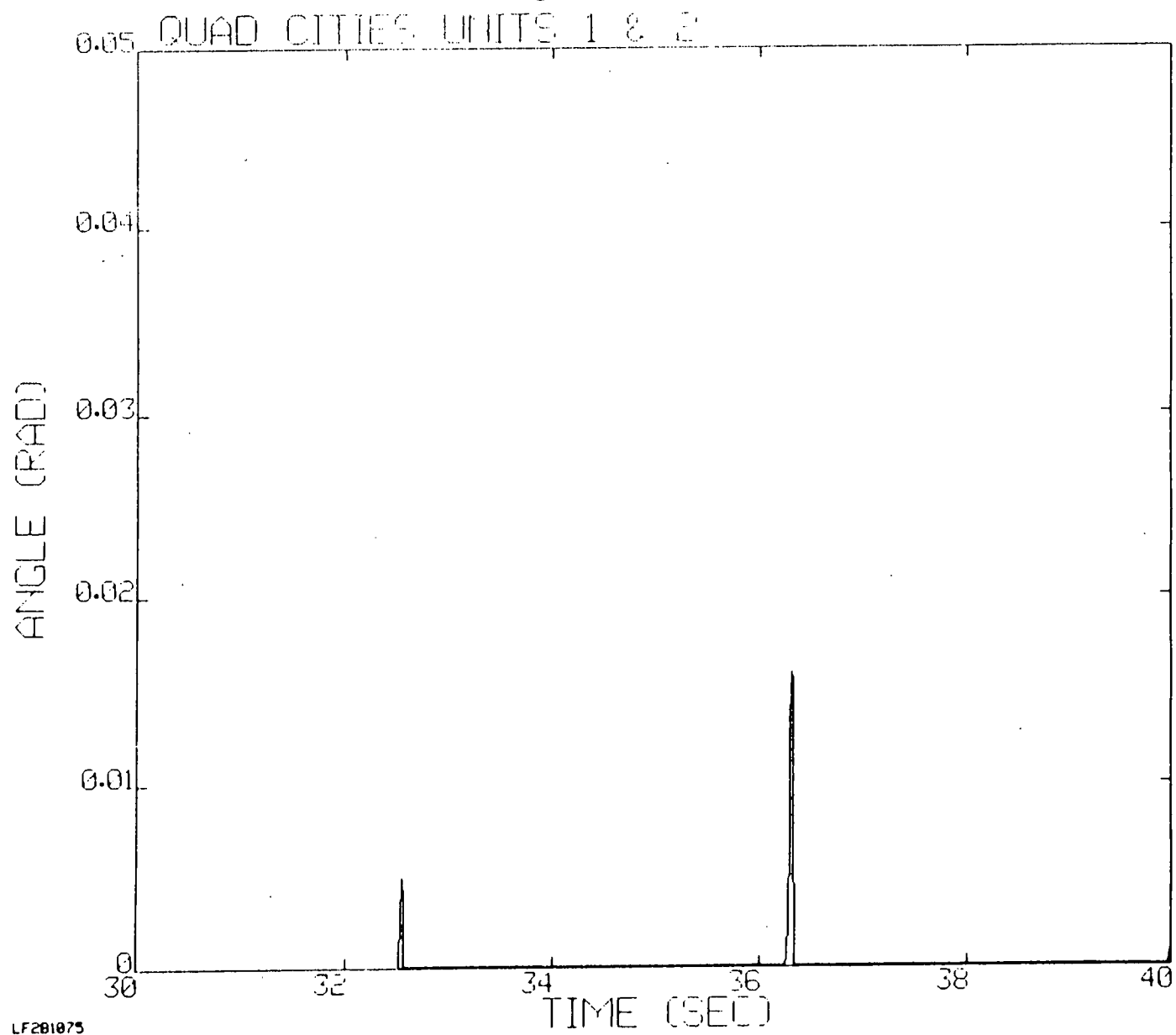


Figure 6d. 30 - 40 seconds.

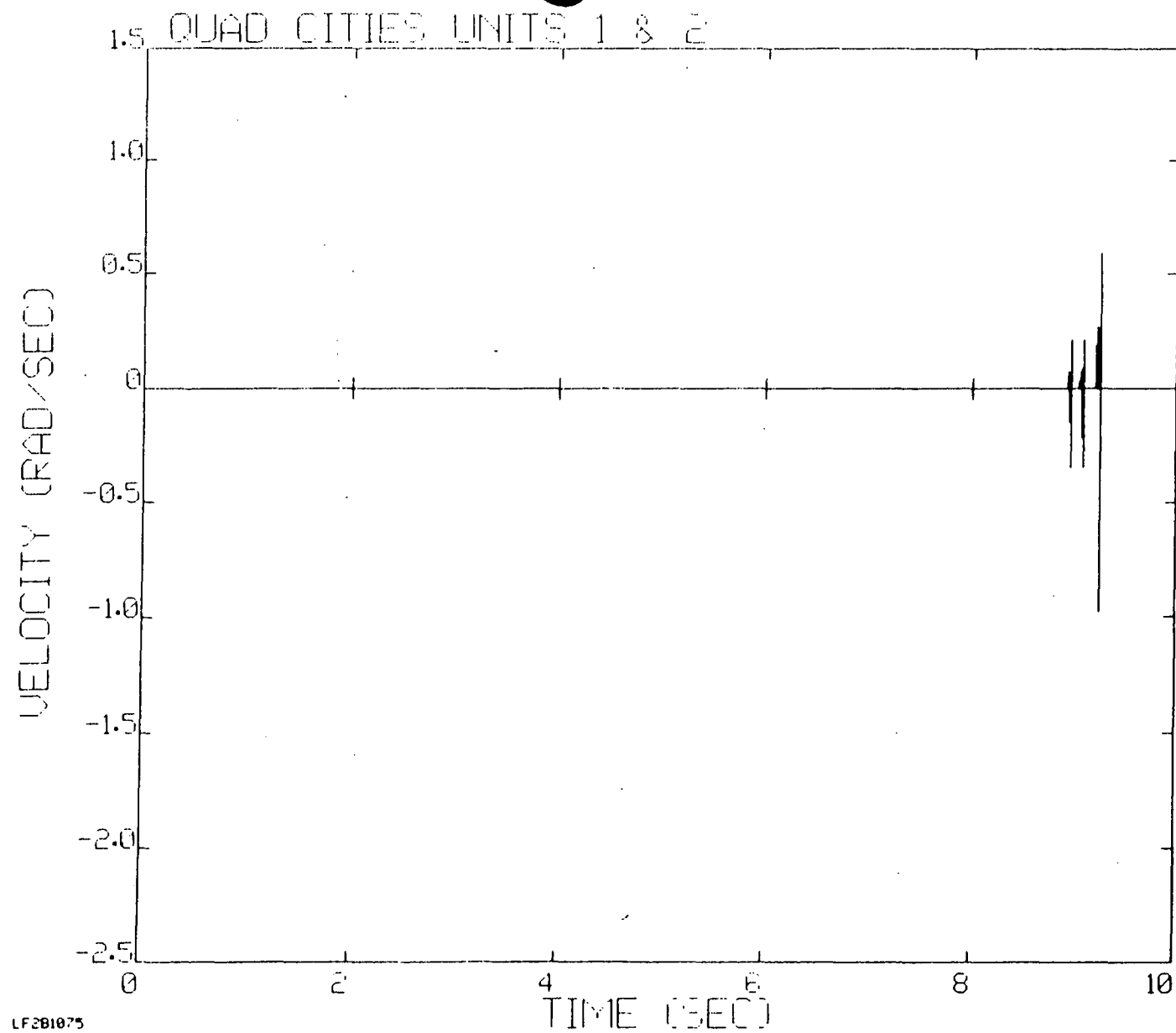


Figure 7a. Angular velocity time history of the 18" A&M internal valve in Quad Cities 1 & 2. 0 - 10 seconds.

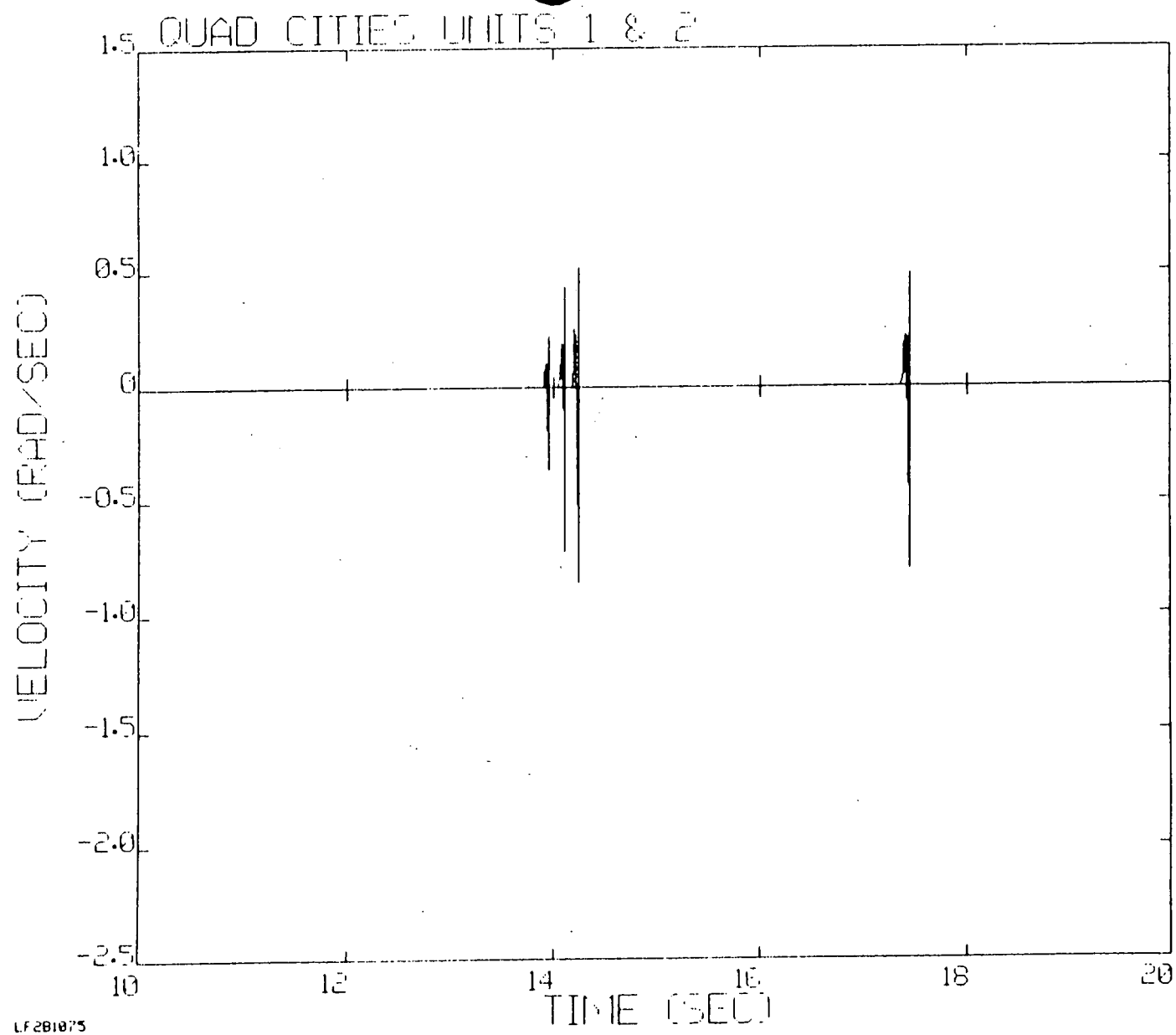


Figure 7b. 10 - 20 seconds.

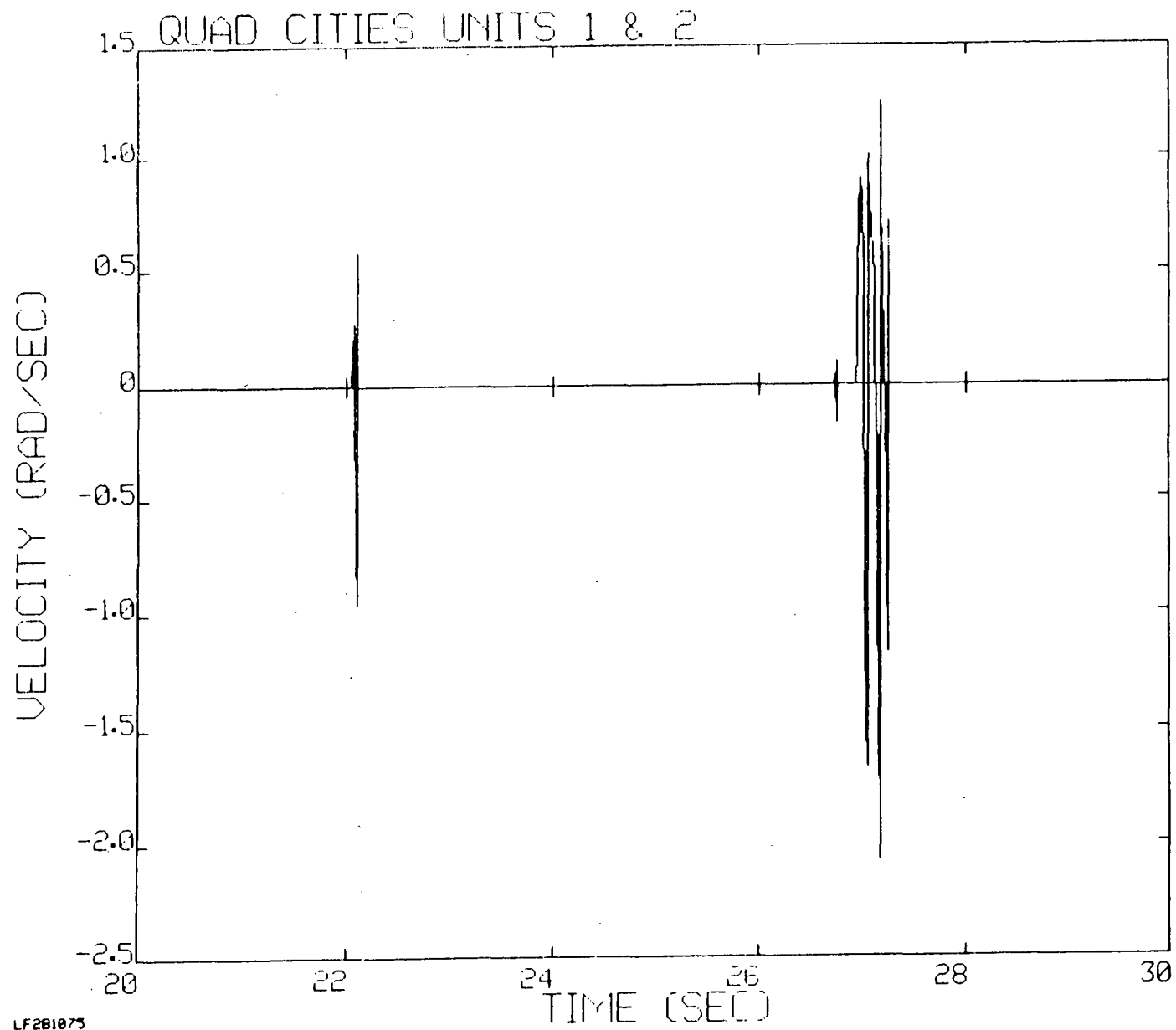


Figure 7c. 20 - 30 seconds.

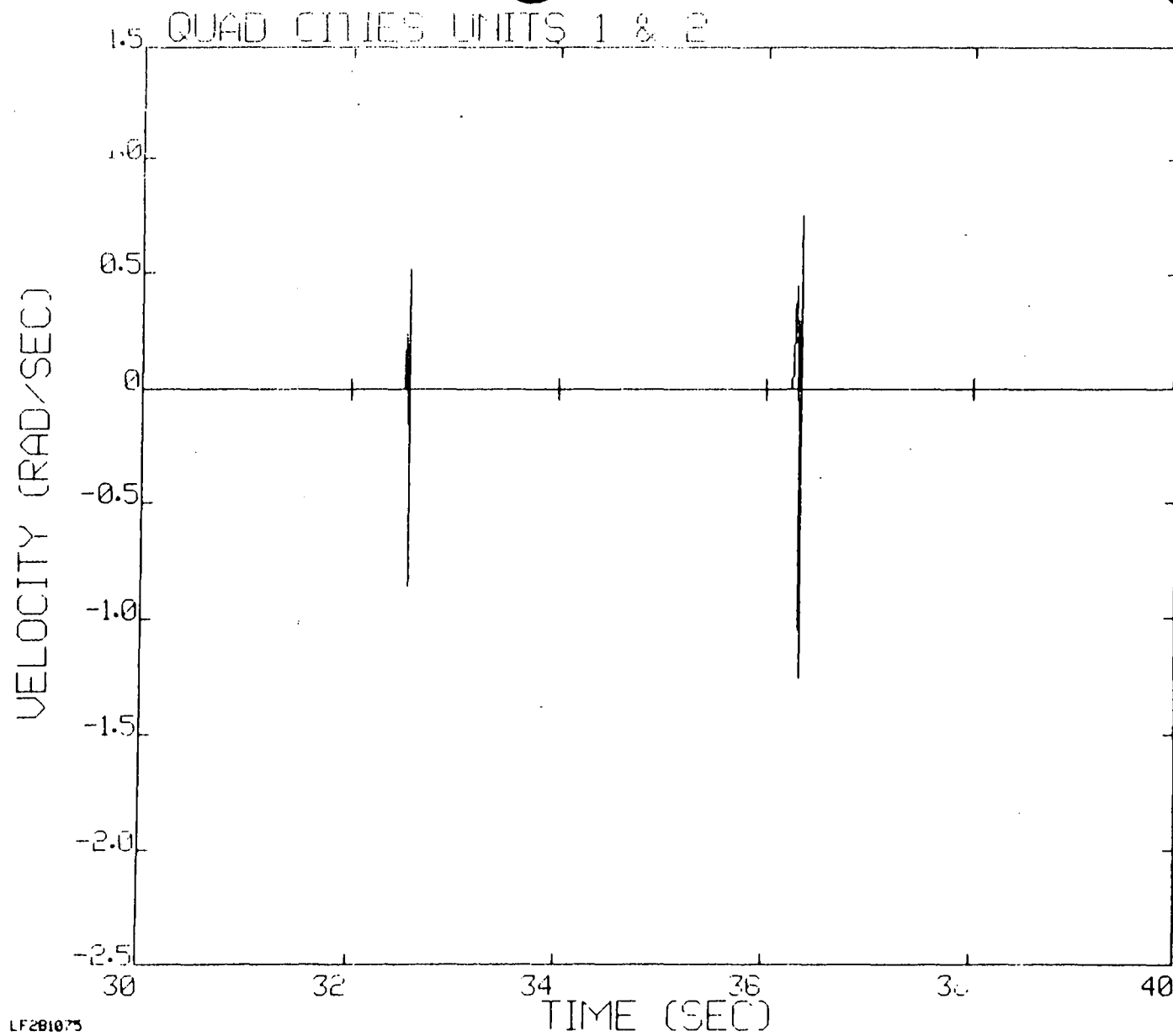


Figure 7d. 30 - 40 seconds.

TABLE 3

Vacuum Breaker Valve Response
for Quad Cities 1 & 2

	Maximum Impact Velocity (rad/sec)	Number of Impacts (2)	Maximum Opening Angle (rad) (3)
Expected Loading Function(1)			
No flow effects	2.62	9	0.060
Flow effects	2.08	4	0.046
Design Loading Function(4)			
No flow effects	3.09		
Flow effects	2.45		

(1) Submergence head is taken as 1.59 psi.
Vacuum breaker assumed to be mounted
at the main vent-header junction. |

(2) Seat impacts above 1 rad/sec.

(3) Body impacts do not occur.

(4) Design impact velocity is 1.18 times
the expected impact velocity (Ref. 3).

Revision 1

REFERENCES

1. "Mark I Vacuum Breaker Dynamic Load Specification, Revision 3," C.D.I. Report No. 80-4, February 1980.
2. "Mark I Vacuum Breaker Improved Valve Dynamic Model - Model Development and Validation," C.D.I. Tech Note No. 82-31, August 1982.
3. General Electric Company letter MI-G-43, July 9, 1982 Mark I Containment Program - Task 9.5.1, Architect Engineer Question Reply No. 315.